UNIVERSIDAD COMPLUTENSE DE MADRID
FACULTAD DE CIENCIAS QUIMICAS

TESIS DOCTORAL

Mitophagy regulators as innovative drugs for neurodegenerative diseases

Moduladores de mitofagia como fármacos innovadores en enfermedades neurodegenerativas

MEMORIA PARA OPTAR AL GRADO DE DOCTOR

PRESENTADA POR

Inés Maestro Inarejos

Directoras

Ana Martínez Gil
Patricia Boya Tremoleda

Madrid

UNIVERSIDAD COMPLUTENSE DE MADRID
FACULTAD DE CIENCIAS QUÍMICAS

TESIS DOCTORAL

CONSEJO SUPERIOR DE INVESTIGACIONES CIENTÍFICAS
Centro de Investigaciones Biológicas Margarita Salas

Mitophagy regulators as innovative drugs for neurodegenerative diseases

Moduladores de mitofagia como fármacos innovadores en enfermedades neurodegenerativas

Memoria para optar al grado de doctor

en Bioquímica, Biología Molecular y Biomedicina por la Universidad Complutense de Madrid

PRESENTADA POR

Inés Maestro Inarejos

DIRECTORAS

Prof. Ana Martínez Gil

Dra. Patricia Boya Tremoleda

Madrid 2022

AGRADECIMIENTOS

Como es de suponer, este trabajo no hubiera sido posible sin la ayuda de mucha gente a la que le estoy enormemente agradecida.

Gracias a mis directoras de tesis, Ana y Patricia. Ana, gracias por traer de vuelta a España a científicos españoles como yo. Gracias por darme la oportunidad de realizar este proyecto contigo. Gracias por haberme dejado entrar en la familia tan bonita que son los Chemfinders. Gracias por transmitirme tu amor por la ciencia y por esta profesión. Y, sobre todo, gracias por escucharme y calmarme. Me has dado paz cuando más lo necesitaba. Patricia, gracias por abrirme tu laboratorio de par en par. Gracias por enseñarme a pensar críticamente y a razonar. Gracias por guiarme en todo el proyecto y por confiar en mí. Gracias por contagiarme tu ilusión por entender. Sin vuestro apoyo y consejo este proyecto no hubiera sido igual.

Gracias al Dr. Manuel Guzmán, por tutorizar mi tesis durante estos casi cuatro años. Gracias por estar siempre detrás del correo y atender a todas mis preguntas. Muchas gracias por tu ayuda.

Carmen, gracias por acogerme tan bien. Gracias por el orden y la disciplina que transmites, tan necesarias en un laboratorio. Gracias por ayudarme con nuestros amigos los americanos, que tanta guerra nos han dado. Sin tu organización hubiera sido imposible. Gracias.

Gracias, Nuria y Ruth. Aunque hemos coincidido muy poco, siempre me habéis recibido con una sonrisa.

Como no mencionar a mis compañeros de laboratorio, con los que he compartido cafés, risas y complicidades.

Chemfinders, GRACIAS.

Vanesa, el fruto del amor. Gracias por ser el corazón del grupo. Como bien dice tu rol, Flora, ‘e*s la jefa, y la más inteligente y cuidadosa, aunque a veces es demasiado mandona’.* Creo de verdad que los VNG son increíbles, aunque siempre negaré haberlo dicho. Gracias por los momentos fuera de labo y por tus manos en la costura. Gracias por las discusiones

literarias y por habernos sacado a todos de la poyata para hacer una tourné en la Furgonesa, que tan buenos momentos ha dado.

Loreto, gracias por escuchar mis quejas y darles coherencia. Gracias por las risas y por los desayunos de los viernes. Aunque también nos has enseñado a comer sano. Y, sobre todo, gracias por enseñarme y acompañarme en esta última etapa que hemos compartido, ¡qué aventura la maternidad!

Carlota, Fauna de los montes de Huesca. Gracias por todos los ratos compartidos en cultivos y en poyata. Gracias por comprender momentos clave de estos años y siempre estar dispuesta a todo con una sonrisa. Y gracias por estos últimos meses espalda con espalda. Ánimo en tu recta final.

Enriquito de mi corazón. Gracias por traer tu humor tan inteligente al labo. Gracias por explicarme con tanta paciencia cositas compus, y tantas cosas varias de gente joven que ya se me escapan de las manos.

Marcos, mi paisano. Gracias por ser tan cercano. Gracias por los ratos de descanso y por habernos amenizado con tus historietas. Por esas conversaciones fugaces en los pasillos. ¡Gracias!

Elena, gracias por estos últimos meses. Gracias por esa simpatía que transmites. Gracias por la predisposición que tienes y por mantenerme un poco al día de las novedades del mundo joven. Aunque sólo sea un poquito.

A los referentes del grupo. Gracias Valle. Porque siempre sacas un hueco para escuchar, sea científico o no. Por esos desayunos. Y por ese buen rollo que transmites. Alfonso, gracias por la disponibilidad y ayuda con tantos papeleos de envíos y contratos. Y Eva. Mil gracias por responder a todas mis preguntar, una y otra vez, y echarme una mano en cualquier momento. Gracias por todo vuestro conocimiento y experiencia.

Rocío, hemos coincidido muy poquito por los laboratorios, pero siempre me has respondido con una sonrisa. Gracias. Andrea, gracias por hacernos un huequito a las bioderivadas en tu laboratorio. Mucho ánimo también en tu recta final.

Y a las nuevas incorporaciones. Mikel, desde el primer día me has sabido escuchar y aconsejar. Gracias por nuestras conversaciones madrugadoras. Y Javi, que has venido a revolucionar el laboratorio con tus canciones y tus fábulas con moraleja. ¡Gracias a los dos y bienvenidos!

Gracias por supuesto, a los doctores que ya han echado a volar. Roca, gracias por tantos cafés en los que me has introducido en el mundo computacional. Gracias por las risas y por la tranquilidad, que es lo que se valora. Pero, sobre todo, gracias por escucharme y solucionarme tantos momentos de estrés en esta última etapa. Te deseo lo mejor por GLPG. Víctor, gracias por los grandes momentos durante las comidas y por tu predisposición siempre. Requena, qué gran descubrimiento. Gracias también por los cafés y por las conversaciones enriquecedoras. Josefa, gracias porque, aunque no hemos coincidido apenas, guardo un gran recuerdo de ti. Me quedo con la espinita de no haber podido disfrutar de tu defensa. Y Eli, muchísimas gracias por amenizarnos cada día con tus canciones. Por ser tan luchadora y transmitir tanta alegría.

Por supuesto muchas gracias a todos los miembros del BoyaLab, por haberme recibido en vuestro labo y haberme hecho un hueco entre vuestras poyatas.

Petra, thanks for sharing these three years. Thanks for your help and for the funny and stressful moments. I wish you the best in your next phase! Bea, muchas gracias por tu predisposición desde el minuto cero y por tener siempre una gran sonrisa. Espero volver a coincidir contigo, aunque sea por festivales. Iñaqui, mil gracias por tu ayuda, sobre todo durante mi último empujón. Me has hecho el camino más fácil. ¡Ánimo con tu proyecto! Elena, gracias por acogerme y por las enseñanzas. Juan, hemos coincidido poquito, pero te deseo lo mejor durante tu andanza en el BoyaLab. Raquel y Sandra, muchísimas gracias por resolverme todas mis dudas cuando he llamado a vuestra puerta. Me habéis dado mucha paz. Y como no acordarme de la gente que ya no está. Natalia, gracias por ser ejemplo de disciplina científica. Ines y Katharina, thanks for your support when I needed!

No puedo dejar de agradecer a la Dra. Ángeles Martín Requero el haberme dejado un trocito de su poyata al final de esta etapa. Gracias por acogernos con tanta ternura y por ser ejemplo de dedicación a la ciencia. Y por supuesto, gracias a Gracia, por haberme

introducido en el mundo de los linfos, gracias por tu orden y tu constancia. Y, sobre todo, gracias por tantas conversaciones y desahogos en cultivos.

También me gustaría agradecer a Carmen y Zaira, del servicio de cultivos, por su buen hacer en el servicio y por ayudar siempre. Y por supuesto muchísimas gracias a Gema, María y Maite, del servicio de confocal, donde tantas y tantas horas he pasado. Gracias por todos los momentos de ayuda que me habéis brindado, que no han sido poco.

I have to write some words to thank all the ITN members. Thanks for the amazing group of young scientists we have formed. Thanks for the meetings, for the feedbacks and for all the knowledge we could share during these three years. Specially, thanks to Prof. Anne Simonsen. Thanks for receiving me in your lab during those two months. Thanks for making me be part of your group. Thanks for listening, for the scientific discussions and for all the advice you gave me. Y como no, gracias Laura. Gracias porque fuiste mi madrina durante esos dos meses. Gracias por enseñarme con tanto cuidado y por introducirme en el mundo del análisis de imagen. Gracias por las cervezas de después y por los ratos fuera del labo. Pero, sobre todo, muchísimas gracias por tantísimas risas. Aún tengo el recuerdo del dolor de tripa de tanto reír. Gracias, porque sin ti, mi estancia no hubiera sido igual.

Y gracias también a mucha gente ajena a la ciencia por su apoyo. Gracias a mis amigas. A Ruth, Isa, Cris y Bea. Gracias por hacerme desconectar.

A Pepe, Tere y Alba, siempre atentos e interesados por mis celulitas.

A mi hermano, por preguntar y estar. Por escuchar, porque eso es suficiente.

A mis padres, por el apoyo incondicional. Por ser los que más creen en mí y transmitírmelo. Por enseñarme la dedicación y la disciplina.

Y a Ponseti. Por estar sin entender. Por escuchar y tranquilizarme en mis malos momentos. Por razonar y darle la importancia a las cosas que lo merecen. Por apoyarme siempre. Por hacer que crezca y por haberme dado lo más bonito que tenemos. Por Abril.

¡Gracias!

RESUMEN

Moduladores de mitofagia como fármacos innovadores en enfermedades neurodegenerativas

La mitofagia es la degradación selectiva de la mitocondria mediante autofagia. A través de una estructura de doble membrana, conocida como autofagosoma, las mitocondrias defectuosas o que no hacen falta son llevadas al lisosoma, donde son degradadas. Se trata de un proceso clave en el mantenimiento de la homeostasis celular. Una acumulación de mitocondrias defectuosas o la falta de mitocondrias sanas causadas por un exceso o un defecto de mitofagia, afectan a la homeostasis celular. De hecho, es un proceso alterado en diferentes enfermedades, como en cáncer, enfermedades cardíacas y especialmente en enfermedades neurodegenerativas, como en la enfermedad de Parkinson, la enfermedad de Alzheimer, o en la esclerosis lateral amiotrófica.

Así, la mitofagia aparece como una diana terapéutica muy interesante en el campo de la química médica y el descubrimiento de fármacos. Es por ello, que el objetivo principal de esta tesis doctoral ha sido la búsqueda de moduladores de mitofagia y su caracterización, así como su aplicabilidad terapéutica en modelos de neurodegeneración.

Para ello, se partió de dos quimiotecas con más de 3700 compuestos en total. Se filtraron los compuestos mediante técnicas computacionales y diversidad química. Finalmente se analizaron 90 compuestos en un ensayo fenotípico de mitofagia, encontrándose dos inductores y un inhibidor.

Los inductores, JAR1.39 y VP07, pertenecen a una familia de compuestos diseñados para inhibir alostericamente la quinasa GSK3. Sin embargo, la modulación de la mitofagia por parte de estos compuestos es independiente de la inhibición de GSK3, siendo su estructura la responsable de su actividad en mitofagia. Los compuestos fueron evaluados en modelos celulares de la enfermedad de Parkinson y recuperaban los bajos niveles de mitofagia que presentaban los modelos y que son característicos de la enfermedad.

El inhibidor, IGS2.7, inhibe la proteína quinasa CK1, pero la inhibición de mitofagia es independiente de su diana. Proponemos ULK1, una proteína quinasa que participan en las fases iniciales del proceso de autofagia, como una nueva diana de IGS2.7. La aplicabilidad

terapéutica del inhibidor se estudió en modelos de esclerosis lateral amiotrófica. Linfoblastos de pacientes con mutaciones en SOD1 y TDP-43, así como modelos murinos con mutaciones en los mismos genes, mostraron mayor flujo de autofagia comparado con sus controles. El tratamiento de ambos modelos celulares y el modelo animal de TDP-43 con el inhibidor IGS2.7 recuperó los niveles de autofagia a los del control.

Por último, se propone a la proteína quinasa SGK1 como una diana para modular la homeostasis mitocondrial. Mediante un cribado virtual y posterior validación de los hits *in vitro,* se estudiaron los compuestos más potentes en el ensayo fenotípico de mitofagia, observándose una disminución de la mitofagia junto a un aumento de biogénesis mitocondrial. Se ensayaron en un modelo celular de la enfermedad de Alzheimer y se observó una recuperación de la muerte celular.

Así, concluimos que la mitofagia y la homeostasis mitocondrial son procesos alterados en diferentes patologías y que su modulación es clave para recuperar los niveles adecuados de mitocondrias sanas. Por ello, aparecen como dos buenas estrategias terapéuticas para el descubrimiento de fármacos en enfermedades neurodegenerativas, en los que el proceso aparece alterado.

ABSTRACT

Mitophagy regulators as innovative drugs for neurodegenerative diseases

Mitophagy is the selective degradation of mitochondria by autophagy. It consists in the recruitment of defective mitochondria or non-needed in a double-membrane structure, called autophagosome, which transports the mitochondria to the lysosome, where it will be degraded. It is an important process in the maintenance of the cellular homeostasis. The accumulation of defective mitochondria due to a block in mitophagy, or a lack of healthy mitochondria due to excessive mitophagy, can cause a detrimental effect on cellular homeostasis. In fact, it is known to be altered in several pathological conditions, such as in cancer, heart diseases and especially in neurodegenerative diseases like Parkinson's disease, Alzheimer's disease, or Amyotrophic Lateral Sclerosis.

Thus, mitophagy rises as an interesting therapeutic target in the field of medicinal chemistry and drug discovery. The main objective of this thesis was the discovery of new mitophagy modulators, their characterization, and their therapeutic applicability on models of neurodegeneration.

Starting from two chemical libraries with more than 3700 compunds, several filters like computational tools and selection of compounds based on chemical diversity were applied to reduce the number of compounds to be evaluated. Finally, 90 compounds were studied in a phenotypic mitophagy assay. Two mitophagy inducers and one inhibitor were obtained.

The inducers, named JAR1.39 and VP07, belong to a family of compounds designed to allosterically target GSK3. However, their ability to induce mitophagy was independent of their role against GSK3, being their structure the responsible of their activity on mitophagy. They were evaluated in Parkinson’s disease cellular model, and they rescued the defective mitophagy characteristic of the disease.

The inhibitor, known as IGS2.7, targets the kinase CK1. Anyhow, mitophagy inhibition appeared to be CK1-independent, being ULK1, a kinase involved in autophagy initation, proposed as the key in its role in autophagy. The therapeutic applicability of the inhibitor was evaluated in amyotrophic lateral sclerosis cellular and animal models. SOD1- and TDP43-lymhoblasts of patients showed higher autophagy flux compared to control. Mice

carrying a mutation in the same genes showed lower protein level of p62, an autophagy surrogate and TOMM20, a mitochondrial mass protein, thus suggesting higher mitophagy activity. The treatment of both cellular models and TDP-43 animal model with the inhibitor IGS2.7, restored autophagy flux and protein levels to control.

In addition, the kinase SGK1 was found to be implicated in autophagy regulation. Thus, using a different approach, a virtual screening was done against the kinase. Then, we evaluated the inhibitory ability of the compounds against SGK1. The more potent compounds were studied in a mitophagy assay, and a decrease in mitophagy was obtained when SGK1 was inhibited. Interestingly, this mitophagy decrease came along with an increase in mitochondrial biogenesis. Their therapeutic applicability was studied in an Alzheimer's disease cellular model. The inhibition of the kinase restored cell death.

Thus, we conclude that mitophagy and mitochondrial homeostasis are defective processes in several pathological conditions and their modulation is interesting to recover good levels of healthy mitochondria. Thus, these two therapeutic strategies can be used in the treatment of neurodegenerative diseases, where the processes are altered.

ABBREVIATIONS

6-OHDA	6-hydroxydopamine
AD	Alzheimer's disease
ALS	Amyotrophic lateral sclerosis
APP	Amyloid precursor protein
ATG	Autophagy-related proteins
BafA1	Bafilomycin A1
BBB	Blood-brain barrier
CCCP	Carbonyl cyanide m-chlorophenyl hydrazone
CK1	Casein kinase 1
CL	Cardiolipin
DFP	Deferiprone
FCCP	Carbonyl cyanide-p-trifluoromethoxyphenylhydrazone
FDA	U.S. Food and Drug Administration
GSK3	Glycogen synthase kinase 3
HCQ	Hydroxychloroquine
HD	Huntington's disease
IC_{50}	Concentration that reduces the effect by 50%
iMLS	Internal mitochondria localization signal
LBDD	Ligand-based drug discovery
LC3	Light chain 3
LIR	LC3-interacting reagion
MBC	Medical and biological chemical library
MN	Motoneuron
MS	Multiple sclerosis
mTOR	Mechanistic target of rapamycin
OA	Okadaic acid
OMM	Outer mitochondrial membrane
P	Postnatal day
PD	Parkinson's disease

PDB	Protein data bank
PQ	Paraquat
PS1	Presenilin 1
ROS	Reactive oxygen species
SAR	structure–activity relationship
SBDD	Structure-based drug discovery
SD	Standard deviation
SEM	Standard error of the mean
SGK1	Serum- and glucocorticoid-induced kinase
SOD1	Superoxide dismutase 1
TDP-43	TAR DNA-binding protein 43
ULK1	UNC51 like kinase-1
WT	Wild-type

1. INTRODUCTION

1.1 Autophagy

Autophagy is a highly conserved cellular pathway that degrades cytoplasmic content in the lysosomes to be recycled into the cytosol. The term was first coined in the 1960s by Christian de Duve, the discoverer of lysosomes, to describe the event by which lysosomes contained degrading cytoplasmic content.[1] In normal conditions autophagy is used to eliminate damaged organelles, like mitochondria, or toxic aggregated proteins and to break down long-lived proteins.[2] Basal autophagy is needed especially in non-dividing cells, due to its inability of diluting damage organelles within daughter cells through cell division.[3] In starvation or stress conditions, autophagy is boosted to provide cells with amino acids or fatty acids to maintain metabolism and ATP levels for cell survival.[2]

1.1.1 Types of autophagy

Depending on the way that the cargo is delivered to the lysosomes, we can distinguish three types of autophagy (Figure 1):

- **Macroautophagy**, (hereafter referred to as 'autophagy'). Cytoplasmic content is sequestered in a double-membrane vesicle, called autophagosome. Then, autophagosomes fuse with lysosomes, where the cargo is degraded.[2] This process is extensively explained in the following sections.

- **Microautophagy**. Cargo is taken by the invagination of the lysosomal membrane itself.[4] This process is the least understood and further tools are needed to elucidate its mechanism and function.

- **Chaperone-mediated autophagy (CMA)**. It allows degradation of proteins that have a specific motif in their sequence. This motif is recognized by the chaperone heat shock-cognate protein of 70 kDa (Hsc70) and targeted to the lysosomal surface, where the protein interacts with lysosome-associated membrane protein type 2A (LAMP2A). Then, the protein is unfolded and gets into the lysosome to be degraded.[5]

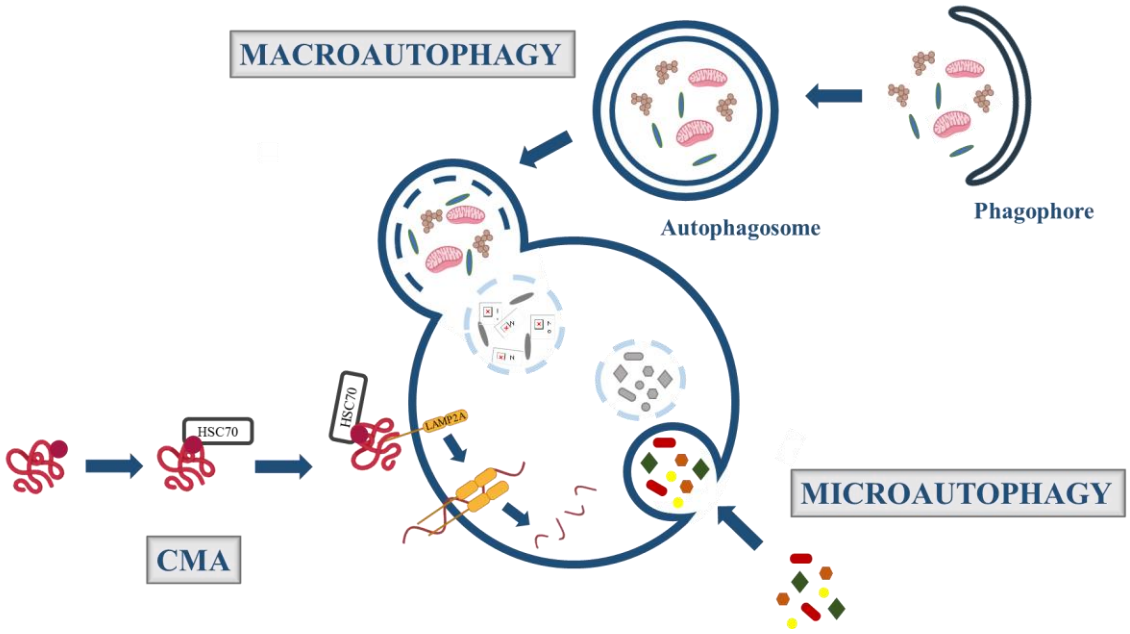

Figure 1. Types of autophagy**.** Representation of the three types of autophagy based on the way the cargo is delivered to the lysosome.

1.1.2 Autophagy Process

Autophagy process is conserved from yeast to humans, and it is regulated by AuTophaGy-related proteins (ATG).[2] Its machinery is constituted by several complexes that are disclosed below (Figure 2).

- **Initiation**. Autophagy starts with the activation of UNC51 like autophagy activating kinase (ULK1) complex (ULK1, FIP200, ATG13, and ATG101) and its activity is regulated by post-translational modifications. The mechanistic target of rapamycin complex 1 (mTORC1), a nutrient sensor, maintains ULK1 complex in an inactive state by phosphorylating ULK1 and ATG13. On the other hand, in the absence of amino acids or in a low energy scenario, an increase in cAMP activates AMP-activated protein kinase (AMPK), which in turn phosphorylates and activates ULK1 complex.[6]

- **Nucleation**. ULK1 complex activity triggers the formation of the Class III phosphatidylinositol 3-kinase (PtdIns3K) complex or vacuolar protein sorting 34 (VPS34) complex. It is a lipid kinase, which is integrated by VPS34 itself, BECLIN-1, VPS15 and ATG14L. Its components are phosphorylated by ULK1, which allows the

translocation of the complex to the phagophore. This translocation is driven by ATG14L.[7] There, the complex provides the cell with their enzymatic product, phosphatidylinositol 3-phosphate (PI3P). This allows the recruitment of lipid-binding proteins, which boosts phagophore growth.[6]

- **Elongation and closure**. Phagophore elongation needs the activity of two conjugation systems. ATG12 is activated by the E1 ubiquitin-activating enzyme, ATG7, and conjugated to ATG5 by the E2 ubiquitin-conjugating enzyme, ATG10. Then, ATG12-5 complex binds to ATG16L forming the ATG12-5-16L complex, which dimerizes and is bound to the membrane of the phagophore. For the formation of the second complex, the protease ATG4 cleaves light chain 3 (LC3) protein, now called LC3-I. ATG7 actives LC3-I and the E2 ubiquitin-conjugating enzyme ATG3 conjugates LC3-I to phosphatidylethanolamine (PE) to form LC3-II, with the assistance of ATG12-5-16L.[8] These two complexes together with ATG9-containing vesicles, which are thought to supply proteins and lipids to the autophagy membranes, promote phagophore elongation.[9] Subsequently, endosomal sorting complexes required for transport (ESCRT) proteins help closing the phagophore to form autophagosomes.[10]

- **Fusion**. The autophagosome becomes mature when ATG4 cleaves LC3 from its surface.[11] Then, it fuses with lysosome with the cooperation of three protein families: Rab GTPases, soluble NSF attachment receptors (SNAREs) and membrane-tethering complexes.[12]

- **Degradation**. After autolysosome formation, the inner autophagosome membrane and the cargo are available to be degraded by acidic lysosomal enzymes into basic building blocks, such as aminoacids, fatty acids and nucleotides. Then, the resulting products are recycled to the cytoplasm. However how this recycling step is taking place needs still further investigation.[13]

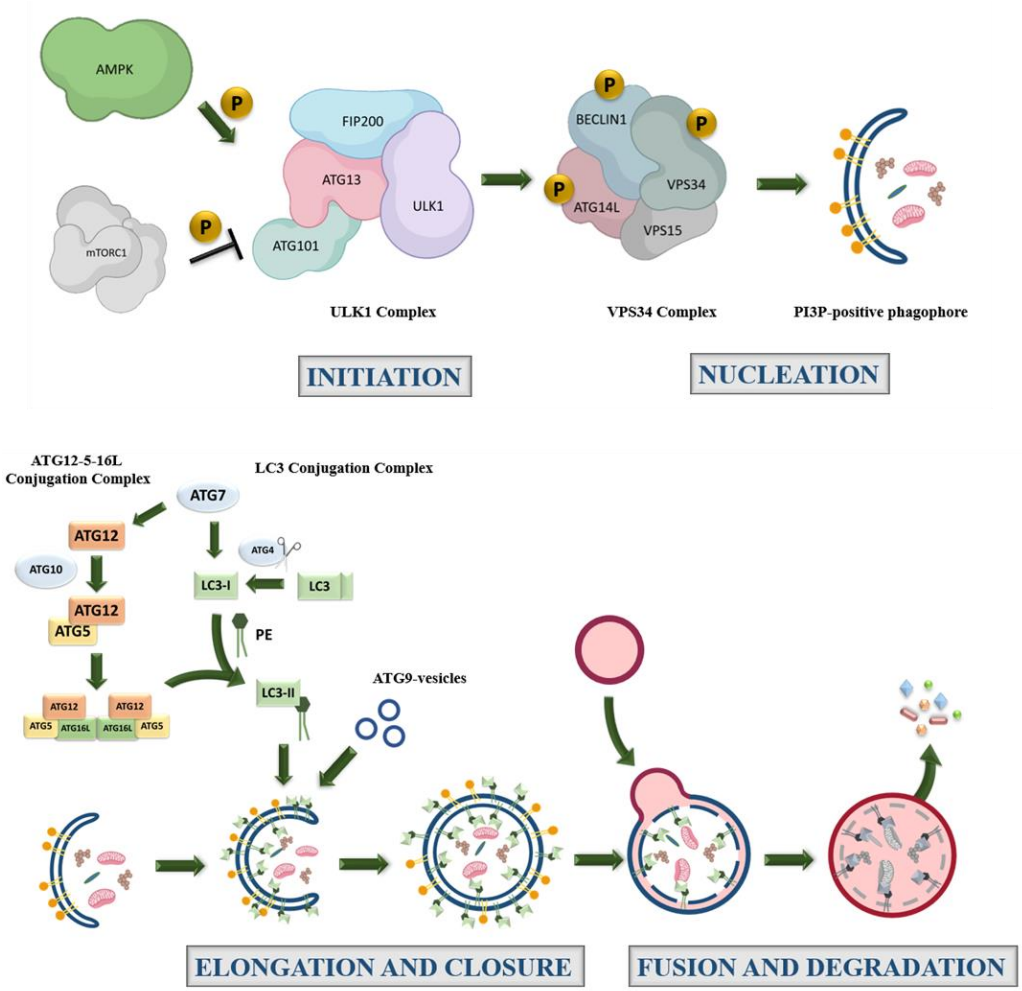

Figure 2. Phases of macroautophagy**.** Representation of macroautophagy process and key players involved in the different phases.

1.1.3 Autophagy Regulation

Autophagy is mainly regulated by post-translational modifications, which activate or inactivate key players of the process or allow them to interact with other partners.[14] In fact, autophagy is usually modulated mainly by the presence or absence of nutrients, which are detected by the already mentioned nutrient and energy sensors mTOR and AMPK. These two kinases regulate by phosphorylation the activity of ULK1, which in turn phosphorylates its substrates to enhance autophagy.[15] Besides, autophagy mRNA levels can also be regulated. The master regulator of autophagy gene transcription is the transcription factor EB (TFEB), which regulates not only autophagy genes, but also lysosomal biogenesis.[16] Its activity is also regulated by phosphorylation. In nutrient-rich conditions,

TFEB stays phosphorylated in the cytosol, but under several stress conditions, it translocates to the nucleus and allows the transcription of genes to enhance autophagy and lysosomal biogenesis.[17]

1.1.4 Autophagy in physiology

All the above-mentioned events allow autophagy to respond against different stress conditions, but it is also needed as a cellular quality control. Basal levels of autophagy are used to maintain cellular homeostasis by getting rid of protein aggregates or defective organelles that will be recycled, which will decrease reactive oxygen species (ROS) production. This is essential especially for post-mitotic cells, like neurons, due to their inability to dilute their aberrant cytoplasmic content by mitosis.[3]

Besides, autophagy plays a role in various physiological conditions, from development to aging. There is a basal autophagic level in oocytes, which is boosted when it is fertilized. Maternal content in the oocyte is degraded and new zygotic material is synthesized.[18] The next autophagic wave occurs at birth, when the newborn is not supplied by the placenta anymore and an increase in autophagy gives nutrients to the neonate during the transition to breastfeeding.[19] During post-natal development, autophagy also plays a role in erythrocyte maturation, in adipogenesis or immune cells differentiation and self-tolerance.[18]

Then, a decline in autophagy has been reported in aging in several organisms, in which there is a decrease in autophagy gene transcripts. Accumulation of autophagosomes and autolysosomes points out a deficit in autophagy and lysosome degradation, which disrupts cellular homeostasis.[20] The inability of degradation makes the cell to accumulate damage mitochondria or other defective organelles, increasing ROS production and heading to dysfunctional cells.[21]

1.1.5 Autophagy in pathology

As autophagy has a role in controlling cellular homeostasis, alterations in the pathway are implicated in several pathologies like cancer, immune diseases, or neurodegeneration.[22]

In cancer, autophagy can be a double-edged sword. On one hand, reduced autophagy leads to defective organelle accumulation, which induces cell stress, heading to cancer development.[23] In fact, expression levels of BECLIN-1 have been found to be low in several tumors, and its overexpression reduced tumor progression.[24] That is why autophagy could be considered as a cancer suppressor. On the other hand, tumors are under stressful and hypoxic conditions. Autophagy has been found to be upregulated in those situations to supply the tumor cells with nutrients and to be able to success in adverse environments.[25] So, in this case, autophagy could be considered as a tumor promoter. At the same time, it can have pro- or anti-metastatic roles.[23]

Like cancer, in cardiovascular diseases, the level of autophagy could be beneficial or detrimental. Basal levels are needed to avoid heart failure or to overcome a hypoxic situation during ischemia. But excessive autophagic activity could lead to cardiomyocyte death.[26]

In immunity, autophagy has several roles: (i) elimination of intracellular pathogens at different stages of infection,[27] (ii) control inflammation by suppressing inflammasome activation or degrading proinflammatory signaling factors,[28] (iii) antigen presentation[29] and lymphocyte homeostasis[30] and (iv) secretion of immune mediators.[31] In fact, mutations in autophagy-related genes are linked to Crohn's Disease, in which autophagy is defective, affecting its immunological roles.[32-33]

Lysosomal storage disorders (LSD) are also linked to autophagy. In LSD, lysosomes are defective and cannot degrade its content to be recycled, what accumulates autophagosomes, causing stress and leading to damage to different tissues, like brain.[34] In this group, there are several pathologies whose defects in the degradation steps produce cardiomyopathies, like Pompe or Danon disease.[35]

β-cells homeostasis and diabetes can also be regulated by autophagy. In an *Atg7*-deficient mouse model, a decrease in β-cell mass is related to an unbalance in glucose tolerance and less insulin secretion, which could culminate in diabetes development.[36]

The role of autophagy in neurodegeneration is extensively disclosed in Section 1.3.

The elucidation of the role of autophagy in these diseases highlights the importance of a correct balance in the process. Although there is still a big field to be explored, autophagy is nowadays the focus of attention of several clinical trials. Not only to increase the knowledge of its status in several pathological conditions, but also as a potential therapeutic target.[37-38]

1.1.6 Selective Autophagy

Autophagy was originally considered as a non-selective process, called bulk autophagy, in which some cytoplasmic content was recycled induced by the lack of nutrients. Now it is known to be also a selective autophagy pathway, responsible for the removal of specific cargo.[39] For that, the pathway needs specific receptors that recognize the cargo and link it to the autophagosome by a LC3-interacting region (LIR) motif.[40]

Depending on the nature of the cargo, selective autophagy can be classified in mitophagy (mitochondria degradation), aggrephagy (protein aggregates degradation), lipophagy (lipids degradation), nucleophagy (nucleus degradation) or xenophagy (pathogen degradation), among others.[41] Each specific cargo is recognized be certain receptors with a LIR motif. The list of cellular components that are removed by selective autophagy is still growing and the latest examples include for example the golgi apparatus.[42]

Like bulk autophagy, selective autophagy must be balanced to maintain cellular homeostasis, since dysregulations in the pathway are also related to pathological conditions.

1.2 Mitophagy

1.2.1 Mitochondria

Mitochondria are organelles composed of four different compartments: the outer membrane (OMM), the inner membrane (IMM), intermembrane space (IMS) and the matrix. They contain their own proteins that are mainly encoded by nuclear DNA, but they also contain their own DNA (mtDNA).[43]

They are considered as the powerhouse of the cell due to their cellular functions in energy production. Inside the mitochondria, it takes place the final oxidation of sugars, lipids, and proteins. They are all converted into Acetyl-CoA to enter the Kreb's cycle, which takes place in the matrix. In the case of proteins, some amino acids are converted into intermediates of the cycle. The Kreb's cycle consists in eight enzymatic steps after which, reducing agents, nicotinamide adenine dinucleotide (NADH) and flavin adenine dinucleotide ($FADH_2$) are produced. These two agents transfer electrons to the mitochondrial respiratory chain to start oxidative phosphorylation (Figure 3).[44]

In the mitochondrial respiratory chain, electrons move from the reducing agents to the respiratory complexes anchored in the IMM. This electron transport triggers a pumping of protons through the complexes from the matrix to the intermembrane space, which generates a potential difference that is used to synthetize ATP.[45]

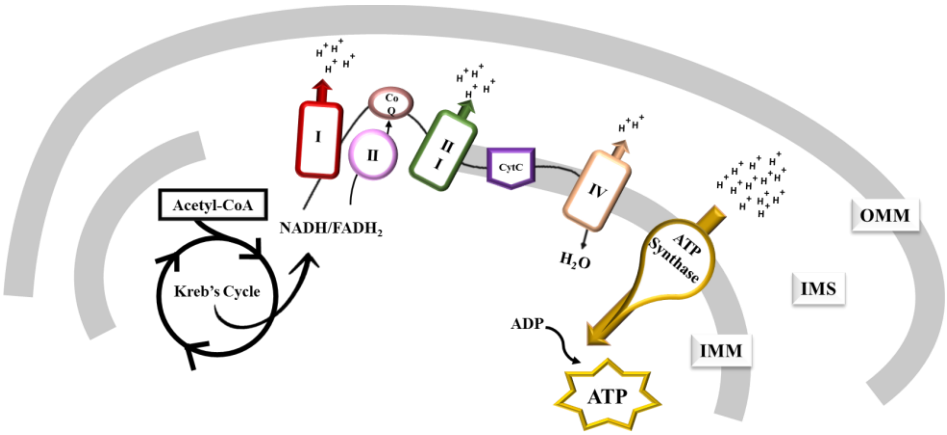

Figure 3. Oxidative Phosphorylation. Representation of oxidative phosphorylation.

Besides its energetic roles, mitochondria play important roles in Ca^{+2} signaling and iron homeostasis, apoptosis, and programmed cell death. Also, they are key players in carbon and nitrogen metabolism, and they are an important source of ROS, which is harmful to cells. So, an important ROS balance is needed to allow mitochondria to achieve completely their functions.[46]

1.2.2 Mitochondrial Quality Control

Mitochondria are highly dynamic and follow cycles of fusion and fission (Figure 4) that allow them to exchange materials among them and with other organelles, like endoplasmic reticulum or lysosomes.[47] This dynamic process is orchestrated by GTPases. The proteins called mitofusins 1 and 2 (MFN1/2) carry out outer membrane fusion, while optic atrophy 1 (OPA1) is in charge of inner membrane fusion.[48] Mitochondrial fission is arranged by dynamin-related protein 1 (DRP1), another GTPase that is present in the cytosol and is recruited to the mitochondria by the mitochondrial receptors fission protein 1 (FIS1) or mitochondrial fission factor (Mff), when the fission is produced.[47] Then, cells can get rid of those dysfunctional mitochondria by its selective degradation, mitophagy.[48]

However, as a decrease in mitochondrial mass is detrimental to cells due to the important roles they have, the degradation of these defective organelles must be counteracted with the generation of new mitochondria, a process known as mitochondrial biogenesis. Mitochondria cannot be synthetized *de novo*, so new mitochondrial components are integrated in pre-existing mitochondria.[49] When peroxisome proliferator co-activator 1 alpha (PGC1α), considered as the master regulator of mitochondrial biogenesis, becomes active, it in turn activates nuclear transcriptional factors, like nuclear respiratory factor 1/2 (NRF1/2). Next, NRF1/2 boosts the synthesis of mitochondrial proteins by nuclear DNA on one hand and TFAM expression on the other one, which is needed for mtDNA transcription. The former will be imported into the mitochondria through the translocases of the inner and outer membrane (TIM and TOM, respectively) complexes and guided to their final location by their mitochondrial targeting sequence. Finally, growing mitochondria fission to give rise to a new organelle.[50]

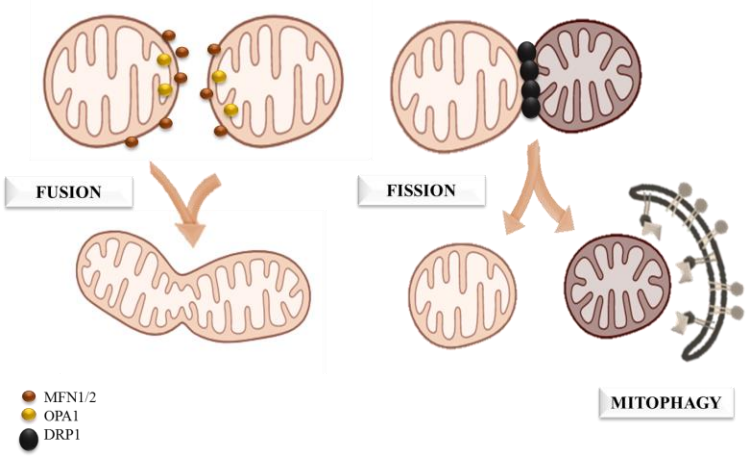

Figure 4. Mitochondrial dynamics. Representation of the cycles of mitochondrial fusion and fission as part of the mitochondrial quality control system. After fission, mitophagy get rid of defective mitochondria.

1.2.3 Mitophagy. General Aspects

Mitophagy is the selective degradation of mitochondria by autophagy. Although it follows the same process than bulk autophagy described in 1.1.2, some of the machinery differs. This will be explained in the following sections, in which we distinguish three types of mitophagy (Figure 5).

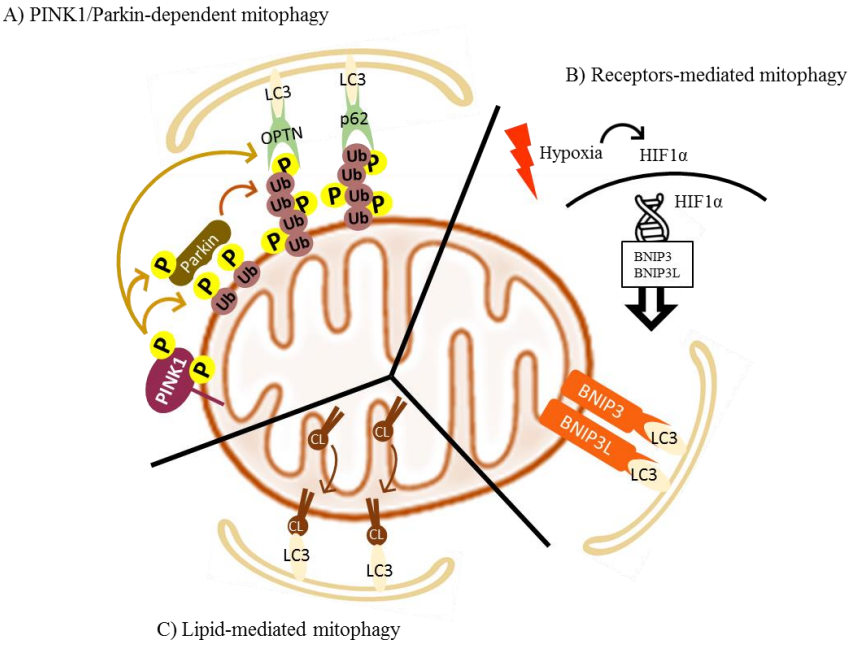

Figure 5. Types of mitophagy. Representation of the different types of mitophagy, based on the way the mitochondria are linked to the growing autophagosome.

1.2.4 PINK1/Parkin-dependent mitophagy

This is the most studied mitophagy pathway, and it is the responsible of the degradation of damaged mitochondria. In normal conditions, the kinase PINK1 is transferred to the IMM, where it is cleaved by proteases and degraded by the proteasome. But, if mitochondria are defective, the transfer of PINK1 to the IMM is blocked and it stays in the OMM, where it becomes active by autophosphorylation. Then, it phosphorylates ubiquitin residues in the mitochondrial surface and activates Parkin by the phosphorylation in Ser65, located in the ubiquitin domain.[51-52] Then, Parkin, an E3 ubiquitin ligase, is recruited to the mitochondria, where it ubiquitinates proteins in the surface of the mitochondria, which in turn are phosphorylated by PINK1. This creates phospho-ubiquitinated proteins chains that are recognized by autophagy adaptors, like p62, NDP52, OPTN, TAX1BP1 and NBR1 by their ubiquitin-binding domain. These adaptors count on a LIR motif that links the mitochondria to the autophagosome. In addition, TFEB is activated,[53] and ULK1 complex and ATG9 are recruited to the mitochondria by NDP52 and OPTN.[54] After, mitophagosome fuses with lysosomes, forming a mitolysosome, where the content is degraded.[55]

1.2.5 Receptors-mediated mitophagy

This mitophagy pathway relays on the ability of receptors of binding LC3 or GABA type A receptor-associated protein (GABARAP) in an ubiquitin-independent way. The most studied are the homologues BNIP3 and BNIP3L.

BNIP3 and BNIP3L are members of the pro-apoptotic mitochondrial protein family that are anchored in the surface of the mitochondria. Although their functions are cell death-related, recently, they were found to be involved in mitophagy. In hypoxic, conditions, HIF1α stabilization increases the expression of the proteins and their activity is enhanced by phosphorylation.[56-57]

1.2.6 Lipid-mediated mitophagy

As an alternative to these two pathways, mitophagy can be also mediated by lipids. Cardiolipin (CL) is a phospholipid mostly present in the IMM. Due to its characteristic structure (four acyl chains bound to a polar head), CL has key functions in mitochondrial

morphology, like in areas with high curvature,[58] and now it is known to be involved in mitophagy. Upon mitophagy stimuli or mitochondrial damage, CL externalized to the OMM, where it interacts with LC3.[59]

Another lipid that can mediate mitophagy is ceramide. It is a sphingolipid present in the cytosol and in the mitochondria. There, it can interact with LC3, connecting mitochondria to autophagosomes.[60]

1.2.7 Mitophagy in physiology and pathology

As the powerhouse of the cell, mitochondria levels should be maintained in quality and quantity enough for their proper functioning. That is why mitophagy plays a key role in mitochondrial quality control, getting rid of damaged mitochondria.

During development, paternal mitochondria are removed by mitophagy and only the maternal ones are inherited. This process takes place via Parkin.[61] In erythroid differentiation, mitophagy is the responsible of mitochondria removal, which is known to depend on BNIP3L-mediated mitophagy. At the same time, mitophagy also participates in cell programming or immunity. It allows a metabolic shift from glycolysis to oxidative phosphorylation, needed during myoblast differentiation and it reduces inflammasome activation in case of infections.[62] The opposite shift, towards glycolysis, is seen during retinal ganglion cells differentiation driven by BNIP3L-mediated mitophagy.[63]

Defects in mitophagy are clearly linked to pathological conditions, mainly aged-related or neurodegenerative diseases, which will be further discussed in the following section.

Swollen mitochondria, as well as inhibited mitophagy have been described in non-alcoholic fatty liver disease patients. On the contrary, smaller mitochondria were found in type 2 diabetes patients and obese people, due to an increase in mitochondrial fission, although it is not translated into mitophagy induction. Defects in mitophagy have been also described in cardiovascular diseases, like atherosclerosis or in heart failure, where patients presented low levels of PINK1. And in cancer, receptor-mediated mitophagy allows the cells to survive in hypoxic conditions by facilitating the metabolic switch.[64]

As in the case of bulk autophagy, the importance of mitophagy in pathology is having more relevance nowadays. This is boosting the discovery of new pharmacological tools to modulate mitophagy for the treatment of those conditions.

1.3 Autophagy and mitophagy in neurodegenerative diseases

Life expectancy is rising worldwide, which is increasing the incidence of age-related pathologies, like neurodegeneration. Neurodegenerative diseases include a group of pathologies characterized by the progressive death of neurons, causing nervous system degeneration.

Although they differ in the type of neuron and brain region affected, they have several hallmarks in common. In general, neurodegenerative diseases manifest i) protein aggregates, due to errors in the protein quality control, ii) propagation and prion-like manifestations of the aggregates, iii) stress granules formation in combination with protein aggregates, iv) defects in the autophagy pathway and v) aberrant mitochondrial homeostasis (Figure 6).[65]

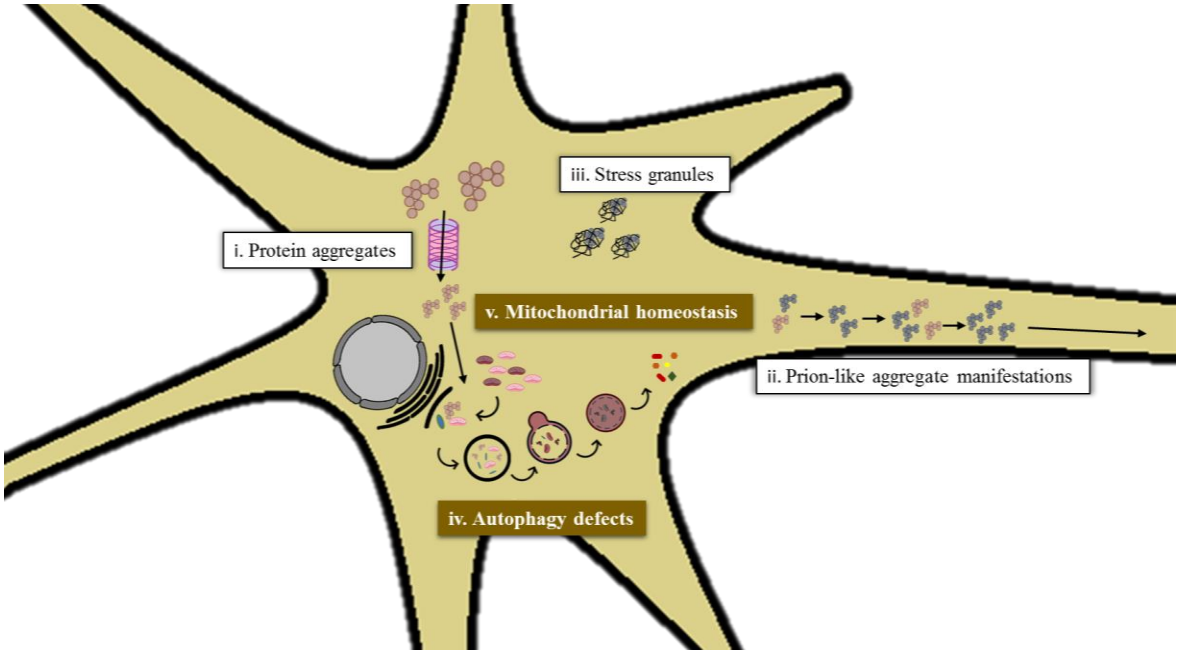

Figure 6. Neurodegeneration hallmarks. Representation of the most common pathological features in neurodegenerative diseases. Modified from Ref [65].

There are several models in which key autophagy genes are knockout to understand the link between autophagy and neuronal death. Studies in *Drosophila* showed that genetic ablation of genes like, *Atg7*, *Atg5*, *Ulk1* or *Fip200*, among others, fall into neurodegeneration.[66] In mice, knockout of *Atg7*[67] or *Atg5*[68] genes in central nervous system, leaded to neurodegenerative manifestations by behavioral disorder, neuronal cell death and accumulation of ubiquitinated proteins. Moreover, overexpression of autophagy genes, like *Ampk* or *Atg8a*, in *Drosophila* or *Atg5* in mice, not only induces autophagy, but extends lifespan.[69]

An overview of the stage of autophagy and mitophagy in neurodegenerative diseases are exposed below.

1.3.1 Parkinson's disease

Parkinson's disease (PD) appears between the ages of 55 and 65 years, being 10% of the cases familial and 90% sporadic. It is characterized by the loss of dopaminergic neurons in the *substantia nigra* and the accumulation of aggregates of α-synuclein forming Lewy bodies.[70] This neuronal death causes a motor symptomatology, characterized by bradykinesia, rest tremor or rigidity.[71]

Studies done in post-mortem brains showed defects in autophagy and mitophagy pathway, colocalization of LC3 with α-synuclein, mitochondria accumulation in autophagosomes in neurons,[72] as well as low levels of lysosomal activity,[73] In fact, in a 1-methyl-4-phenyl-1,2,3,6-tetrahydropyridine (MPTP) mouse model mimicking PD, lysosomal depletion occurred before autophagosome accumulation in dopaminergic neurons.[74]

In a *Drosophila* model, α-synuclein overexpression hinders autophagy flux and leaded to autophagy protein accumulation. Moreover, some Parkinson-related mutations are found in genes with a key role in mitophagy, like *PINK1* and *PARKIN2*, encoding for PINK1 and Parkin. The inability of Parkin to ubiquitinate mitochondria reduces their recognition by autophagy receptors. So, this pathway is being extensively studied. Moreover, α-synuclein degradation depends on Parkin and mitochondrial fission, so when Parkin is reduced, α-synuclein is not degraded and impairs mitochondrial function.[64]

Other autophagy-related PD mutations are found in the genes *PARK8,* which codifies the leucine rich repeat kinase 2 (LRRK2) or *GBA-1* (GBA-1). Mutations in LRRK2 are the most common genetic risk factor in PD. The kinase, which also presents a GTPase domain in its structure, has functions related to vesicle trafficking, so it is not surprising to think that defects in its role involve autophagy impairment.[75] LRRK2 knock-out mice, LRRK2 knock-in mice with a mutation in G2019S (in the kinase domain) and WT mice expressing the mitoQC (to study mitophagy) or autoQC (to study autophagy) reporter were generated. While no changes in autophagy were observed, mitophagy was induced in MEFs when LRRK2 was knock-out and was reduced when LRRK2 was knock-in.[76] However, data from patients with a mutation in R1441G in the GTPase domain reflected an increase in autophagy and mitophagy markers.[77] This manifests the controversy of the role of LRRK2 in autophagy. GBA1 is a lysosomal enzyme involved in sphingolipids metabolism. As proper lysosomal function is needed during the autophagic process, mutations in a lysosomal gene interrupt the process.[73]

Since the 1960s until now, levodopa is the most effective treatment for PD patients, although its chronic administration can trigger dyskinesia (involuntary movements).[78] Autophagy modulation by levodopa has been studied in a 6-hydroxydopamine (6-OHDA)-induced PD mice model. After the treatment, mTORC1 was activated in association with increased levels of p62 in the striatum, indicating impairment in autophagy. The co-treatment with rapamycin, an mTORC1 inhibitor, prevents autophagy impairment and reduced levodopa-induced dyskinesia.[79]

These data suggest that autophagy enhancers could be a promising chemical tool to restore the impairment of autophagy found in the pathology, and the one induced by the treatment with levodopa.

1.3.2 Alzheimer's disease

Alzheimer's disease (AD) is the most common form of dementia, characterized by the progressive reduction of cholinergic neurons, which triggers loss of memory and deficiency in cognitive functions. Many of the cases are sporadic, and aging is the main risk factor.

One of its hallmarks is the deposition of extracellular plaques of β-amyloid (Aβ) and intraneuronal tau neurofibrillary tangles.[80]

An increase in the activity of the endosomal-lysosomal system has been reported at early states of the disease, which becomes defective as AD progresses. As late endosomes fuse with autophagosomes, this defective process leads to the accumulation of autophagic vacuoles, which interestingly are rich in presenilin 1 (PS1), a key player in Aβ generation.[81]

In fact, the APPS/PS1 is a mouse model widely used in AD field, due to their prone of amyloid plaque formation.[82] As lysosomes are reported to be defective in AD, this model has been injected with adeno-associated virus particles (AAV8) encoding a cytomegalovirus promoter-driven construct to transduce TFEB in the hippocampus to study lysosomal activity enhancement to reduce Aβ production. TFEB transduction promoted a reduction in amyloid precursor protein (APP) accumulation, as well as Aβ in the interstitial fluid, and in consequence, a decrease in extracellular amyloid plaques.[83]

The same APP/PS1 mouse model was crossed with CAG-mRFP-GFP-LC3 transgenic mice, to study autophagy and there was reported an increase in the number of autophagosomes compared to littermate at different stages of the disease in the hippocampus. However, the number of autolysosomes decreased with the progression of AD, indicating the blocking of the fusion between autophagosomes and lysosomes.[84]

Autophagy was also studied in another amyloid mouse model with five AD-linked mutations (5xFAD mouse) crossed with an autophagy-induced mouse model (*Becn1*$^{FA/FA}$). A decrease in soluble and insoluble Aβ in the brain of these mice was confirmed by dot blot assay, ELISA, and microscopy.[85]

Moreover, Aβ was showed to interact with DRP1 in postmortem brains from AD patients and primary neurons from AD mouse models (Tg2576 and APP/PS1), suggesting an abnormal balance in mitochondrial dynamics.[86] The same group confirmed later an increase in mitochondrial fission proteins (FIS1, DRP1) in hippocampal tissues, while mitochondrial fusion proteins (MFN1/2, OPA1), mitochondrial biogenesis proteins (PGC1α, TFAM), and autophagy and mitophagy proteins (ATG5, LC3-II, PINK1) were decreased.[87]

One could think of boosting autophagy and mitophagy to treat AD, however, as a block in the fusion between autophagosomes and lysosomes are reported, an excessive increase in autophagy could be detrimental. So other strategies, like lysosome activity enhancement should be considered.

Despite the big efforts done to find a disease-modifying treatment to target Aβ and tau proteins aggregates, current treatments for AD patients only slow down the progression but they do not restore cognitive functions. Inhibitors of acetylcholinesterase, like donepezil, rivastigmine or galantamine, or *N*-methyl-D-aspartate receptor (NMDA) antagonist, like memantine, are the most used.[88] The neuroblastoma cell line SH-SY5Y was treated with galantamine, revealing an increase in proteins involved in different phases of the autophagic process, as well as mitophagy-related proteins.[89] In an AD cellular model, PI3K/AKT/mTOR signaling pathway was inhibited, which resulted in autophagy increased. This condition was reversed by the inhibition of NMDA receptors with memantine.[90] However, in a recent work, memantine increased autophagy and Parkin-independent mitophagy.[91]

Thus, there is still a gap of information about basal levels of autophagy/mitophagy in AD, as well as the correct modulation of this condition.

1.3.3 Amyotrophic Lateral Sclerosis

Amyotrophic lateral sclerosis (ALS) is a devastating disease caused by the death of both upper and lower motoneurons (MN). Like other neurodegenerative diseases, ALS is predominantly sporadic, and only a small percentage is caused by mutations in several genes, some of them, like *SQSTM1* (encoding p62), *OPTN* or *TBK1*, are related to autophagy or mitophagy.[92]

Around 97% of patients, sporadic or familial, present protein aggregates of TAR DNA-binding protein 43 (TDP-43), which accumulates in the cytoplasm with post-translational modifications.[93] Other kind of aggregates are found in patients, like aggregates of superoxide dismutase 1 (SOD1) or fused in sarcoma protein (FUS).[94]

Nowadays, there are only two drugs approved for the treatment of ALS, which increase life expectancy several months, but they do not cure the disease. Rilutek® (riluzol) was approved in 1995 by the U.S. Food and Drug Administration (FDA). It is a benzothiazole derivative that decreases excitotoxicity caused by glutamate. It is also used for the treatment of pancreatic cancer, where it has been reported to reduce autophagy.[95] The second one, approved in Japan in 2015 and by the FDA in 2017, is edaravone. It has antioxidant properties, although the mechanism of action remains unknown.[96] Similar to riluzol, edaravone seems to inhibit autophagy in neurons after oxygen-glucose deprivation,[97] and in an *in vivo* model of cerebral ischemia.[98]

Although there is a lack of studies done to establish the modulation of autophagy/mitophagy by these two drugs in ALS, there is increasing and controversial information regarding the level of autophagy/mitophagy in the disease.

One of the most studied ALS mouse models is hSOD1^{G93A} mouse. mTOR low levels were detected in this model, as well as an increase in LC3 turnover in MN cell cultures expressing SOD1^{G93A} and in spinal cords of SOD1^{G93A} mice.[99] This indicates that autophagy is increased. But this model showed defective mitochondrial morphology,[100] as well as defects in mitochondrial axonal retrograde transport, which occurs only in MN.[101] In addition, autophagy cargo accumulation reported defects in lysosomal degradation, indicating a block in autophagy flux.[102] Other work done in the same model reported enhanced mitophagy at early stages of the disease and a survival increased with *PARKIN* depletion.[103]

However, the upregulation of autophagy in this model has controversial results. On one hand, the treatment with trehalose increased lifespan and improved the symptoms, only during the first stages of the disease.[104] Conversely, rapamycin worsened MN loss.[105] Interestingly, autophagy inhibition protected from MN loss and from detrimental accumulation of autophagosomes.[106] In other ALS models, rapamycin ameliorates the disease in a TDP-43 mouse, but in TDP-43 *Drosophila* model, the condition was worsened, and autophagy inhibition ameliorate it.[107]

Moreover, as it is well reviewed in Madruga *et al*., when autophagy or mitophagy is deleted in these mice, there is an early onset of the disease, but survival is extended.

Authors argued that this survival increase is due the role of glial cells in neuro-inflammation.[108]

These data highlight the complexity of this pathology, as well as the large amount of information that is lacking. Thus, it provides the opportunity to continue exploring the role of autophagy/mitophagy in ALS from a basic to a translational approach perspective.

1.3.4 Other neurodegenerative diseases and aging

Although aging is not a neurodegenerative disease, most of them are related to lifespan increase. So, the study of autophagy during aging could be very useful to understand the process during neurodegeneration. In fact, autophagy decline is seen during aging, and there are evidence of aging delay and lifespan prolongation by autophagy induction.[109] In a recent work done in an aging model, memory, synaptic plasticity as well as autophagy were compromised compared to control. The treatment with spermidine, spermine and rapamycin, compounds described to increase autophagy, restored brain aging.[110]

Similarly, the treatment of eighteen month-old male C57BL6/J mice for ten days with metformin**,** which has shown to increase autophagy[111] and lifespan in mice,[112] improved cognitive function, as well as reduced neuro-inflammation.[113]

Huntington's disease (HD) is a neurodegenerative disease caused by a mutation in a gene, whose protein product is degraded by autophagy. In a mouse model in which the disease was induced by the striatal injection of mutant huntingtin, autophagy was induced at the early time point (ten days). After three weeks, time enough for mutant huntingtin to aggregate, autophagy was blocked. The genetic overexpression of *Tfeb* or *Beclin1* could modulate autophagy, but they could not rescue HD phenotype at the late stage. However, at early time point, *Beclin1* overexpression could reduce aggregates.[114] This highlights the complexity of autophagy through different stages of the diseases, and the deeply study to determine the therapy. In a previous work, rilmenidine, an antihypertensive agent, was used as a treatment for a HD mouse model, obtaining a reduction in the pathology signs and mutant huntingtin.[115]

Protein aggregates have been detected in the brains of multiple sclerosis (MS) patients,[116] as well as in experimental autoimmune encephalomyelitis (EAE) mouse, an *in vivo* model to study MS. In fact, this model showed a decreased in LC3-II/LC3-I ratio.[117] In a similar mouse model, autophagy flux in spinal cords was impaired compare to control, and the protein levels of BECLIN1 and p62 were reduced, which was restored by the treatment with rapamycin. Nevertheless, as different cell types participate in the pathobiology of MS, autophagy enhancement appeared to be beneficial in neurons and glia cells, but detrimental in immune cells, which play an important role in the development of the disease.[118]

1.3.5 Autophagy/mitophagy modulators in clinical trials for neurodegeneration

As autophagy appears as a neuroprotective and anti-aging mechanism, its enhancement has been studied not only *in vitro* and *in vivo* but also in clinical trials. The current autophagy modulators in clinical trials ongoing to treat neurodegeneration and aging and their structures are summarized in Table 1 and Figure 7.

Table 1. Autophagy inducers in clinical trials

Condition	Autophagy modulator	Study phase	CT id.
ALS	Rapamycin Colchicine Tamoxifen	II II I/II	NCT03359538 NCT03693781 NCT02166944
AD	Rapamycin	II	NCT04629495
HD	Rilmenidine	II	EudraCT number 2009-018119-14
Subjective cognitive decline	Spermidine	II	NCT02755246
Amnestic mild cognitive impairment	Metformin	II	NCT00620191
Aging	Metformin	IV III	NCT02432287 NCT03309007

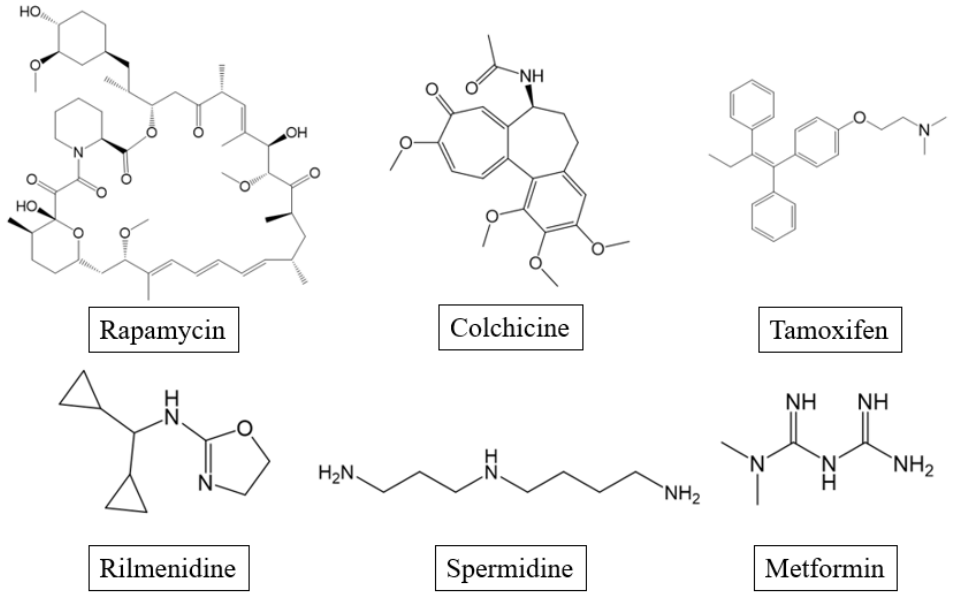

Figure 7. Chemical structure of selected autophagy modulators in clinical trials.

1.4 Tools to study autophagy and mitophagy

In 1993 Yoshinori Ohsumi described the first genes related to autophagy[119] and later, in 2016, he was awarded with the Nobel Prize in Physiology or Medicine for his discoveries in autophagy. Thus, during the last twenty years, when selective autophagy of mitochondria, mitophagy, was also described, there has been a great interest in the autophagic field, clearly seen by the increase in the number of published papers (Figure 8).

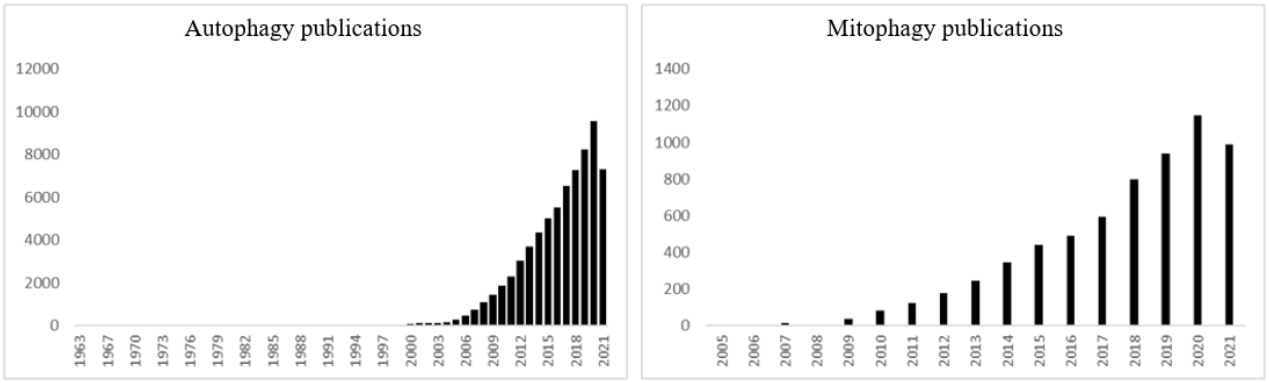

Figure 8. Number of articles published in the autophagy field. Graph representation of the increasing number of autophagy-related papers since the early 60s and mitophagy related papers since 2005.[120]

As autophagy is a dynamic and complex process, there is an urgent need to unify concepts and the tools to monitor the pathway. Since 2008, Daniel Klionsky has joined the knowledge of the experts in the field to develop a Guideline for the use and interpretation of assays for monitoring autophagy. In 2021, the fourth edition has been released,[121] and it has been used to summarize several techniques to monitor autophagy, which is disclosed below:

- **Transmission Electron Microscopy (TEM).** With TEM, autophagic structure morphology can be studied in high quality. It can distinguish between bulk autophagy or selective autophagy based on the nature of the cargo. However, this technique is time-consuming and needs expert personnel in the skill and in the autophagy field.

- **LC3-family protein (WB, GFP-ATG8).** LC3 is the most extensively used protein to study autophagy, and there are several techniques based in this protein to monitor it.
    - Western Blot. When autophagy is induced, LC3-I is lipidated to obtain LC3-II, which is the autophagosome marker. However, an increase in LC3-II is not always indicative of autophagy activation, as LC3-II degradation can be very fast. To ensure autophagy activation or inhibition, 'autophagy flux' is determined. An increase in autophagy is considered if LC3-II is accumulated in the presence of an inhibitor. These can be protease inhibitors (leupeptine) or compounds that neutralize lysosomal pH (NH_4Cl, bafilomycin or chloroquine). The last ones also block the fusion between autophagosome and lysosome.

    - Fluorescence microscopy. Autophagosome formation can be monitored by fluorescence microscopy by LC3 coupled with GFP. GFP fluorescent is sensitive to acidic environments, like lysosomes. So, an increase in GFP-LC3 fluorescence over time can suggest a block in the fusion, and a decrease in the signal denotes the proper degradation of the protein. Again, to confirm it, autophagy inhibitors should be used.

- **Tandem fluorescence reporter.** To improve fluorescent microscopy-based assays to study autophagy flux, new assays have been developed. They are based on the

conjugation of LC3 to two fluorescent proteins. GFP, which has been already mentioned to be pH sensitive and mCherry or RFP, which is more stable. Colocalization of both fluorophores, seen in yellow, identifies autophagosomes and red only puncta distinguish autolysosomes. Interestingly, this tandem can be used to monitor mitophagy, if conjugated to a mitochondrial protein.

- **Flow cytometry**. Like fluorescent microscopy, both, GFP-LC3 or tandem-LC3 can be monitored by flow cytometry.

- **Immunofluorescent staining.** Immunodetection of autophagy and mitophagy related proteins are also used to monitor the processes. Again, LC3 is the standard gold, but in some tissues LC3 can be localized in other organelles besides autophagosomes. So, other proteins can be monitored.

- **p62.** p62 and cargo targeted by p62 are incorporated in the autophagosome and degraded in the autolysosome. So, p62 is considered as a surrogate for autophagy flux. When autophagy is blocked, p62 accumulates. The level of p62 is usually measured by western blot or by immunofluorescent. Simultaneously the mRNA levels of p62 should be assessed as this protein in tightly regulated at the translational level.

The tools used in this project were Western Blot, tandem fluorescent reporter to study both autophagy and mitophagy, and immunodetection of autophagy and mitophagy related proteins.

1.5 Drug discovery and development

Now that we are aware of the lack of autophagy/mitophagy modulators to treat neurodegenerative diseases and the tools to study the modulation of the pathway, the next step is to be conscious of the challenging process of drug discovery and development, which is explained in the following sections.

1.5.1 Drug discovery and development. Process

Drug development is a time-consuming and expensive process that needs at least 15 years and more than one and a half million euros.[122] Only 10% of the drugs that start the process end up in the market. Failure is usually related to undesirable ADME effects or toxicity.[123]

Drug development includes early drug discovery, preclinical and clinical studies, and approval for commercialization (Figure 9).

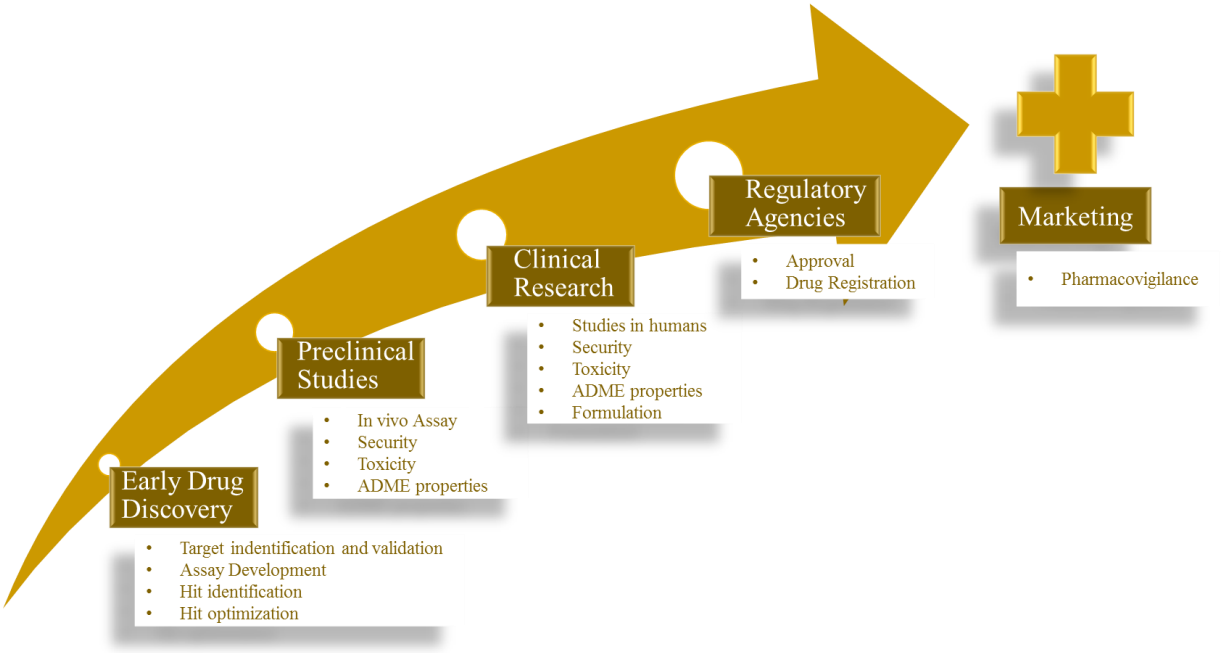

Figure 9. Scheme of phases in drug discovery and development process.

The first steps have been the scope of this project and it can be divided in several phases:

- **Target identification**. A target is considered any biological entity that can be modulated by a drug (druggable). The identification can be done by several routes, like searching in publications, measuring its protein or mRNA levels, among others.[124] Among all the possible targets, protein kinases are being exetensively study, as they have been found altered en diverse pathological conditions.[125]

- **Target validation.** Once the target is identified, it must be validated. Again, there are several methods for that purpose. For example, classical genetics using different tools widely used such as antisense oligonucleotides, which block the synthesis of the desired protein. However, the use of these tools *in vivo* is limiting, due to low bioavailability and toxicity. Another validation tool is the use of transgenic animals, where the gene expressing the desired target may be knock-out or over-expressed, but their use is expensive, time-consuming, and due to ethical rules, the animal use in research should be reduced being limited to exceptional cases. More recently, with the development of biological chemistry, a new strategy to identify and validate a target has emerged. This is chemical genetics.[124]

  Chemical genetics is defined as the use of small molecules and/or chemical probes, to perturb a biological system to explore the outcome. Its analogue term, classical genetics studies protein function by mutations in genes. Here, the chemical probes are used to study the function of a desired protein. Although they are complementary, the use of small molecules is faster and reversible, and the activity of the target can be differently modulated varying the concentration of the drug.[126] Interestingly, chemical genetics can be carried out with chemical tools with the sole objective of validating the target. In that case, pharmacokinetic properties of the probes are less severe. However, if small molecules are also used with the final aim of turning into a drug candidate, then, more requirements in the following steps of the process must be fulfilled.[127]

  There are two approaches in chemical genetics to identify the small molecules (Figure 10):

  - Direct chemical genetics. This approach is selected when the target is not known. Thus, the hits are identified from a chemical library in a phenotypic assay, which can be done in different cellular and/or animal models. Compounds able to modulate the phenotype are selected to be further

studied. The next step is target deconvolution for each of these compounds resulting in target identification.

- Reverse chemical genetics. This strategy is used when the target is known. In that case, the library of compounds is usually screened against the target to determine protein activity. The most effective compounds can be further validated in a phenotypic assay selecting, in that way, the desired molecular tools.

- **Hit identification and optimization.** A hit is considered any molecule with activity in a biological screening. To identify new hits, there are several approaches. Among them, high throughput screening (HTS) is one of the most used and allows the testing of thousands to million molecules in 384-well or 1536-well plates. It needs automated equipment, which is expensive but affordable for the pharmaceutical industry. Academics usually work with a smaller set of compounds in 96-well or 384-well plates.

  To identify hits among a library of compounds, those are tested in assays that allow the study of the biological activity of the compounds against the drug target and/or in a phenotypic assay that modulates the desired property. These screens can be simple biochemical-based assays (such as kinase assays) or a more complex one such as cellular-based assays.[128]

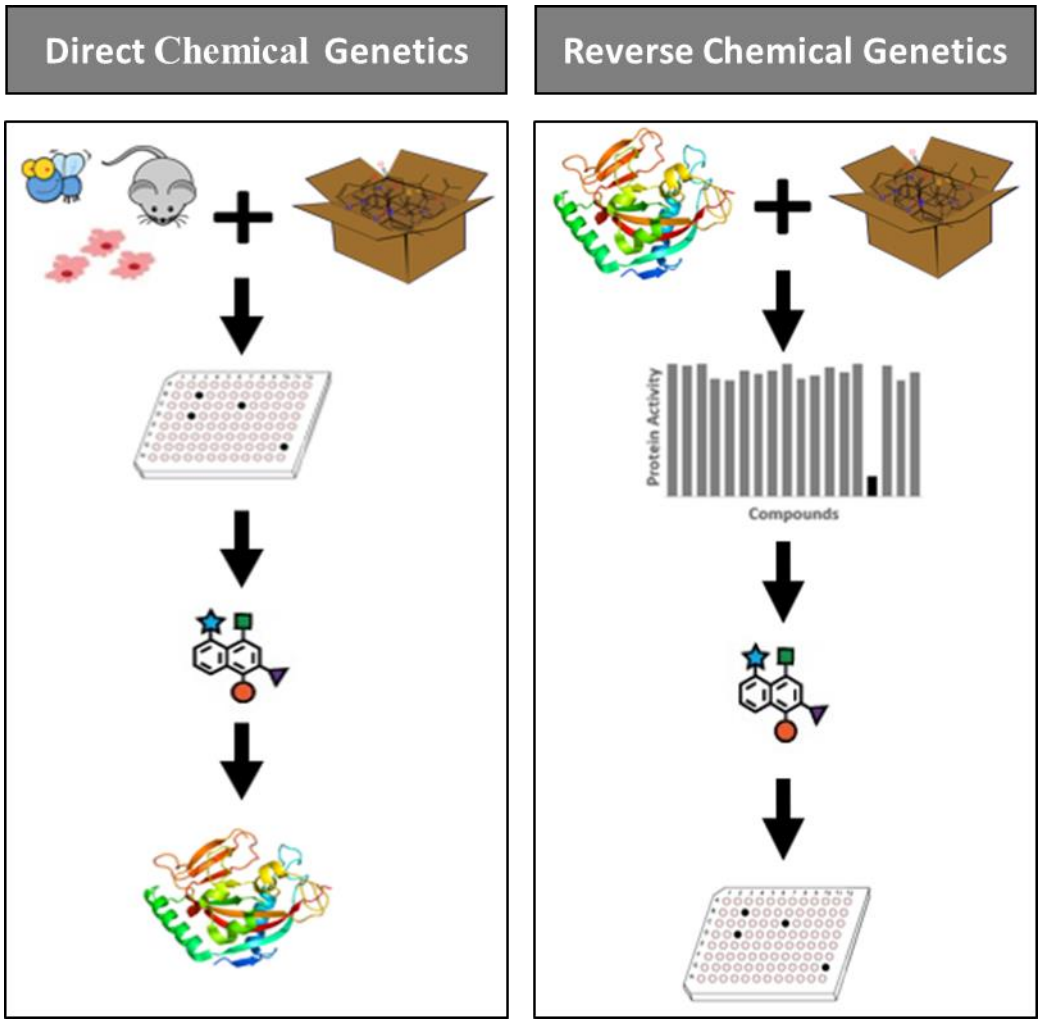

Figure 10. Types of chemical genetics. General workflow of the two strategies in chemical genetics: direct and reverse.

Once hits are identified, they are usually tested in a dose-response curve in the primary assay. With that, the maximal activity of the hits can be obtained to compare their potency. Afterwards and with the aim to optimize the hit, cluster of compounds with similar structure or with the same chemical motif are identified or synthetize for establish structure–activity relationship (SAR) studies. Thus, the chemical features responsible for the activity against the drug target can be distinguished and identified a lead.

Next, leads are tested for ADME (absorption, distribution, metabolism. and excretion) properties as well as physicochemical and pharmacokinetic measurements. In addition, to avoid off-targets effects, for instance in kinase

targeting, the hits can be tested in an *in vitro* kinase assay against a big panel of different kinases to determine their selectivity.[124]

Last, the most promising compounds will be tested in preclinical models to evaluate the security and toxicity of the drug in animals before moving on clinical trials with humans. Clinical trials are divided in four phases, with increasing number of participants to identify the correct dose, ADME properties, security, or off-targets effects before being approved by the pharmaceutical regulatory agencies for marketing. Once in the market, the last phase (pharmacovigilance) controls the drug in real society to identify adverse events not known to date.[129]

1.5.2 Drug discovery to target protein kinases

Protein kinases are responsible of phosphorylating residues of serine, threonine or tysorine in proteins. They are found in important cellular processes, like proliferation, apoptosis, and other cell signaling pathways. Dysregulation on these proteins have been reported in several pathologies, including neurodegenerative diseases. Thus, they have become a perfect target to develop a drug discovery program in order to find compounds to modulate them.[130-131] In fact, in December 2021 there were 68 protein kinase inhibitors approved by the FDA, most of them for oncology therapy.[132]

In autophagy and mitophagy we can distinguish different serine/threonine kinases, like mTOR, AMPK and ULK1, or PINK1 in the case of mitophagy, which orchestrate the initiation of autophagy. New kinases are being investigated nowadays and their relation to autophagy or mitophagy is under study. This is the case of serum- and glucocorticoid-induced kinase 1 (SGK1), a protein involved in channel regulation, with new roles in the autophagy process.[133] It was considered as a negative regulator of autophagy, as it interacts and activates mTOR.[134] However, recently its inhibition has been described to inhibit autophagy.[135] Interestingly, it has been reported to be upregulated in neurodegenerative diseases. Thus, its possible role in autophagy and mitophagy and in neurodegeneration makes it a perfect target to find new inhibitors in order to restore those pathological conditions in which the kinase is altered.

1.5.3 Drug discovery in Neurodegeneration

As we have already mentioned, neurodegenerative diseases are everyday more prevalent in the society due to lifespan increase. In all these pathologies an effective treatment does not exist. Moreover, there is a lack of biomarkers during early stages of the diseases which difficult the outcomes from clinical trials. When neuroprotective agents are given to patients, a big number of neurons are already lost. In addition, the amount of information underlying the pathophysiology of the disease is still missing,[136] and the animal models do not recapitulate all the features of the pathology, which explains the number of drugs that fail during the *in vivo* phase.[137] In fact, due to their complexity, scientists are designing drugs that act in parallel over several targets. This is the case of AD, in which multitarget directed ligands have been synthetized to target several proteins responsible of different mechanisms involved in the development of the disease.[138]

Crossing the blood-brain barrier (BBB) is another challenge for central nervous system therapies market. BBB is a protective barrier that divides peripheral blood circulation from neuronal tissue. However, this protective barrier prevents the entrance of large molecules and around 98% of small molecules. Moreover, development periods as well as regulatory approval are longer and more expensive.[137]

So, as population ages, pharmaceutical companies and academia are getting over these challenges by mimicking better the microenvironment and pathophysiology of the disease. For that, improvements at the technical level are done, for instance with 3D cultures, but also with the help of computational tools which will decrease the time and the cost of the development periods.

1.5.4 Computational tools in drug discovery

As mentioned, HTS needs the testing of huge volume of compounds, after which some of them will be selected as hits and optimized to become more efficient. However, the rate of success is very low. With the introduction of computational tools in the field, compounds predicted to be inactive will be removed from the list, maintaining only the most favourable ones. With that, both time and price are reduced.

Depending on the starting information, computational tools can be divided in ligand-based drug discovery (LBDD) or structure-based drug discovery (SBDD).

In LBDD, there is no or little information of the target, so it is based on ligands with a known biological activity. One of the methods that are used in LBDD is the selection of compounds based on similarity to the reference ones. In general terms, similarity can be studied by comparing chemical structures by fingerprints or physicochemical properties. Fingerprints are a binary representation that describes the presence or absence of a determine fragment or descriptor. It is used when the objective is to find active compounds with similar structure. However, if the goal is to discover compounds with the same biological activity but with new chemical structure, physicochemical properties are more convenient. Predictions of these features can be simple, like molecular weight or the number of hydrogen bond donor. But they become more complex when comparing polarity or solubility.[139]

In SBDD, the first step is to identify the target to modulate. It must be involved in the pathology or pathway of interest; it must be druggable and it is important to have the crystal structure of the target (available in Protein Data Bank (PDB))[140]. However, if the crystal lacks, the structure can be obtained by homology modeling comparing the sequence of the target with the sequence of related proteins.

One of the most used techniques of SBDD is virtual screening. It consists in several steps by which big chemical libraries can be filtered based on different predictive parameters in order to reduce the number of compounds tested in a biological assay. Those filters can be physicochemical properties, drug-like properties or based on molecular docking.

Molecular docking studies the interactions of the ligands with the target in a determined spatial region in the structure of the protein, known as grid. It uses algorithms to determine different ligand poses in the grid and score them based on the predictive affinity of the ligand for the target (docking score). Thus, a classification of the best poses is obtained to select the best one for further biological studies.[141]

Hence, molecular modelling is an interesting field with more presence in drug discovery as computational capacity is also growing. In addition, there are many other techniques in the area, including molecular dynamics, machine learning or artificial intelligence.

2. HYPOTHESIS AND OBJECTIVES

One of the features of **neurodegenerative diseases** is a defect in the **autophagic pathway** and detrimental **mitochondrial homeostasis**. So, the hypothesis of this PhD project is that the **modulation** of the selective autophagy of mitochondria, **mitophagy,** is a potential **target** for the treatment of neurodegenerative pathologies.

Thus, the main objective of this PhD is the **discovery of small molecules able to modulate mitophagy** and the study of their therapeutic applicability in different neurodegenerative disease models. Both direct and reverse chemical genetics approaches will be followed to achieve this task.

Specific goals are the following:

1. Set up of mitophagy phenotypic assay and medium throughput screening of compounds
2. Characterization and therapeutic potential of mitophagy enhancers
3. Characterization and therapeutic potential of mitophagy inhibitor
4. Inhibitors of SGK1 as a promising tool to restore mitochondrial homeostasis in neurodegenerative diseases

3. MATERIALS AND METHODS

3.1 Compound preparation

All the compounds were prepared with a stock concentration of 25 or 10 mM in DMSO. The final % of DMSO in cell culture was not higher than 0.1%. Bafylomycin A1 (Baf1), carbonyl cyanide 3-chlorophenylhydrazone (CCCP), MRT68921 and okadaic acid (OA) were also prepared in DMSO. Deferiprone (DFP), hydroxychloroquine (HCQ) and 6-OHDA were dissolved in water. Paraquat (PQ) (Sigma, 856177-1G) was prepared in PBS 1X. Carbonyl cyanide-p-trifluoromethoxyphenylhydrazone (FCCP) (Sigma, C2920) was dissolved in ethanol.

3.2 Cell culture

3.2.1 Cell lines

The cell lines used in this project were:

- U2OS-iMLS (±Parkin). Human osteosarcoma U2OS cell line with stable inducible expression of the internal mitochondrial localization signal (iMLS) (NIPSNAP1$_{1-53}$)-EGFP-mCherry.[142] They were generated with the FlpIn system using the pcDNA5-MLS-mCherry-EGFP plasmid. As those cells do not express Parkin, U2OS-iMLS were transduced with a lentiviral particle expressing Parkin. Both cell lines were culture with DMEM with glutamine supplemented with 10% FBS and 1% Pen-Strep at 37 ºC and 5% CO_2. Cells were selected with 100 µg/mL hygromycin and 5 µg/mL blasticidin. Additional 2 µg/mL puromycin were used for U2OS-iMLS-Parkin cells. To induce the expression of the mitophagy reporter, 500 µg/mL doxycycline was added for the last 24h. These cells were obtained from Prof. Anne Simonsen Lab (Faculty of Medicine, Institute of Basic Medical Sciences and Centre for Cancer Cell Reprogramming, Institute of Clinical Medicine, University of Oslo, Norway).

- ARPE-19 MitoQC. Human retinal pigment epithelial cell line stably expressing the mitophagy reporter mCherry-GFP-FIS1$_{101-152}$.

- SH-SY5Y MitoQC. Human neuroblastoma cell line stably expressing the mitophagy reporter mCherry-GFP-$FIS1_{101-152}$.

These two lines were maintained in DMEM:F12 (1:1) supplemented with 15% de FBS, 1% glutamine 2 mM and 1% de pen-strep (0.5 mg/ml) at 37 ºC and 5% CO_2.

MitoQC reporter was obtained as follow: mCherry, GFP and $FIS1_{101-152}$ residues cDNA were cloned into a pBABE.hygro vector.[143] The construct was co-transfected into 293FT cells with GAG/POL and VSV-G expression plasmids (Clontech, Saint-Germain-en-Laye, France) for retrovirus production using Lipofectamine 2000 (Life Technologies) in accordance with manufacturer's instructions. Virus was harvested 48h after transfection and applied to cells in the presence of 10 μg/mL polybrene. Cells were selected with 500 μg/mL hygromycin, and stable pool used for experiments. In order to maintain in culture only the cells with reporter, 800 μg/mL and 500 μg/mL hygromycin are used for ARPE-19 MitoQC and SH-SY5Y MitoQC, respectively. These two cell lines were obtained from Dr. Ian Ganley Lab (School of Life Sciences, University of Dundee, Scotland).

- Lymphoblasts from ALS patients

Peripheral blood samples were obtained from thirteen control subjects, four sporadic (sALS) patients, four ALS patients carrying a mutation in SOD1 (SOD1-ALS) and two ALS patients carrying a mutation in TDP-43 (TDP43-ALS). Patients were diagnosed by neurologistS from the Hospital Universitario 12 de Octubre (Madrid, Spain) applying El Escorial criteria.[144] Samples were obtained after signing an informed consent. All procedures were approved by the Hospital Doce de Octubre and the Spanish Council of Higher Research Institutional Review Board and are in accordance with National and European Union Guidelines.

Blood samples were used to isolate peripheral blood mononuclear (PBMC) on Lymphoprep™ density-gradient centrifugation.[145] Granulocytes and erythrocytes have a higher density (> 1.077 g/mL) than mononuclear cells and therefore they sediment through the Lymphoprep™ (1.077 g/mL) layer during centrifugation. Thus, 10 mL of blood were diluted with 10 mL of PBS 1X (Sigma-Aldrich). Then, 12 mL of Lymphoprep™ were

added and centrifuged for 45 min at 1400 rpm (Figure 11). PBMC were extracted, washed with PBS 1X and centrifuged for 10 min at 1300 rpm. In order to immortalize the lymphocytes, pellets were mixed with 8 mL of RPMI (Invitrogen), 1 µg/mL cyclosporine (Sigma-Aldrich) to block T cells and one aliquot of Epstein-barr virus obtained from Burkitt lymphoma cell line (B-95-6) given by Logina Akhatat (National Institute of Alcohol and Abuse Disorders, NIH, Bethesda, USA). Cells were maintained in suspension in a concentration of 10^6 cells/mL in RPMI-1640 (Invitrogen) supplemented with 1% L-glutamine 2 mM, 1% pen-strep and 10% FBS at 37 ºC and 5% CO_2.

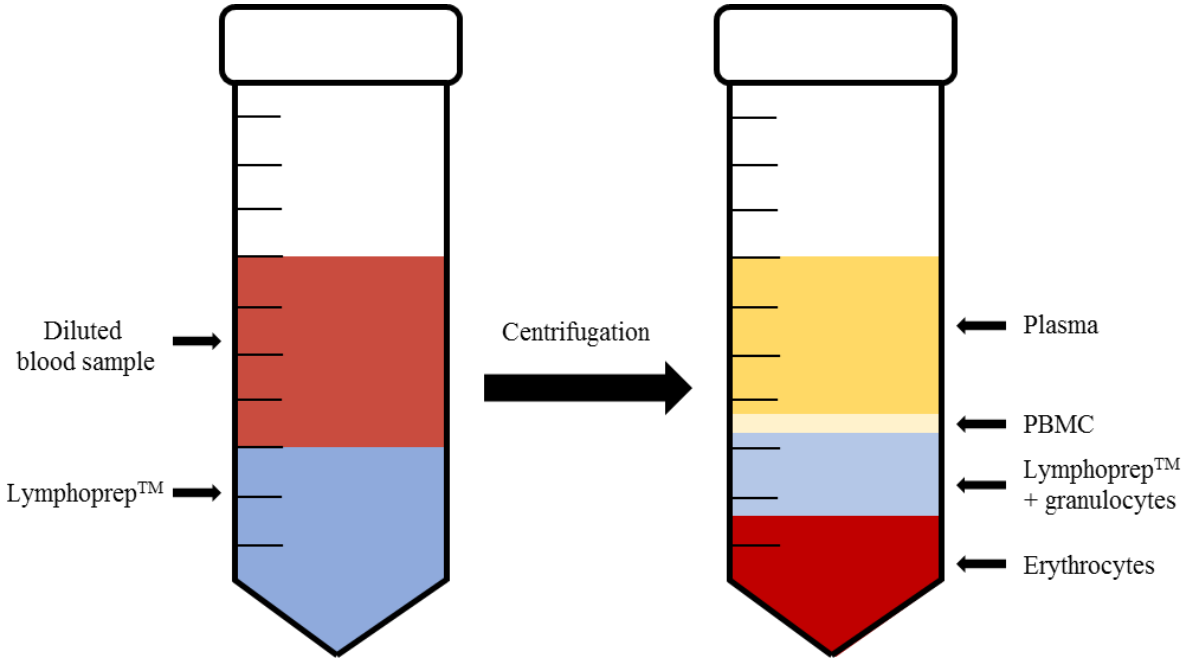

Figure 11. Isolation of PBMC by Lymphoprep™ density-gradient centrifugation.

3.2.2. Fluorescence microscopy

3.2.2.1 Mitophagy assay

U2OS-iMLS ±Parkin and ARPE-19 MitoQC cells were seeded at a final concentration of 50,000 cells/mL in a 96-well plate and in crystals in a 24-well plate, respectively. In the case of the SH-SY5Y MitoQC cells, 100,000 cells/mL were seeded in a 24-well plate. The next day, the cells were treated as indicated. In the case of U2OS-iMLS ±Parkin, 500 µg/mL doxycycline was added to medium to induce the expression of the reporter. After

24h, the cells were fixed with 3.7% N-(2-hydroxyethyl)piperazine-N′-ethanesulfonic acid (PFA) 200 mM Hepes pH 7 and incubated with Hoechst (Invitrogen, H1399) to stain the nuclei. The U2OS cells were maintained in the plates in PBS until images were acquired. The ARPE-19 and SH-SY5Y MitoQC cells were seeded in crystals and incubated with DAPI (Sigma-Aldrich─2D9542) to stain the nuclei. Then, the crystals were mounted over slides with ProLong Diamond Antifade Mountant (Thermo, P36961). The slides were kept for 24h at RT and then at 4 °C until images were acquired.

3.2.2.2 Immunostaining

The U2OS-iMLS ±Parkin cells were seeded at a final concentration of 50,000 cells/mL in a 96-well plate. The next day, the cells were treated as indicated, and 500 μg/mL doxycycline was added to medium to induce the expression of the reporter. After 24h, the cells were fixed with 3.7% PFA 200 mM Hepes pH 7 and incubated with Hoechst (Invitrogen, H1399) to stain the nuclei. The cells were washed with 0.2% NP-40 to permeabilize the cells. Then, the cells were washed with 1% BSA in PBS 1X and incubated with the primary antibody (LC3; 1:500, MBL-PM036) for 1h at 37 °C. After washing steps, the cells were incubated with the secondary antibody Rabbit DayLight 649 (1:500) for 30 min at RT. Finally, the cells were kept in PBS until imaged.

3.2.2.3 Image Acquisition

Images of the U2OS-iMLS ±Parkin cells in 96-well plates were obtained under an ImageXpress Micro Confocal microscope (Molecular Devices), placed in the Advanced Light Microscopy Facility at Gaustad (University of Oslo, Norway). Six images per well were automatically taken at 20x in order to quantify around 1000 cells per condition.

Images of the ARPE-19 MitoQC and SH-SY5Y MitoQC cells in 24-well plates were obtained with an AF6000 LX widefield multidimensional microscopy system and CLSMLEICA TCS SP8 STED 3X placed in the confocal laser and multidimensional microscopy *in vivo* facility at CIB Margarita Salas (Madrid, Spain). Five to six images were manually taken at 40x and 63x, respectively, to have around 100 cells per coverslip.

3.2.2.4 Image analysis

Image analysis was done with CellProfiler.[146] In order to identify red-only structures per cell segmentation of nuclei, cells and mitochondrial network were performed. Mitochondrial structures were further filtered as "yellow" or "red-only" based on the ratio between their EGFP and mCherry integrated intensities. The final number of red-only structures per cell was used as a mitophagy rate readout. Later, this pipeline was modified in order to analyse mitophagy in cells seeded in 24-well plates. The final number of yellow structure per cell was used to measure mitochondrial mass.

For the mitochondrial morphology study, segmentation of mCherry structures was done and the mean area of each mitochondrial fragment per image was used as a final readout.

3.2.3 Western Blotting

3.2.3.1 Cell seeding

U2OS-iMLS-Parkin and ARPE-19 MitoQC cells were seeded at a final concentration of 200,000 cells/mL in a 6-well plate. After 24h, the cells were treated as indicated. Proteins were extracted with lysis buffer [50 mM Tris-HCl pH 6.8, 10% glycerol (v/v) and 2% sodium dodecyl sulfate (w/v), in distilled water] with protease inhibitors 1X (Sigma, P8783) and phosphatase inhibitors [1 mM sodium orthovanadate (Sigma, S6508), 1 mM sodium fluoride (Sigma, 201154), and 5 mM sodium pyrophosphate decahydrate (Sigma, 221368)]. The proteins were scrapped and transferred to a tube. The samples were heated at 95 °C for 15 min and spin and stored at −20 °C until used.

Lymphoblasts were seeded at a final concentration of 10^6 cells/mL in a 24-well plate and treated as indicated. After washing steps, pellets were stored at -80 °C until used or treated with the lysis buffer to extract the proteins. The samples were heated at 95 °C for 15 min and spin and stored at −20 °C until used.

3.2.3.2 Protein quantification and immunoblotting

To quantify proteins, a bicinchoninic acid protein assay kit (Pierce, 23227) was used, and 12-15 μg of proteins was loaded with 10 mM dithiothreitol and 0.005% bromophenol blue in Criterion TGX Precast Midi Protein gels (BioRad, 5671124) and transferred to

polyvinylidene fluoride membranes (BioRad, 170–4157) activated with 100% methanol (Panreac, 131091.1214) for 2 min. The transfers were done with Trans-Blot Turbo Transfer (BioRad) for 14 min (two waves of 7 min each) at 25 V. After the transfers, protein bands were detected with Ponceau Red (Sigma, 78376). Membranes were washed with PBS 1X-Tween20 (Bio-Rad, 170-6531) (PBS-T) and blocked with 5% (w/v) milk in PBS-T for 1h, shaking at RT. After blocking, membranes were washed with PBS-T and incubated with primary antibodies (Table 2) in 3% (w/v) BSA, 0.01% azide in PBS overnight, shaking at 4°C.

Table 2. Antibodies used in western blotting

Antibody	Provider	Ref	Species	Dilution
LC3	Sigma	L7543	Rb	1:1000
P62	Abcam	56416	Ms	1:1000
TOMM20	Santa Cruz	sc-11415	Rb	1:1000
TIMM23	BD Bio.	611222	Ms	1:1000
Vinculin	Abcam	ab129002	Rb	1:1000
GAPDH	Abcam	ab8245	Ms	1:1000

Next day, membranes were washed with PBS-T and incubated with secondary antibodies in PBS-T for 1h, shaking at RT. For band detection, membranes were incubated for 3 min with Pierce ECL Western Blotting Substrate (Thermo Scientific, 32106). Images were obtained with the Chemiluminescent system of ChemiDoc™ MP Imaging System from Bio-Rad. Quantification was done with Image Lab Software of Bio-Rad.

3.2.4 Citrate synthase assay

Citrate synthase participates in Kreb's cycle, converting acetyl-CoA to CoASH with the help of oxaloacetate. Its activity could be related to the number of mitochondria in a sample.

A total of 200,000 cells/mL were seeded in a 6-well plate. After 24h, the cells were treated as indicated. Then, the cells were washed with cold PBS 1X. The cells were resuspended in NP-40 lysis buffer in water (150 mM NaCl, 1% NP-40, and 50 mM Tris pH

8), rotated in a cold room for 30 min, and centrifuged at 13,000 g for 20 min in cold. Then, the supernatant was collected and stored at −20 °C until used.

Citrate synthase activity was determined by incubating 5 µL of proteins with 995 µL of 100 mM Tris pH 8, 0.1% Triton, 0.1 mM acetyl-CoA (Sigma, A2181), and 0.2 mM 5,5′ dithiobis(2-nitrobenzoic acid) (Sigma D8130-1G). 198 µL of the mix was pipetted in triplicates on a 96-well plate, and 2 µL of oxaloacetate (Sigma O4126-1G) was added to the sample wells. Absorbance was measured at 412 nm every 30s for up to 60 min at 30 °C. The results were normalized to protein concentration.

3.2.5 Viability assay. Crystal Violet.

Cell death was evaluated with crystal violet, a dye that binds to DNA and protein of remaining adherent cells.

300,000 cells/mL were seeded in a 96-well plate. Next day cells were treated as indicated and 1h later OA was added to induce cell death. To stop the treatment, cells were washed with PBS 1X and fixed with PFA 3.7% Hepes 200 mM for 30 min. Then, 0.1% crystal violet (Sigma, C0775) in distilled water was added for 30 min at RT in a shaker. Plates were carefully washed with distilled water to remove crystal violet in excess and faced down to dry overnight. Next day, cells were resuspended in 10% acetic acid (Merck) in distilled water. Absorbance at 590 nm was measured and quantified in a plate reader.

3.2.6 RT-qPCR

3.2.6.1 RNA extraction and quantification

Cells were seeded at a final concentration of 100,000 cells/mL in a 6-well plate. Next day, cells were treated as indicated. RNA from cells was extracted using the RNeasy Plus Mini Kit (Qiagen, Hilden, Germany) and quantified with NanoDrop™ 2000 (Thermo Fisher Scientific). Samples were stored at -80 °C.

3.2.6.2 Reverse Transcription

From each extract, 1 µg was reverse-transcribed into cDNA using the High-Capacity cDNA Reverse Transcription Kit with RNase Inhibitor (Applied Biosystems, Cheshire, UK). Reverse transcription was performed in a thermal cycler at 25 °C for 10 min, 37 °C for 120 min, 85 °C for 5 min and then cooled to 4 °C. Samples were stored at -20 °C.

3.2.6.3 cDNA amplification

For each sample, Master Mix 2X and H_2O PCR grade from Light Cycler® 480 Probes Master (Roche) were mixed with primers of the gene of interest (*PPARGC1A*, Mm01208835_m1, Thermo Fisher). The housekeeping gene *18S* (Hs99999901_s1, Thermo Fisher) was used for internal normalization.

3.2.6.4 Analysis RT- qPCR

For the analysis of the results, the Light Cycler® 480 Software, Version 1.5 was used. First, absolute quantification was determined in order to remove deviated replicates (Cp Error must be lower than 0.5). Then, relative quantification was assessed.

3.3 Biochemical kinase assays

3.3.1 International Centre for Kinase Profiling

Assays of kinase inhibition were done in the the MRC Unit of Dundee University, under the following methods:

- SGK1 (5-20 mU diluted in 20 mM MOPS pH 7.5, 1 mM EDTA, 0.01% Brij35, 5% glycerol, 0.1% b-mercaptoethanol, 1 mg/mL BSA) is assayed against a modified Crosstide peptide GRPRTSSFAEGKK in a final volume of 25.5 µL containing 8 mM MOPS pH 7.0, 0.2 mM EDTA, 30 µM substrate peptide, 10 mM magnesium acetate and 0.02 mM [33P-g-ATP] (50-1000 cpm/pmol) and incubated for 30 min at room temperature. Assays are stopped by addition of 5 µL of 0.5 M (3%) orthophosphoric acid and then harvested onto P81 Unifilter plates with a wash buffer of 50 mM orthophosphoric acid.

- ULK1 (5-20 mU diluted in 50 mM Tris pH 7.5, 0.1 mM EGTA, 1 mg/mL BSA, 0.1% mercaptoethanol) is assayed against MBP in a final volume of 25.5 µL containing 50 mM Tris pH 7.5, 0.1 mM EDTA, 10 mM DTT, 0.33 mg/mL substrate, 10 mM magnesium acetate and 0.02 mM [33P-γ-ATP] (50-1000 cpm/pmol) and incubated for 30 min at room temperature. Assays are stopped by addition of 5 µL of 0.5 M (3%) orthophosphoric acid and then harvested onto P81 Unifilter plates with a wash buffer of 50 mM orthophosphoric acid.

3.4 Animal samples analysis

The animal models from which the spinal cords were obtained were:

- mCherry-GFP-FIS1$_{101-152}$ (MitoQC) mice with C57BL/6 genetic background.[147] They were obtained from Dr. Ian Ganley lab and stablished in the CIB animal facility. Two animals per group were treated intraperitoneally at P90 (postnatal day 90) with vehicle or IGS2.7 1 mg/Kg for 8 and 24h and then sacrificed. Vehicle to treat control animals and to dissolve the drug was composed by 5% Tween-80 and 5% DMSO in NaCl 0.9%.

- Prp-hTDP-43(A315T) transgenic mice (TDP-43^{A135T}) and their wild-type (WT) littermate, both with C57BL/6 genetic background, were obtained from Dr. Eva de Lago (Complutense University, Madrid). Four animals per group were treated intraperitoneally with vehicle or IGS2.7 at 0.5 or 1 mg/Kg daily for 30 days from P65 until P95. Vehicle to treat control animals and to dissolve the drug was composed by 6.25% Tween-20 and 0.9% DMSO in PBS (Sigma-Aldrich). Animals were sacrificed 24h after the last drug administration.

- B6.Cg-Tg(SOD1-G93A)1Gur/J transgenic mice (SOD1^{G93A} mice) carrying the G93A mutant form of the human SOD1 transgene, and their wild-type (WT) littermate, both with C57BL/6 genetic background, were obtained from Dr. Silvia Corrochano (Hospital Clínico). In total nine SOD1^{G93A} mice and four WT animals were sacrificed between P112 and P115.

Spinal cords were extracted and fixed with 4% PFA or 3.7% PFA 200 mM Hepes pH 7.0 in the case of MitoQC mice for 24h, cryoprotected in 30% sucrose (Merck Millipore) and stored at -80 ºC. Sections of 20 µm at the lumbar level of the spinal cords were obtained with a cryostat and collected on gelatin-coated slides.

3.4.1 Histological procedures

Sections of the spinal cords were used for immunofluorescence. Samples were washed with PBS 1X and permeabilized with 0.3% Triton X-100 (Sigma) in PBS 1X for 15 min in a wet chamber. Samples were again washed with PBS 1X and blocked with the blocking solution BGT (3 mg/mL Bovine Serum Albumine (Nzytech) 10 mM glycine (VWR Chemicals) and 0.25% Triton X-100 in PBS 1X) for 1h at RT in a wet chamber. Next, sections were incubated at 4 ºC overnight with primary antibodies (Table 3) in blocking solution in a wet chamber. Then, sections were washed and incubated with secondary antibodies in blocking solution for 1h at RT in a wet chamber. In addition, 1 µg/mL DAPI was used to stain the nuclei. Slides were washed with PBS 1X and mounted with Vectashield antifade mounting medium (Vector Laboratories, H-1000-10).

Table 3. List of primary and secondary antibodies used for histological studies in spinal cords

PRIMARY ANTIBODIES			
Antibody	**Provider**	**Species**	**Dilution**
p62	Progen	Guinea Pig	1:100
Tomm20	SCBT	Rabbit	1:100
SECONDARY ANTIBODIES			
Antibody	**Provider**	**Fluorophore**	**Dilution**
Anti-Guinea pig	Invitrogen	Alexa-568	1:200
Anti-Rabbit	M.Probes	Alexa-647	1:200

3.4.1.1 Image acquisition

Spinal cords were imaged in the ventral horn area, where the MN are. Images were obtained under CLSMLEICA TCS SP8 STED 3X microscope placed in the confocal laser and multidimensional microscopy *in vivo* facility at CIB Margarita Salas (Madrid, Spain) with 63x objective. Z-stacks of four to five sections per animal were obtained.

3.4.1.2 Image analysis

Image analysis was done with CellProfiler.[146] p62 and TOMM20 area were measured by MN in TDP-43^{A135T} mice, SOD1^{G93A} mice and their control littermate. Mitophagy, red-only punctae, was measured by MN in MitoQC mice. Ten to fifteen MN were quantified animal. Then, the mean of the animals from the same group was obtained and represented.

3.5 Computational tools

3.5.1 Compound preparation and drug-like properties predictions

Computational preparation of the compounds from the FDA and MBC was done with Maestro,[148] the interface of the chemical simulation software Schrödinger.

Starting from a .sdf file, 2D structures of drugs were processed into 3D structures with LigPrep[149] (Maestro). To obtain the most favourable structures in the most possible physiological environment, ligands were ionized at 7.2±0.2, desalted and one stereoisomer was generated per ligand using OPLS2005 force field, which mimics the forces between atoms within molecules.

Then, ligands were characterized using QikProp.[150] It is another tool from Schrödinger software that predicts absorption, distribution, metabolism, and excretion (ADME) properties and important pharmaceutical descriptors of ligands based on their 3D structure. Compounds were selected based on those descriptors.

Following Lipinski's rule of five, absorption and permeability decrease if molecular weight is greater than 500 Da.[151] So, that was the cutoff applied to reduce the list of compounds to 431.

The second parameter evaluated was LogP. LogP is a value that describes the tendency of a compound to be distributed in a biphasic system of lipid and water. A negative value assumes hydrophilicity and a positive vale determines more concentration of the compound in the lipidic phase.[152] As lipophilicity is essential in absorption, distribution, and penetration across biological membranes, a limit of LogP>0 was applied. Then, 39 compounds more were deleted from the list.

Finally, PSA, which improves cellular potency, intestinal absorption and BBB permeation or restriction to the peripheral circulation, was also determined. PSA is defined by the amount of molecular surface of the ligands that is polar. To cross the BBB and reach the central nervous system, low PSA (<60-70 Å) is needed.[153] Here, we applied a cut-off of PSA<80 Å.

3.5.2 Similarity based on binary fingerprints

In order to compare the 2D structures of the compounds with reference ones, we used Canvas,[154] another graphical interface of Schrödinger. First, hashed binary fingerprints were evaluated. This method splits the ligands in fractions and scores with 0 or 1 the absence or presence of the fragments that grow radially from each atom.[155] To calculate it, discrimination between different types of atoms is relevant. There are several atom-typing schemes that go from the simpler one, in which atoms are equivalents, to more complex ones. In this case, we used the Daylight invariant atom type, which distinguishes atoms by atomic number, formal charge, valence, and the numbers of hydrogen and non-hydrogen.[156]

Hashed radial binary fingerprints from 2D structures were calculated with 64-bit precision. Fingerprints of reference compounds were also obtained. Then, similarity from fingerprints was determined based on Buser metric.

3.5.3 Docking studies

Docking studies were done against the kinase SGK1. Its crystal structure 3HDM, available in PDB was used.[157] First, the protein was prepared with *Protein Preparation Wizard* tool, from Maestro.[158] The ligand, metals and molecules of water were removed, and hydrogens were included. Residues were ionized at a pH 7.2 and minimized with OPLS2005 force field. Ligands from the MBC chemical library were prepared with LigPrep, as previously indicated.

The docking site was defined based on the position of the ligand crystallized in the catalytic site. The compounds were forced to form two hydrogen bonds, with Asp177 and Ile179, like the control ligand. The screening virtual was done with the software Glide,

from Maestro,[159] with extra precision (XP). Results were order based on the docking score (XP Gscore).

3.6 Statistics

Statistics was done with the software GraphPad Prism 7. Analysis was done with the unpaired two tailed t-test to compare two groups or one-way ANOVA followed by Dunnett's multiple comparison test if there are more than two groups. A p-value lower than 0.05 was considered statistically significant.

4. RESULTS

4.1 Set up of mitophagy phenotypic assay and medium throughput screening of compounds

The aim of this chapter is to discover mitophagy modulators that could represent new therapeutic agents for the study and/or treatment of neurodegenerative diseases. For that, phenotypic assays and two different chemical libraries were used. Selected compounds from those libraries have been filtered by cheminformatics tools in order to reduce the number to be tested in the cell-based assay. Then, the ability of those selected compounds to modulate mitophagy was determined by fluorescent phenotypic assay.

4.1.1 Compound selection

Two different chemical libraries containing small molecules were used: the Pharmakon drug collection (US Drug Collection, MicroSource Discovery Systems) (1759 compounds) and our in-house Medicinal and Biological Chemical (MBC) library[160] (>2200 molecules). As the number of compounds included in the final screening had to be reduced due to layout limitations, several filters were applied to reduce and select the number of compounds.

4.1.1.1 Pharmakon drug collection

One of the strategies in drug discovery to reduce costs and time is drug repurposing.[161] It consists in finding new uses to already-marketed drugs. One of the main advantages is a reduction in the rate of failure. Drugs have already been tested in preclinical models and clinical phases, so toxicity effects have been already overcome and safety is guaranteed. Moreover, formulations have been also studied, so the process to get to the market with a new indication is faster and cheaper.[162]

With this concept in mind, the first step in drug selection was to obtain a list with drugs already approved from the company MicroSource Discovery Systems, Inc. The list contained information related to its structure, CAS number, formula, molecular weight, biological profile, and generic and market name of two drug collections: 1360 compounds that reached clinical trials in USA (U.S Drug Collection) and 399 compounds that are or have been marketed in Europe and/or Asia (International Drug Collection). The combination of these two libraries constituted the Pharmakon drug collection.

4.1.1.2 Bibliographic search

The list included drugs approved for other purposes but human intake. Among them, insecticides or pesticides were removed. With them, other drugs, like antibiotics, antitumoral, edulcorants, antiprotozoal, antimalarial, anthelmintic, antiviral, antiseptic, contrast agents or anaesthetics were also discarded to avoid unwanted side effects in a future chronic treatment for neurodegenerative diseases. Thus, a reduction of almost 70% of compounds was obtained. Next, the rest of compounds were filtered with bibliographic information for their ability to cross the human BBB. Finally, 452 compounds out of 1759 were selected for subsequent filtering steps (Table 4).

Table 4. Number of compounds from the Pharmakon drug collection filtered by bibliographic search

Filter	Bibliographic search		
	US Drug Collection	INT Drug Collection	Pharmakon
-	1360	399	1795
Insecticides, pesticides, antitumoral	431	130	561
BBB penetration	336	116	452

4.1.1.3 Computational filtering

- Drug-like properties

To filter the remaining compounds based on their drug like properties, computational tools were used. Schrödinger is a scientific chemical simulation software broadly used in pharmaceutical research and Maestro[148] is one of its graphical interfaces. In order to extract information from the compounds with the program, a first step of ligand preparation is needed.

First, ligands were converted from a 2D structure in .sdf files provided by MicroSource Discovery Systems, Inc into a 3D structure with LigPrep (Maestro).[149] Then, predictions of different characteristics, like ADME properties and important pharmaceutical descriptors of ligands based on their 3D structure were obtained with QikProp (Maestro).[150] To select only the compounds with better drug-like properties, the compounds were filtered based on molecular weight, partition coefficient (LogP) and polar surface area (PSA).

Thus, a final set of 300 compounds were included in the next computational filter step.

- Similarity based on binary fingerprints

As explained in the introductory part, fingerprints are a binary representation that determines the presence or absence of fragments in the structure of the ligands. This tool can be used with another graphical interface of Schrödinger, named Canvas.[154] It encloses cheminformatics techniques that allow us to determine the similarity between several drugs.

The 2D structures of compounds preselected from the drug-like property filter were the input in this step.

The structure of the library compounds were compared to two known mitophagy modulators (Figure 12). Deferiprone (DFP), which is an iron chelator known to induce receptor-mediated mitophagy[143] and carbonyl cyanide m-chlorophenyl hydrazone (CCCP), which reduced mitochondrial membrane potential and induced mitophagy by the recruitment of Parkin.[163] Fingerprints of the reference compounds were also calculated following the same scheme.

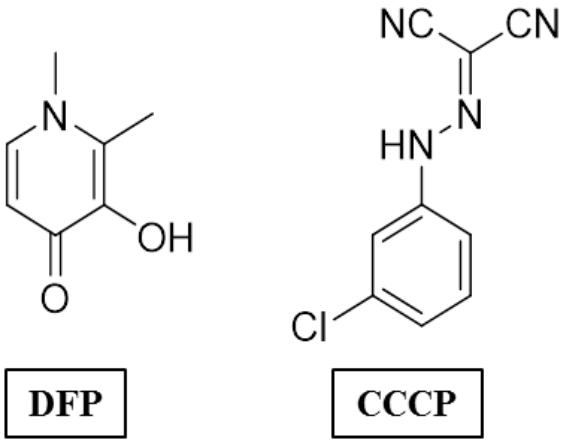

Figure 12. Chemical structure of mitophagy modulators used as reference in compound selection based on binary fingerprint similarity.

Compounds were ordered based on the similarity coefficient and the best 34 compounds with chemical diversity were selected for the screening (Table S1).

4.1.1.4 MBC library

The MBC library is our in-house chemical library, and it counts on more than 2,000 compounds and growing on based on the work of the medicinal chemists of the group. It has been already extensively characterized in terms of drug-likeness and physicochemical properties. One of the main interests of the MBC library is its chemical diversity, as well as its direct availability at work. So, it is a perfect beginning in drug discovery programs.[160]

The filtering process of the MBC library was similar to Pharmakon drug collection but avoiding the bibliographic search. Ligands were prepared and characterized by LigPrep and QikProp (Maestro) and their similarity to mitophagy inducers, DFP and CCCP, was determined by binary fingerprints (Canvas) as explained before. Thus, 37 compounds were selected (Table 5).

Table 5. Number of compounds from the Pharmakon drug collection and MBC library obtained after computational filtering

Computational filters		
Filter	**Pharmakon**	**MBC**
-	452	2077
MW<500 Da	431	1954
LogP>0	392	1862
PSA<80 Å	300	1373
Similarity based in fingerprints	34	37

So, finally 34 compounds from Pharmakon drug collection and 37 compounds from the MBC library were selected for the following phenotypic assay. Additionally, 19 compounds from the MBC library that were discarded previously were rescued, based on their known biological activity and their relevance in other medicinal chemistry programs. In total, 90 compounds were included in the screening (Figure 13).

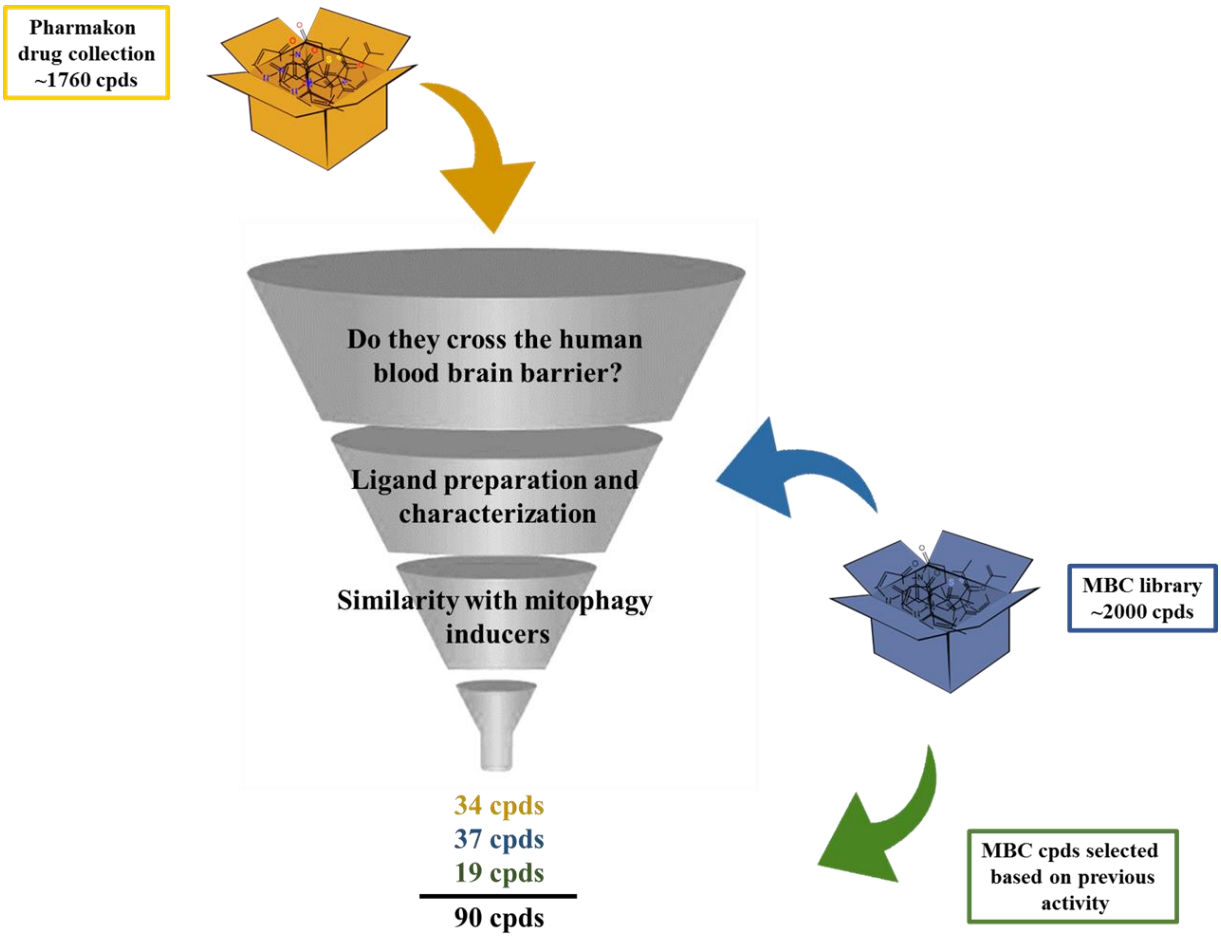

Figure 13. Scheme of filtering steps underwent by the chemical libraries to decrease the number of compounds used in the screening.

4.1.2 Mitophagy phenotypic assay

Once the compounds were selected, an internship was arranged with Fraunhofer IME ScreeningPort (Hamburg, Germany). The aim was to first test the compounds in an autophagy phenotypic assay, to study later in a mitophagy phenotypic assay and determine the specificity of the compounds. After one month setting up the autophagy assay in Hamburg, technical issues hindered the study, so autophagy screening was cancelled. Thus, we proceeded with the mitophagy phenotypic assay in collaboration with Anne Simonsen Lab, in Oslo. With this purpose, we organized an internship of two months in 2019 in the Institute of Basic Medical Sciences (University of Oslo, Norway).

The phenotypic assay consisted in an image-based assay using the human U2OS cell line with doxycycline-inducible expression of the double-tagged NIPSNAP internal mitochondrial localization signal (iMLS, NIPSNAP1$_{1-53}$-EGFP-mCherrry) previously described as a mitophagy reporter.[142] As U2OS cells do not express Parkin,[164] we have also used U2OS-iMLS cells transduced with a lentiviral particle expressing Parkin (U2OS-iMLS-Parkin). In that way we could assess effects of modulators on both, receptor-mediated and Parkin-mediated mitophagy. Like other tandem reporters, iMLS is pH sensitive. When mitochondria are in the cytosol (pH ~7.2), the reporter is seen in yellow as a combination of mCherry and EGFP. However, when the mitochondria are inside the acidic compartments (pH ~4.5-5), the reporter is seen as red-only, due to the EGFP quenching at low pH. To induce the expression of the mitophagy reporter, cells were treated with doxycycline 24h.

In order to assure the correct functioning of the assay, cells were treated with several controls. The vehicle (DMSO 0.1%) in which the compounds were dissolved, was the negative control in both cell lines. As a positive control, DFP 1 mM was used in receptor-mediated mitophagy and carbonyl cyanide-p-trifluoromethoxyphenylhydrazone (FCCP) 5 μM, another mitochondrial uncoupler, was used in Parkin-mediated mitophagy. As seen in Figure 14, both drugs clearly induced mitophagy, by the increase in the number of red dots, which represent mitolysosomes. In both cases, the treatment during the last two hours with bafilomycin A1 (BafA1), the V-ATPase inhibitor, increased the pH, restored EGFP signal in the acidic compartments,[165] and blocked the fusion between autophagosomes and lysosomes, then inhibiting the final step of the pathway.

Additionally, two extra internal controls were used in the assay. The lack of doxycycline was used to ensure the system was not leaky, and complete media to see the effect of the vehicle in mitophagy modulation. Cells that were not treated with doxycycline did not show the reporter, as expected, so mitophagy could not be evaluated. Regarding to cells treated only with complete media, there were no differences with cells treated with the vehicle (data not shown). So, for the rest of the analysis, the effect of the drugs was only compared to vehicle, hereafter control.

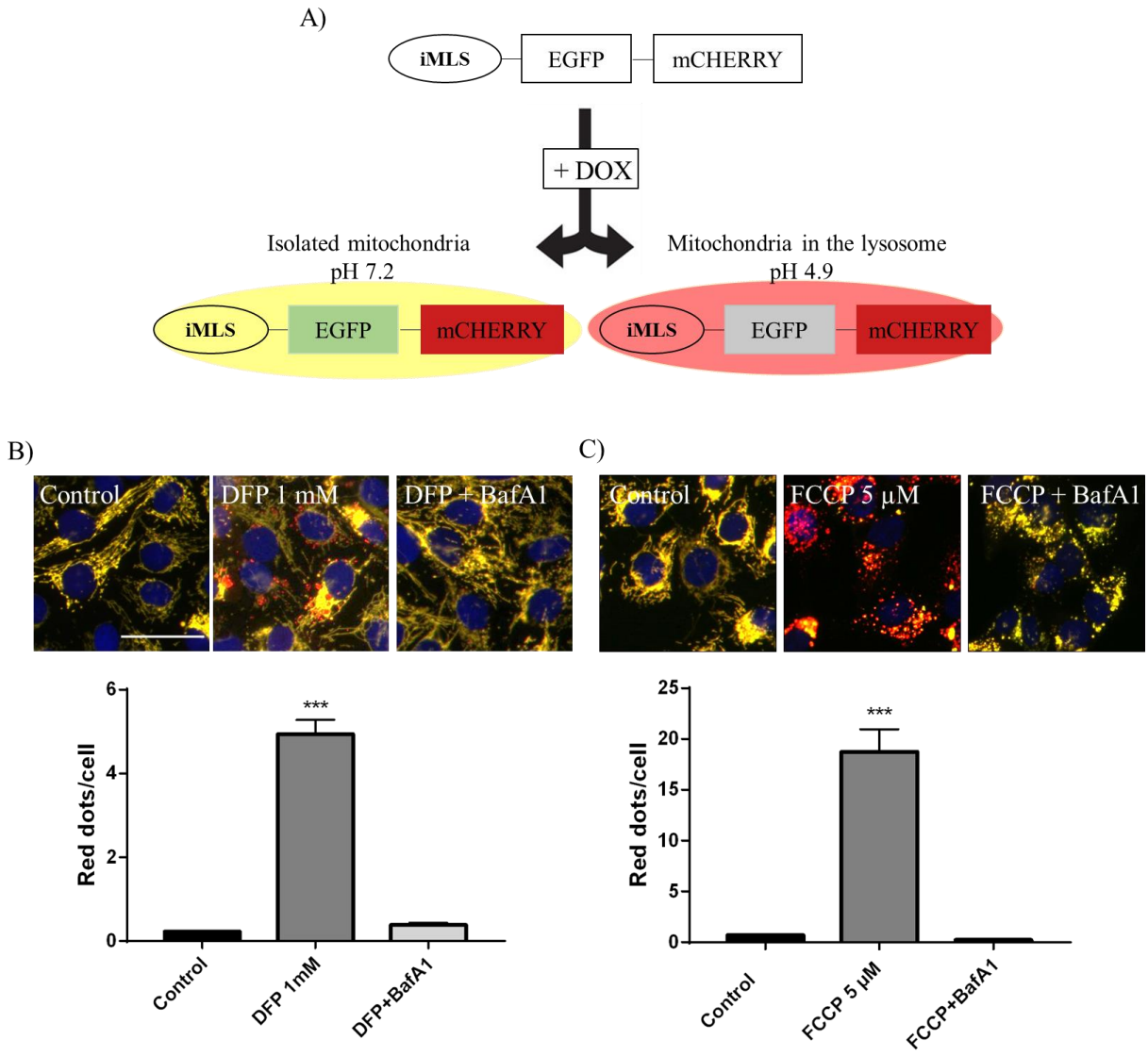

Figure 14. Description of iMLS reporter and assay set up. A) Mitophagy reporter description. B) U2OS-iMLS and C) U2OS-iMLS-Parkin cells were treated with the controls for 24h. BafA1 100 nM was added for the last 2h. Data represent the mean±SEM of three independent experiments. (Significance was determined by one-way ANOVA followed by Dunnett's multiple comparison test to control, where ***p<0.001). Scale bar = 50 µm.

4.1.3 Screening of compounds

When the phenotypic assay was set up, the screening of the compounds preselected as described in previous sections, was carried out. With the objective of discovering mitophagy modulators, we studied the ability of inducing and inhibiting mitophagy in both cell lines. With that, four different screenings were done. In all of them, cells were treated

with the compounds at a final concentration of 25 µM for 24h. Compounds that increased at least 2x mitophagy were considered inducers, while compounds that reduced mitophagy more than 50% were considered inhibitors. Some compounds were deleted from the screening due to cell toxicity or a decrease in cell proliferation.

The structure of the definitive list of compounds and their similarity coefficient with DFP and CCCP can be found in Table S1 (Annexes). Results of the final 78 compounds (28 from the Pharmakon drug collection and 50 from the MBC library) are described in the following sections.

4.1.3.1 Receptor-mediated mitophagy inducers

Non-expressing Parkin U2OS-iMLS cells were treated with the compounds at 25 µM for 24h. The internal controls used in this assay were control, DFP 1 mM and DFP co-treated with BafA1 for the last two hours. Unfortunately, as it can be seen in Figure 15, none of the compounds induced mitophagy in this cell line.

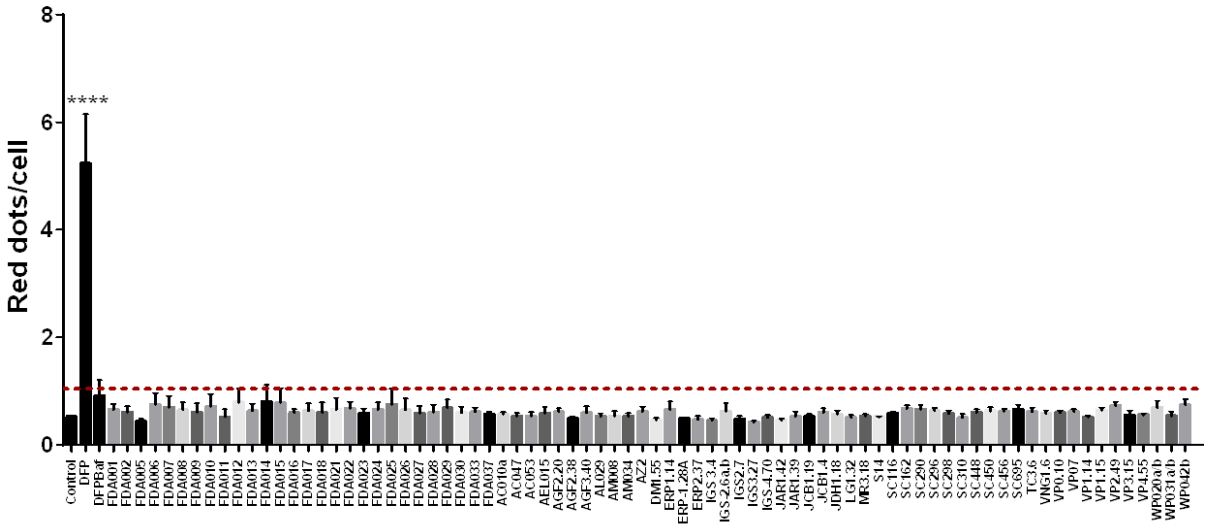

. **Figure 15.** Receptor-mediated mitophagy inducers. U2OS-iMLS cells were treated with control, DFP 1 mM and the compounds at 25 µM for 24h. BafA1 was added the last 2h. Data represent the mean±SEM of three independent experiments. (Significance was determined by one-way ANOVA followed by Dunnett's multiple comparison test to control, where ****p<0.001). Red line indicates 2-fold mitophagy increase compared to control.

4.1.3.2 Parkin-mediated mitophagy inducers

To find Parkin-mediated mitophagy inducers, U2OS-iMLS-Parkin cells were treated with the compounds, same as in the previous section. In this case, the positive control was FCCP 5 µM, whose mitophagy induction was blocked with BafA1 added during the last 2h of treatment. Interestingly, in this case, two compounds, identified as JAR1.39 and VP07, were able to induce 6-fold and more than 3-fold mitophagy, respectively, clearly seen by the increase in red dots (mitolysosomes) (Figure 16). Additionally, both compounds, from the MBC library, also changed the morphology of the mitochondrial network, as another sign of mitophagy induction, but they did not induce massive mitophagy, like FCCP, which would be detrimental.

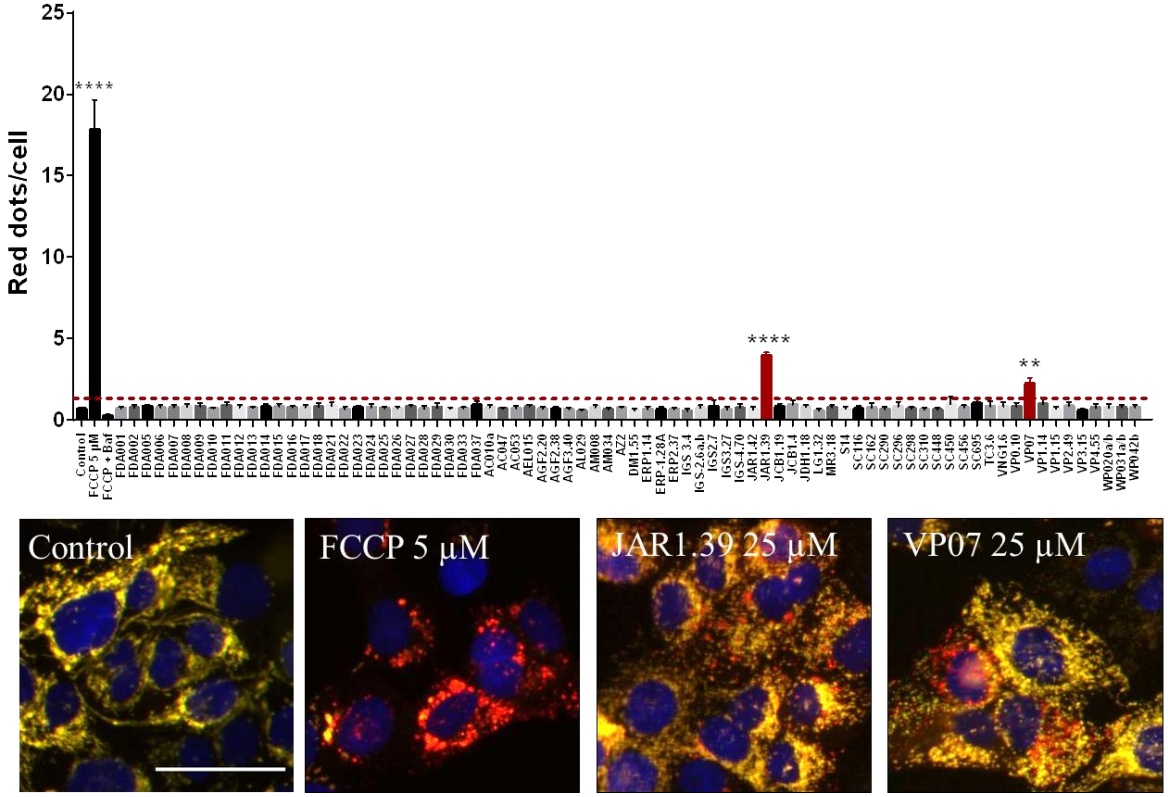

Figure 16. Parkin-mediated mitophagy inducers. U2OS-iMLS-Parkin cells were treated with control, FCCP 5 µM and the compounds at 25 µM for 24h. BafA1 was added the last 2h. Data represent the mean±SEM of three independent experiments. (Significance was determined by one-way ANOVA followed by Dunnett's multiple comparison test to control, where ****p<0.0001, **p<0.01). Red line indicates 2-fold mitophagy increase compared to control. Scale bar = 50 µm.

4.1.3.3 Receptor-mediated mitophagy inhibitors

There is still some controversy on the modulation of mitophagy in neurodegeneration. As aberrant mitophagy induction could reduce the number of detrimental but also functional mitochondria, we decided to look also for mitophagy inhibitors.

An induction of mitophagy was needed to determine the ability of the compounds to reduce the formation of mitolysosomes. For that, U2OS-iMLS cells were co-treated with DFP 1 mM and the compounds at 25 µM. DFP co-treated with the control for 24h and BafA1 for the last 2 hours were used. As expected, the control did not modify mitophagy induction by DFP, while BafA1 completely blocked the increase in red dots. Regarding the rest of the compounds from Pharmakon drug collection and MBC library, only one compound, identified as IGS2.7, from the MBC library, reduced mitophagy induction in more than 50% (Figure 17).

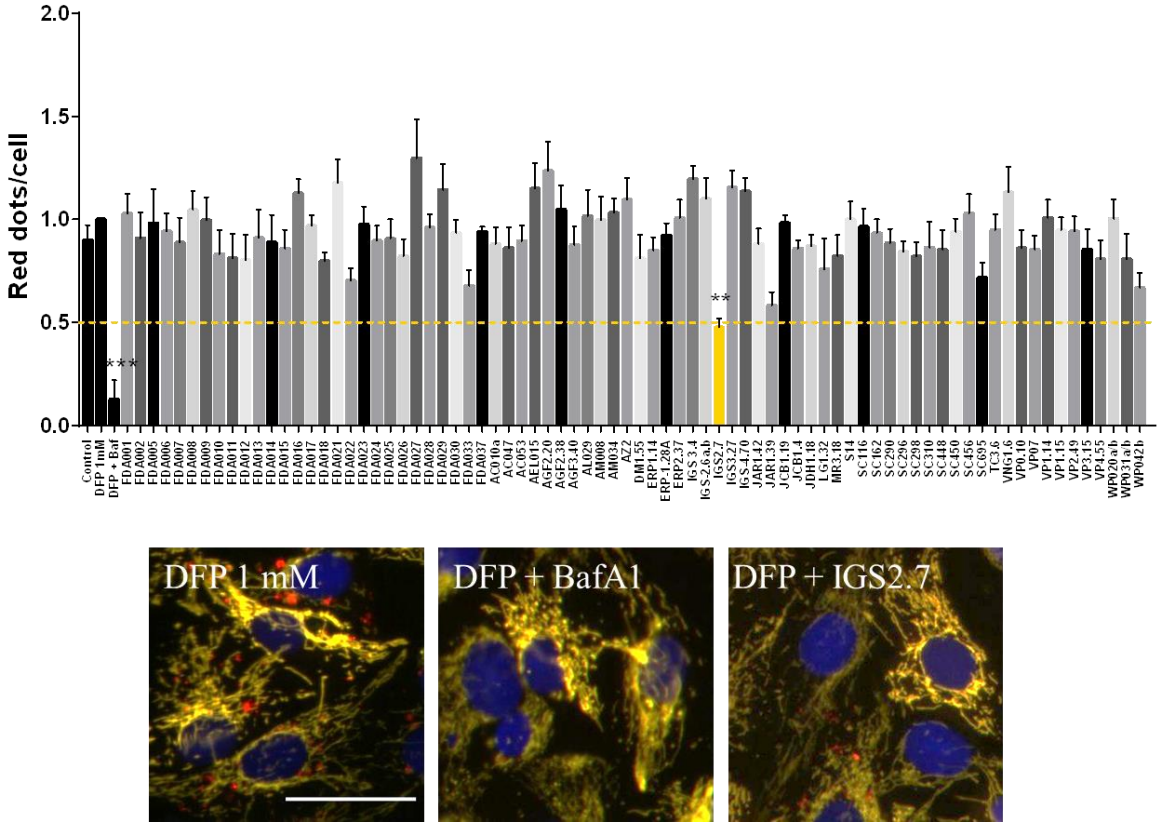

Figure 17. Receptor-mediated mitophagy inhibitors. U2OS-iMLS cells were treated with DFP 1 mM and co-treated with control and the compounds at 25 µM for 24h. BafA1 was added the last 2h. Data represent the mean±SEM of three independent experiments. Results were normalized to DFP 1 mM. (Significance was determined by one-way ANOVA followed by Dunnett's multiple comparison test to control, where ****p<0.0001, **p<0.01). Yellow line indicates 50% mitophagy reduction compared to control. Scale bar = 50 µm.

4.1.3.4 Parkin-mediated mitophagy inhibitors

In the case of U2OS-iMLS-Parkin, mitophagy was induced with FCCP 5 µM. Again, the co-treatment with the control did not reduce mitophagy induction by FCCP, while BafA1 blocked the process. However, none of the compounds co-treated with the inductor inhibited mitophagy (Figure 18). Moreover, the treatment with FCCP induced massive mitophagy which is detrimental and affects cell viability. This, in addition to Parkin overexpression, which also stresses cells and the co-treatment with the compounds, made this condition more complicated and variable for the screening.

Interestingly, WP031a/b induced mitophagy in synergy with FCCP. However, it did not modulate mitophagy alone (Figure 18), so this compound was not considered to be further characterized.

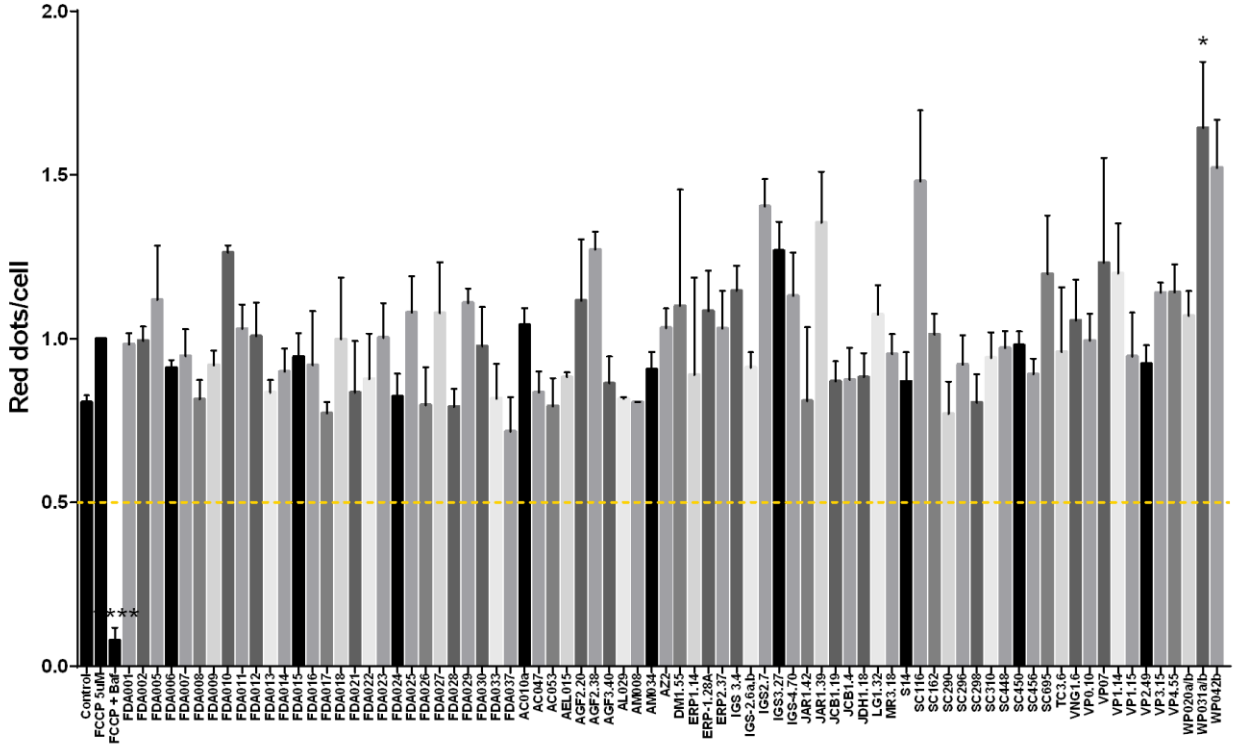

Figure 18. Parkin-mediated mitophagy inhibitors. U2OS-iMLS-Parkin cells were treated with FCCP 5 µM and co-treated with control and the compounds at 25 µM for 24h. BafA1 was added the last 2h. Data represent the mean±SEM of three independent experiments. Results were normalized to FCCP 5 µM. (Significance was determined by one-way ANOVA followed by Dunnett's multiple comparison test to control, where ****p<0.0001, *p<0.05). Yellow line indicates 50% mitophagy reduction compared to control.

4.2 Characterization and therapeutic potential of mitophagy enhancers

In this chapter, the enhancers found in the screening, JAR1.39 and VP07, are further characterized to find their potential mechanism of action and therapeutic applicability.

4.2.1 Hit characterization in U2OS-iMLS-Parkin cells

First, a dose-response relationship of JAR1.39 and VP07 in U2OS-iMLS-Parkin cells was studied. For that, cells were treated with increasing concentrations of the compounds (from 1.56 to 25 µM) for 24h and mitophagy was quantified. Images were used to study both mitophagy and mitochondrial morphology, by measuring fission as the mean area of the segmented mitochondrial network, typically found in Parkin-mediated mitophagy.[166]

JAR1.39 induced mitophagy at the highest concentration and a dose-dependent response trend was observed (Figure 19A and B). Moreover, this dose-response relationship was also observed for mitochondrial fission (Figure 19A and C). The highest concentration caused a significant decrease of the mean area of segmented mitochondria. This effect was lost as the dose decreased.

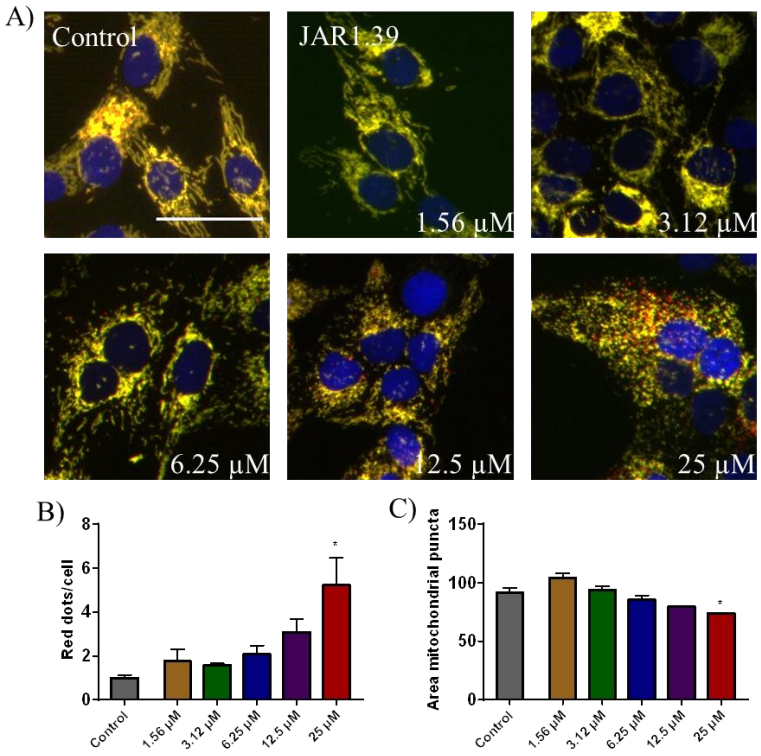

Figure 19. JAR1.39 characterization in U2OS-iMLS-Parkin cells. A) Representation of cells treated with control and increasing doses of JAR1.39. Quantification of B) mitophagy flux (red dots per cell) and C) mitochondrial fragmentation (area mitochondrial puncta). Data represent mean±SEM of two independent experiments. Data from B) were normalized to control. (Significance was determined by one-way ANOVA followed by Dunnett's multiple comparison test to control, where *p<0.05). Scale bar = 50 µm.

The treatment with VP07 induced an increase in red dots compared to control cells at 25 µM (Figure 20A and B). Mitochondrial fragmentation was also determined and a trend in the reduction of mitochondrial network area was observed when mitophagy was induced (Figure 20C).

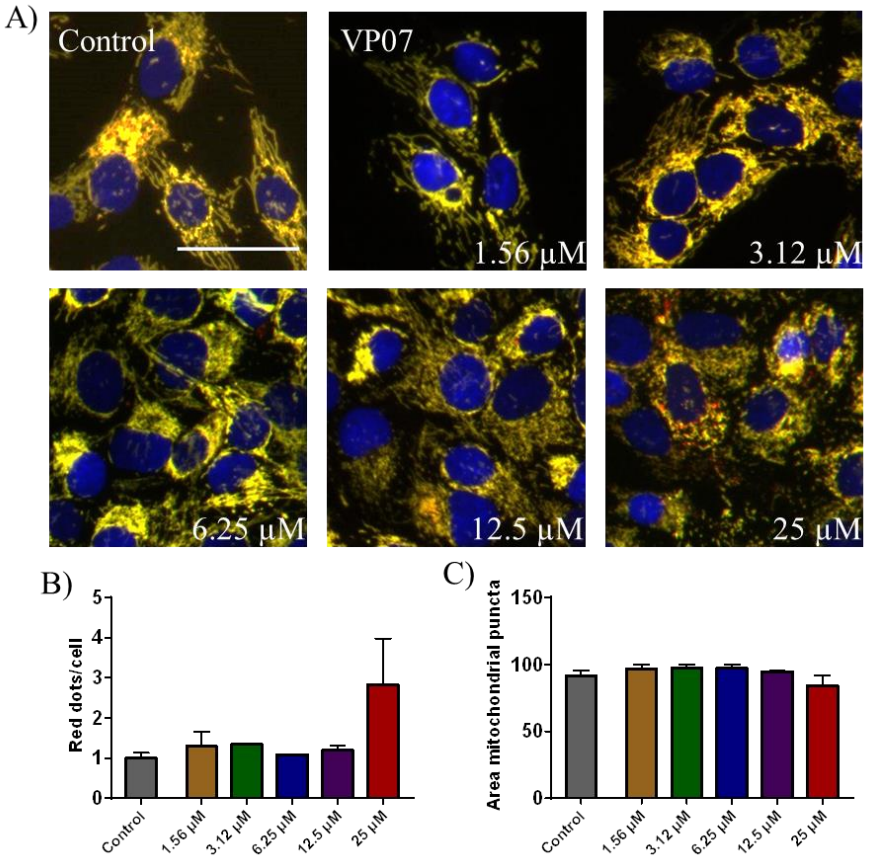

Figure 20. VP07 characterization in U2OS-iMLS-Parkin cells. A) Representation of cells treated with control and increasing doses of VP07. Quantification of B) mitophagy flux (red dots only per cell) and C) mitochondrial fragmentation (area mitochondrial puncta). Data represent mean±SEM of two independent experiments. Data from B) were normalized to Control. Scale bar = 50 µm.

With that, we decided to continue working with these compounds at 25 µM for 24h.

Regarding to fission, it was interested the effect of the JAR1.39 and VP07 in U2OS-iMLS cells. As expected, the compounds did not induce mitophagy, while they changed the morphology of the mitochondrial network. As seen in Figure 21, control cells had elongated mitochondria, while the treatment with JAR1.39 and VP07 rounded the network,

without mitochondria degradation. Thus, we confirmed the compounds needed Parkin to induce mitophagy and this took place downstream of mitochondrial fission.

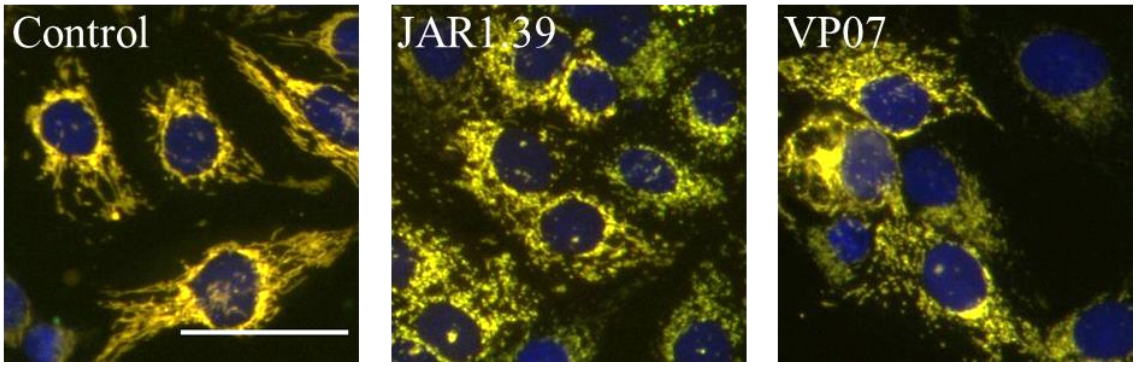

Figure 21. Representation of U2OS-iMLS cells treated with JAR1.39 and VP07 at 25 µM for 24h. They induced fission without mitochondrial degradation.

To corroborate the pro-mitophagy effect of the selected compounds we used other methods. First, the levels of two mitochondrial proteins, TOMM20 (in the outer mitochondrial membrane) and TIMM23 (in the inner mitochondrial membrane) were measured by western blot. Both proteins levels were reduced upon treatment with the positive control, FCCP, as well as with the discovered hits, JAR1.39 and VP07, suggesting an increase in mitophagy (Figure 22).

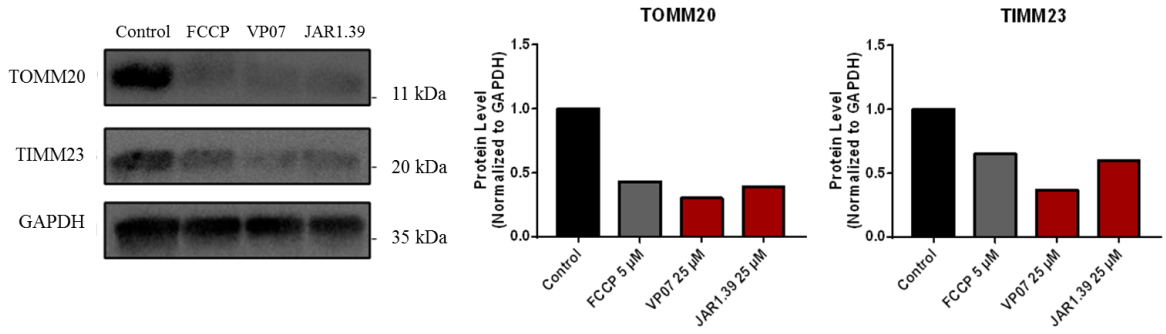

Figure 22. Western blot of mitochondrial proteins from U2OS-iMLS-Parkin cells treated with FCCP 5 µM and VP07 and JAR1.39 at 25 µM for 24h. Data represent values from one experiment, and they were normalized to control. Graphs represent values from a preliminary experiment.

Another method to study mitophagy is the determination of the enzymatic activity of the mitochondrial matrix protein citrate synthase. A clear reduction in the activity of the

enzyme compared to control cells was observed in cells treated with the JAR1.39 and VP07, confirming again mitochondrial degradation by increased mitophagy (Figure 23).

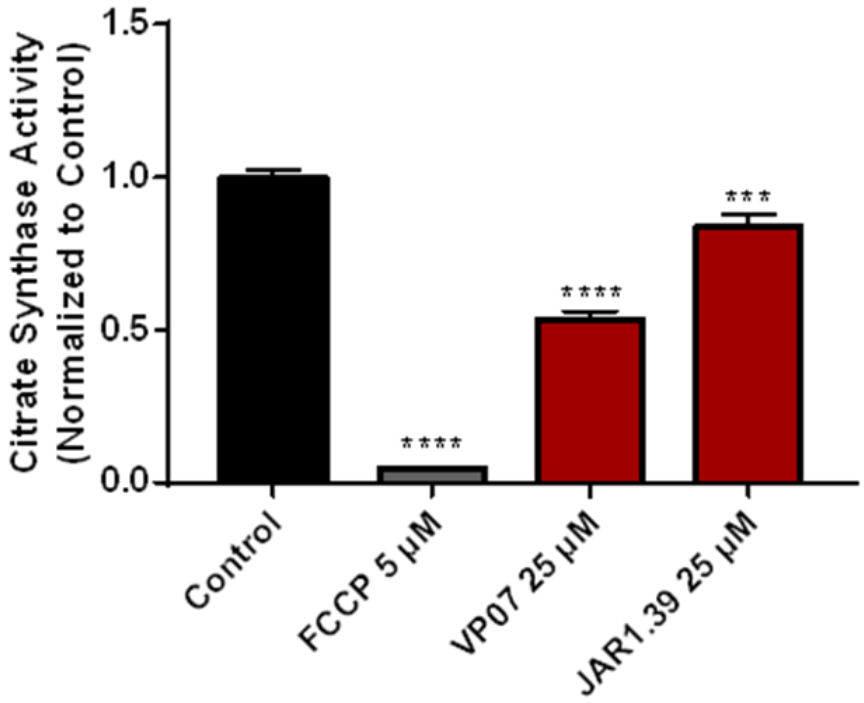

Figure 23. Citrate synthase assay in U2OS-iMLS-Parkin cells treated with FCCP 5 µM and VP07 and JAR1.39 at 25 µM for 24h. Data were normalized to control. Graphs represent the mean±SD of three replicates from one experiment. (Significance was determined by B) one-way ANOVA followed by Dunnett's multiple comparison test to control, where ****p<0.0001, ***p<0.001).

Last, LC3 immunostaining was done in U2OS-iMLS-Parkin cells treated with both, JAR1.39 and VP07. An increase in LC3 punctae was observed in the treated cells compared to control (Figure 24, above graph). In addition, LC3 colocalized more with mitochondria (represented only by the mCherry fluorophore from iMLS reporter) in cells treated with VP07 and JAR1.39 than in control cells (Figure 24, below graph).

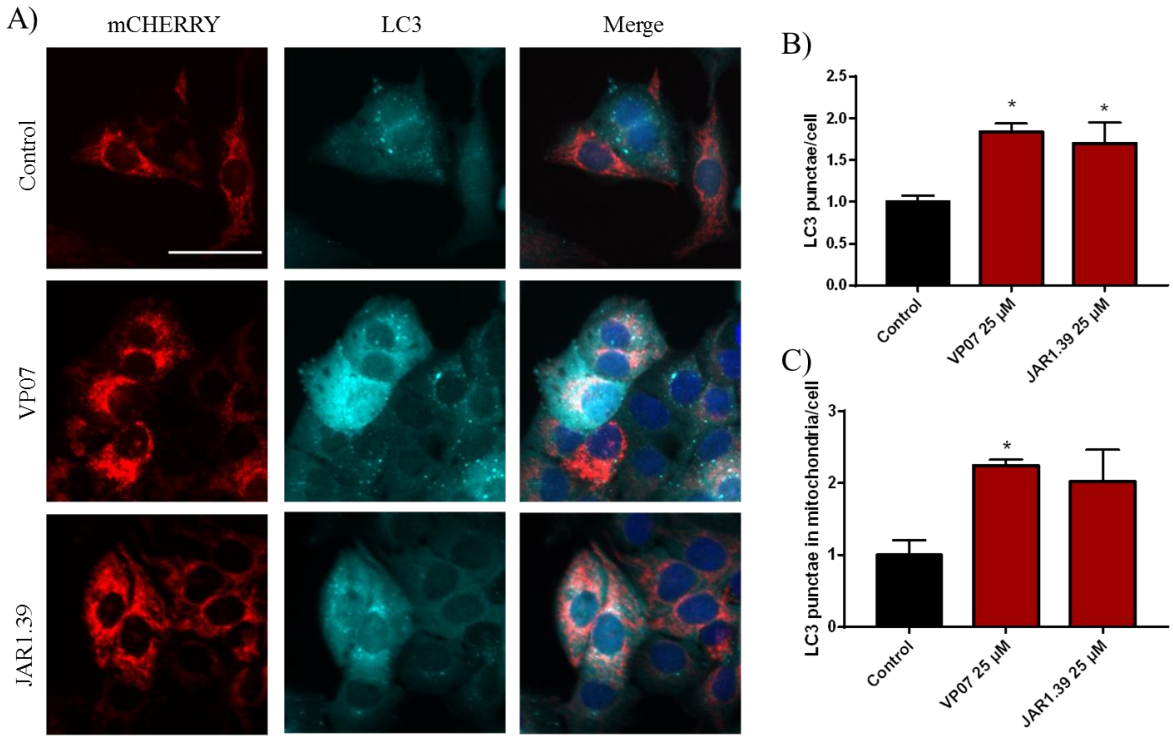

Figure 24. Immunostaining for LC3 in U2OS-iMLS-Parkin cells treated with VP07 and JAR1.39 at 25 µM for 24h. Data were normalized to control. Graphs represent the mean±SEM of three independent experiments. (Significance was determined by one-way ANOVA followed by Dunnett's multiple comparison test to control, where *p<0.05). Scale bar = 50 µm.

4.2.2 Hit confirmation in ARPE-19 MitoQC cells

Next, we validated the mitophagy-inducing capacity of both compounds using another cell type, ARPE-19, a human retinal pigment epithelial cell line that constitutively expresses Parkin.[167] In addition, this cell line expresses a different mitophagy reporter, mCherry-GFP-FIS1$_{101-152}$ (known as MitoQC), based on fusion of mCherry-GFP to the OMM protein FIS1.[143] Thus, this differs from the iMLS reporter, which contains a portion of NIPSNAP1, a matrix protein.[142]

As shown in Figure 25, both hits induced mitophagy at 25 µM for 24h. Thus, these results validated the efficacy of JAR1.39 and VP07 to enhance mitophagy in two different cell lines expressing two different mitophagy reporters.

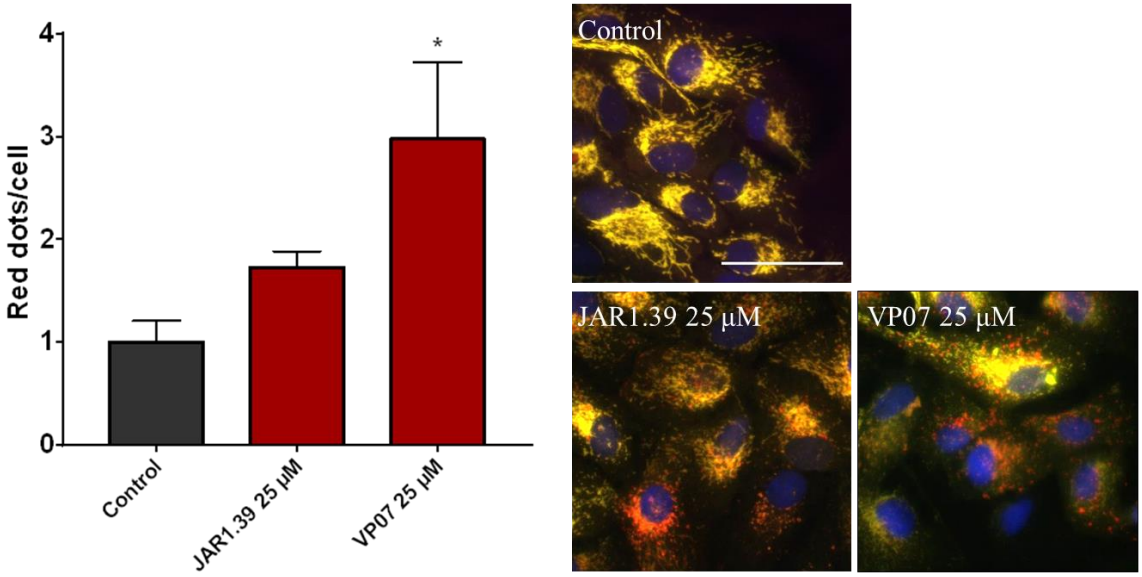

Figure 25 Validation of mitophagy inducing capacity of the compounds in the cell line ARPE-19 MitoQC. Cells were treated with the hit compounds, JAR1.39 and VP07, at 25 µM for 24h. Values were normalized to control (DMSO 0.1%). Data represent the mean±SEM of three experiments. (Significance was determined by one-way ANOVA, followed by Dunnett's multiple comparison test to control, where *p<0.05). Scale bar = 50 µm.

4.2.3 Finding the potential mechanism of action

4.2.3.1 Biological activity-based decoding

JAR1.39 and VP07 belong to the MBC library and were originally synthetized in a medicinal chemistry program designed to discover allosteric and brain permeable inhibitors of glycogen synthase kinase 3 (GSK3),[168] a kinase involved in neurodegeneration and several cellular processes like autophagy, inflammation, or oxidative stress.[169-170] Based on that, GSK3 inhibition was firstly considered a potential mechanism by which these two hits induced mitophagy. Nevertheless, the initial mitophagy screening (Figure 16) included other GSK3 inhibitors with diverse chemical structures such as iminothiadiazoles,[171] or thiadiazolidindiones[172] (Table 6). None of them induced mitophagy as it was observed by fluorescence microscopy. Thus, as all these diverse small molecules, VP1.14, VP1.15, VP3.15 and VP4.55 (Table 6), were GSK3 inhibitors, we concluded that mitophagy induction by JAR1.39 and VP07 was independent of their GSK3 inhibitory activity.

Table 6. Chemical structures of GSK3 inhibitors included in the screening phase, their IC_{50}, and images from the cellular assay. Scale bar = 20 µm.

Compound ID	Chemical structure	GSK3 IC_{50} (µM)	Cellular assay
JAR1.39	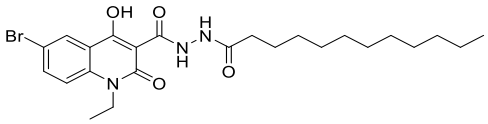	2.01	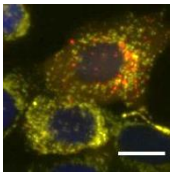
VP07	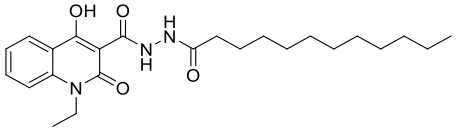	2.8	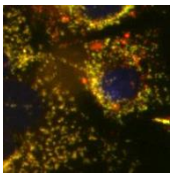
VP1.14	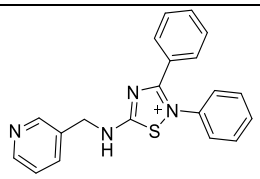	1.28	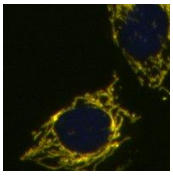
VP1.15	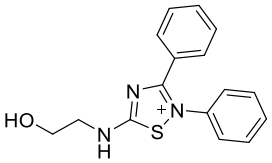	1.95	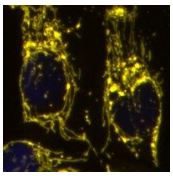
VP3.15	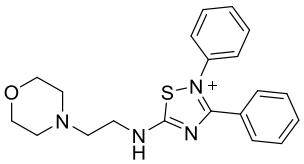	0.88	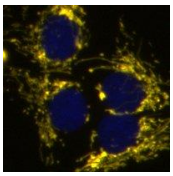
VP4.55	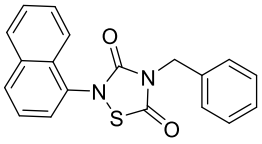	0.32	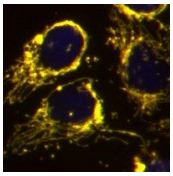

4.2.3.2 Chemical structure-based deciphering. Structure-activity relationship (SAR) studies

Next, we explored the mechanism of action by chemical SAR studies. As it was previously indicated, JAR1.39 and VP07 were synthesized in a medicinal chemistry project to target allosterically GSK3. Based on hydrazide-derivatives of a quinolone scaffold, new compounds were developed.[168]

To evaluate whether JAR1.39 and VP07 were modulating mitophagy due to their chemical structure, we included a set of 34 hydrazide-derivatives containing a quinolone scaffold in our mitophagy assay in ARPE-19 MitoQC cells (Figure 26 and Table 7).

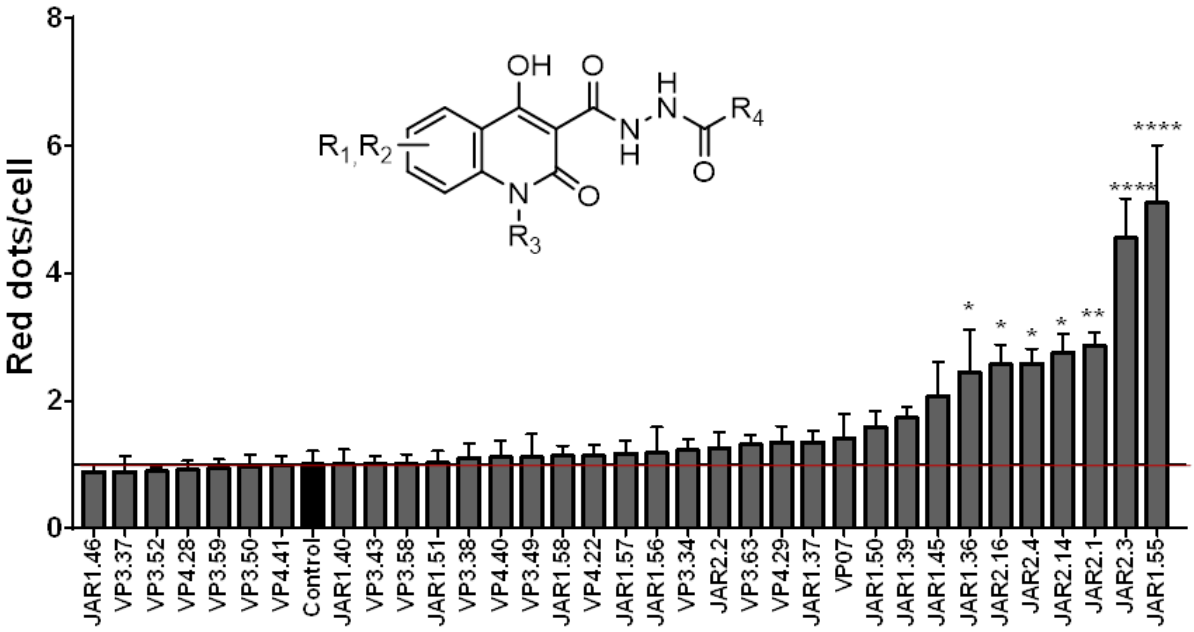

Figure 26. General chemical structure of hydrazide-derivatives of quinolines and evaluation of mitophagy induction of several related compounds. ARPE-19 MitoQC were treated at 25 μM for 24h. Data represent the mean±SEM of three independent experiments. Values were normalized to control. (Significance was determined by one-way ANOVA followed by Dunnett's multiple comparison test to control, where *p < 0.05, **p<0,01 and ****p<0.0001).

Results showed that several of these new compounds behaved as mitophagy enhancers independently of their inhibition on GSK3. They were then classified based on their degree of biological activity and a relationship between their potency to induce mitophagy and their chemical structure was obtained.

Table 7. Structure of hydrazide-derivatives of the quinolone family. ARPE-19 MitoQC cells were treated with the compounds at a final concentration of 25 µM for 24h. IC_{50} values obtained from Palomo *et al.*[168]

Cpd	Structure	IC_{50} GSK3	Cpd	Structure	IC_{50} GSK3	Cpd	Structure	IC_{50} GSK3
JAR1.55	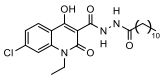	2.48	VP4.29	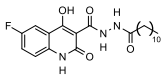	5.8	VP3.58	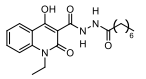	38% @10 µM
JAR2.3	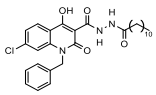	5.99	VP3.63	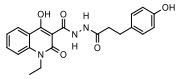	<20% @10 µM	VP3.43	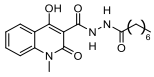	8.7
JAR2.1	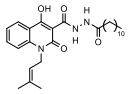	7.78	JAR2.2	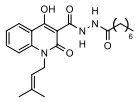	7.11	JAR1.40	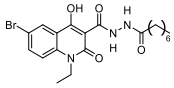	7.34
JAR2.14	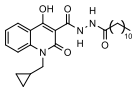	5.25	VP3.34	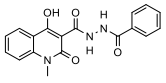	<20% @10 µM	VP4.41	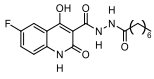	<20% @10 µM
JAR2.4	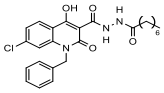	5.96	JAR1.56	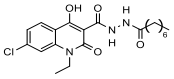	4.83	VP3.50	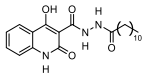	4.5
JAR2.16	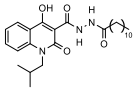	<20% @10 µM	JAR1.57	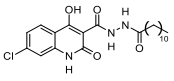	4.03	VP3.59	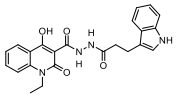	<20% @10 µM
JAR1.36	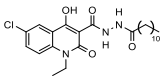	3.18	VP4.22	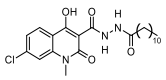	3.12	VP4.28	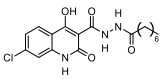	9.0
VP07	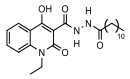	2.8	JAR1.58	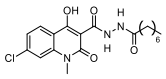	6.66	VP3.52	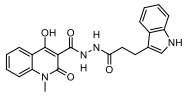	<20% @10 µM
JAR1.45	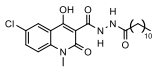	5.95	VP3.49	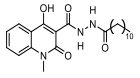	7.3	VP3.37	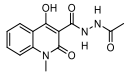	23% @10 µM
JAR1.39	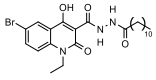	2.01	VP4.40	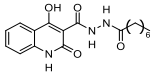	<20% @10 µM	JAR1.46	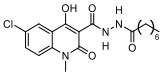	8.48
JAR1.50	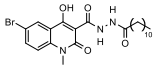	4.28	VP3.38	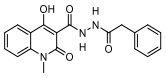	20% @10 µM			
JAR1.37	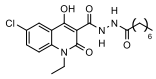	9.42	JAR1.51	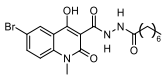	6.28			

In particular, the nature of the substituent in position R_4 (Table 7), aromatic or aliphatic, is of utmost importance for mitophagy induction. When the compound had an aromatic group in R_4, like phenyl, benzyl, or dimethylene heteroaryl fragments (derivatives VP3.34,

VP3.38, VP3.63, VP3.59, VP3.52, Figure 26 and 27 and Table 7), they did not enhance mitophagy.

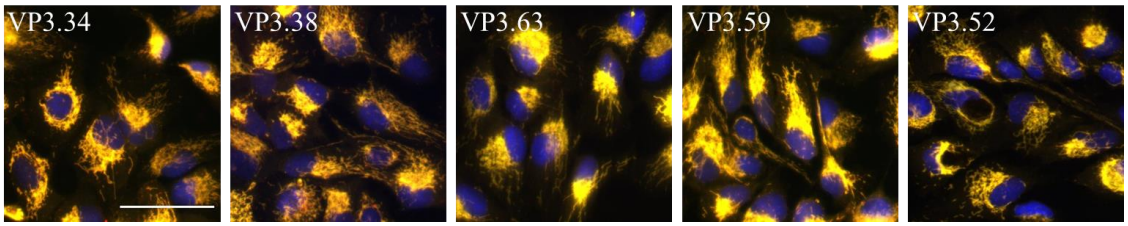

Figure 27. Representation of ARPE-19 MitoQC cells treated with compounds with an aromatic substituent in position R_4 at 25 µM for 24h. Scale bar = 50 µm.

However, if the substituent in R_4 was an aliphatic element, we could distinguish three different situations (Figure 28). If the alkylic moiety was very short, such as a methyl group (VP3.37), mitophagy was not induced. But, when R_4 was an aliphatic chain, their lengths became a key chemical feature for their biological activity.

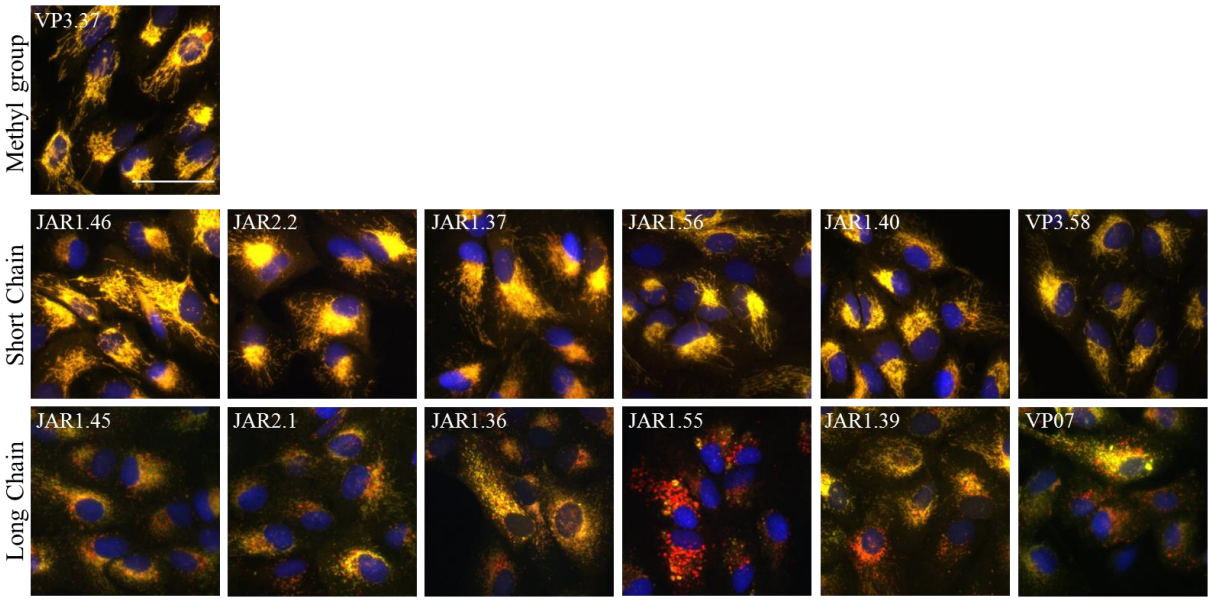

Figure 28. Representation of ARPE-19 MitoQC cells treated with compounds with an aliphatic element in R_4 at 25 µM for 24h. Only compounds with a long aliphatic substituent ($C_{11}H_{23}$) induced mitophagy. Scale bar = 50 µm.

Two situations were differentiated between short (C_7H_{15}) and long ($C_{11}H_{23}$) aliphatic chains. When comparing pairs of compounds with the same substituents in R_1, R_2 and R_3,

and different length of the aliphatic chain in R_4, only compounds with longer aliphatic chains in R_4 induced mitophagy.

As expected, JAR2.16, which also presented a long aliphatic chain composed with eleven carbon atoms, induced mitophagy (Figure 26 and 29). However, it did not inhibit GSK3 (IC_{50}>20 µM) (Table 7). Thus, we confirmed again the results obtained in the previous section 4.2.3.1: their capacity of mitophagy induction is independent of GSK3 inhibition. But the presence of a long aliphatic chain in their chemical structure is of utmost relevance for this biological property.

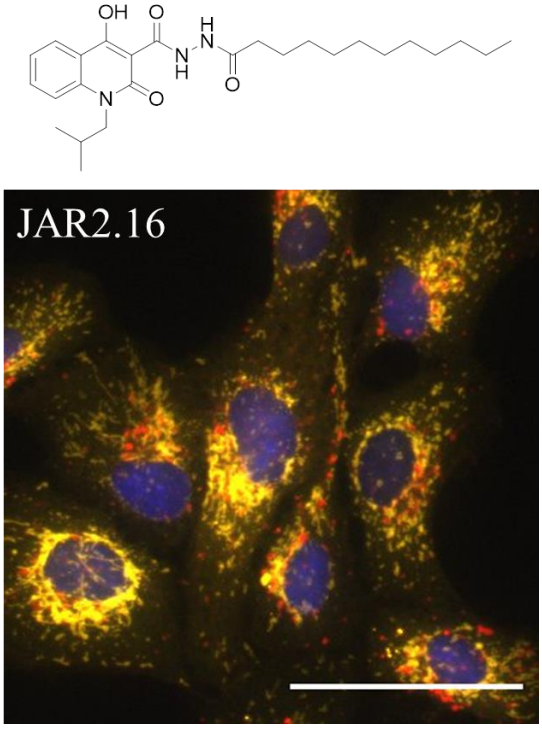

Figure 29. Structure and mitophagy induction by JAR2.16 at 25 µM for 24h. Scale bar = 50 µm.

Based on their chemical structure, the next question was whether the heterocycle was also required for mitophagy modulation. ARPE-19 MitoQC cells were treated with the hydrazides bearing aliphatic chains of eleven and seven carbons atoms, respectively. None of these two compounds induced mitophagy (Figure 30). This result confirmed that, the heterocycle, a quinolone scaffold, and the long aliphatic chain joined to the hydrazide moiety were needed to induce mitophagy.

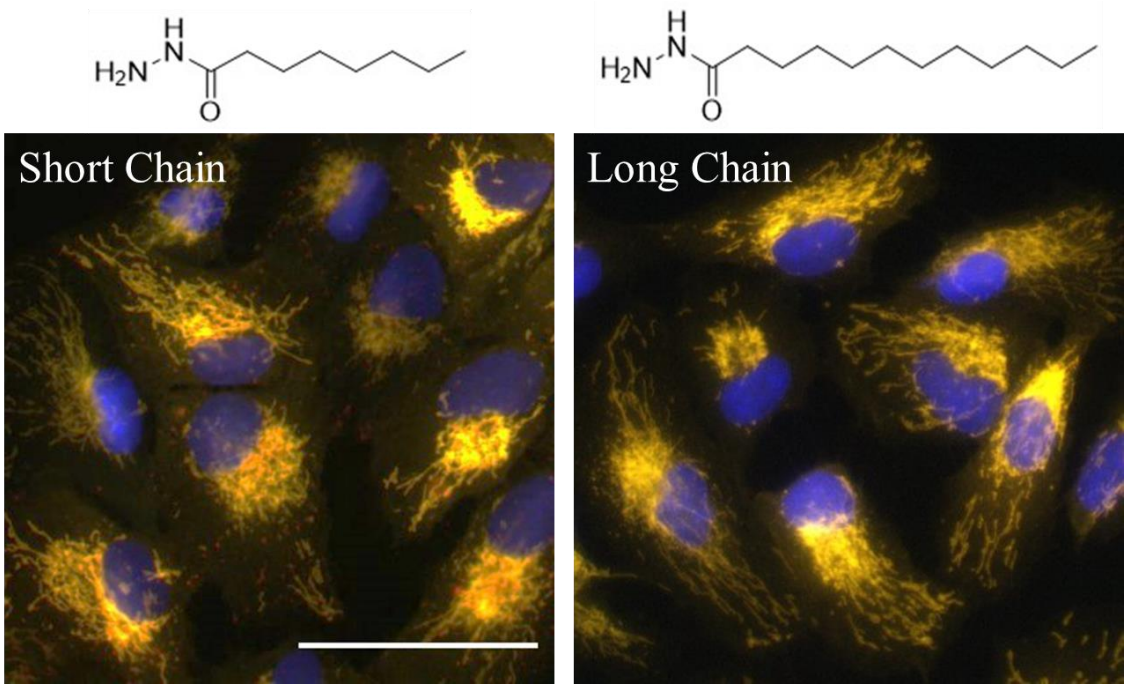

Figure 30. ARPE-19 MitoQC cells treated with the hydrazide with short (C_7H_{15}) and long ($C_{11}H_{23}$) aliphatic chain at 25 µM for 24h. Scale bar = 50 µm.

Further analysis of the biological data and chemical structure revealed the impact on mitophagy modulation by the substituent of the quinolone heterocycle. Interestingly, substituents in the heterocyclic nitrogen had an important function in the biological response, inducing more mitophagy as the lipophilicity of the substituents increased. Accordingly, mitophagy activity was amplified with the number of atoms present in the alkyl moiety (Me<Et<iPr<Bn) attached to the nitrogen aromatic atom, whereas the absence of substituent in this position did not induce it (see VP3.49<VP07<JAR2.16<JAR2.3 compounds, Figure 26 and 31A). In fact, compound JAR2.4, which had a benzyl moiety attached to the aromatic nitrogen, but an aliphatic chain of seven carbon atoms, is a good mitophagy inducer (Figure 26 and 31B).

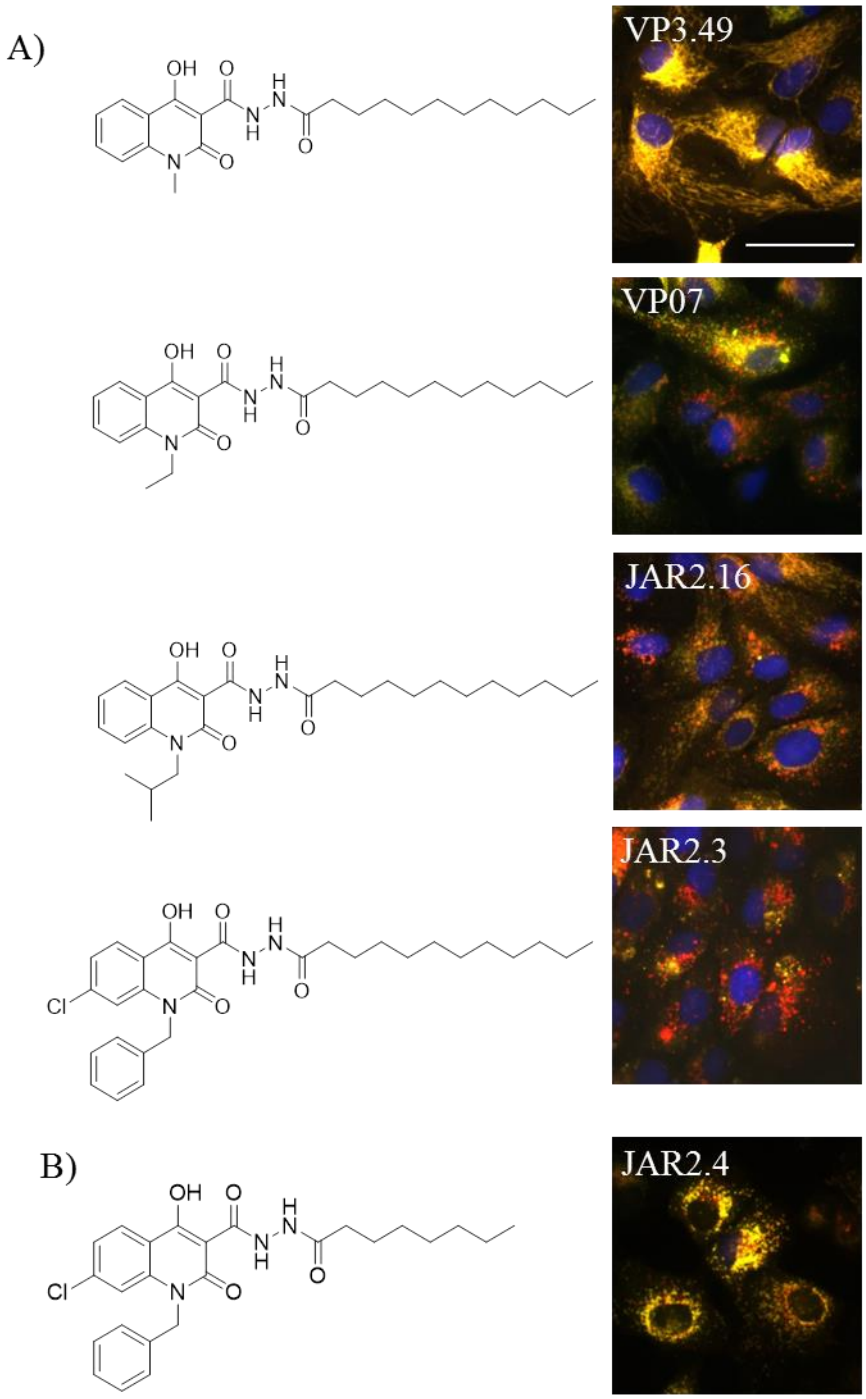

Figure 31. Importance of the lipophilicity of the substituent of the aromatic nitrogen on mitophagy induction. Representation fo ARPE-19 MitoQC cells treated with the compounds at 25 µM for 24h. A) More mitophagy was observed as the lipophilicity of the substituents increased. B) JAR2.4, with a benzyl group in the aromatic nitrogen, induced mitophagy with an aliphatic chain of seven carbon atoms. Scale bar = 50 µm.

4.2.4 Therapeutic potential of mitophagy inducers

Last, we proceeded to study the therapeutic effect of our mitophagy enhancers in cellular models of PD, as mitophagy defects have been reported in the idiopatic form of the disease.[173] For that, we used the human neuroblastoma cell line SH-SY5Y expressing the MitoQC reporter and treated them with PQ and 6-OHDA, two commonly used toxins to mimic PD.

As expected, PQ decreased significantly basal mitophagy compared to control (Figure 32), which confirmed the mitophagy block in this model. The pre-treatment with VP07, avoided this mitophagy reduction caused by PQ while a similar tendency was observed with 6-OHDA treatment. These results confirmed the therapeutic potential of mitophagy inducers, and particularly VP07, recovering the mitophagy deficits observed in PD.[174]

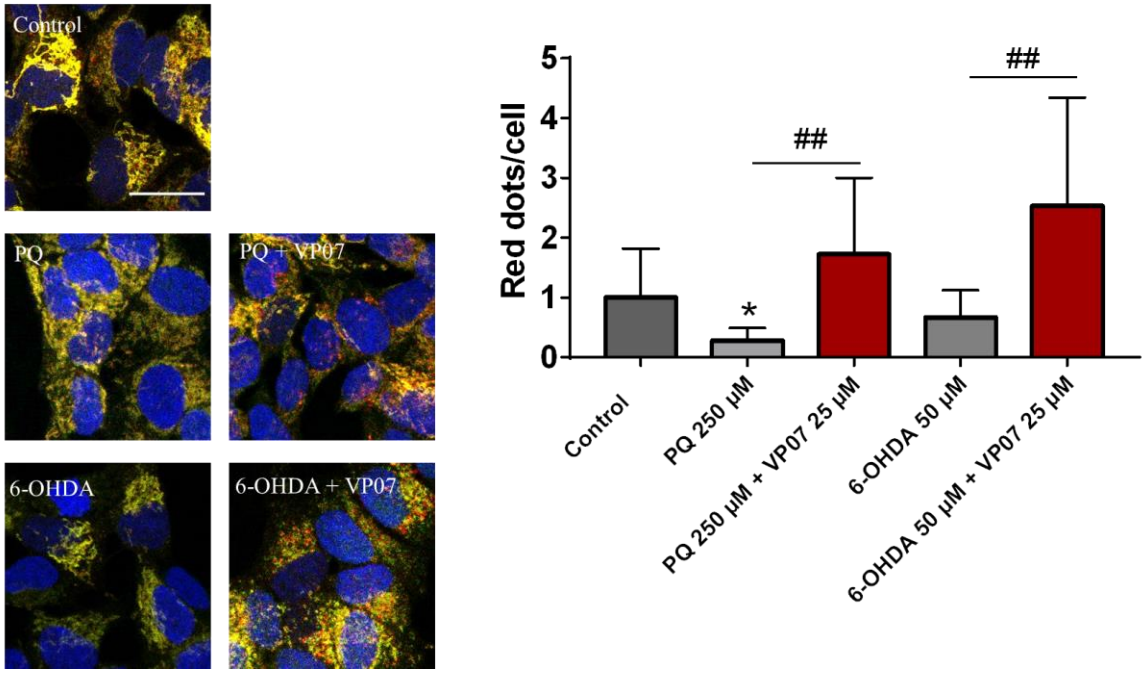

Figure 32. Therapeutic modulation of mitophagy by VP07 in a PD chemical model. SH-SY5Y MitoQC cells (100,000 cells/mL) were pretreated with VP07 25 µM for 1h and treated with PQ 250 µM or 6-OHDA 50 µM for 24h. The graph represents the mean±SD of one independent experiment. Data were normalized to control. (Significance was determined by unpaired two tailed t-test, where *p<0.05, significantly different from control, ## p<0.01 significantly different from PQ or 6-OHDA). Scale bar = 20 µm.

4.3 Characterization and therapeutic potential of a new mitophagy inhibitor

In this chapter, the mitophagy inhibitor identified in the screening described in chapter 1, named IGS2.7, is further characterized to find a possible mechanism of action and to test its therapeutic applicability.

4.3.1 Characterization of IGS2.7 in U2OS-iMLS cells

In a first approach we stablished a dose-response relationship of the inhibitor. U2OS-iMLS cells were treated with the mitophagy inducer DFP at 1 mM with increasing concentrations of IGS2.7 from 1.56 to 25 µM (Figure 33). When cells were treated only with DFP, the formation of mitolysosomes (red-only punctae) was seen. As shown in Figure 33 the co-treatment with IGS2.7 reduced mitophagy as its concentration increased, being almost completely blocked at the highest concentration, 25 µM.

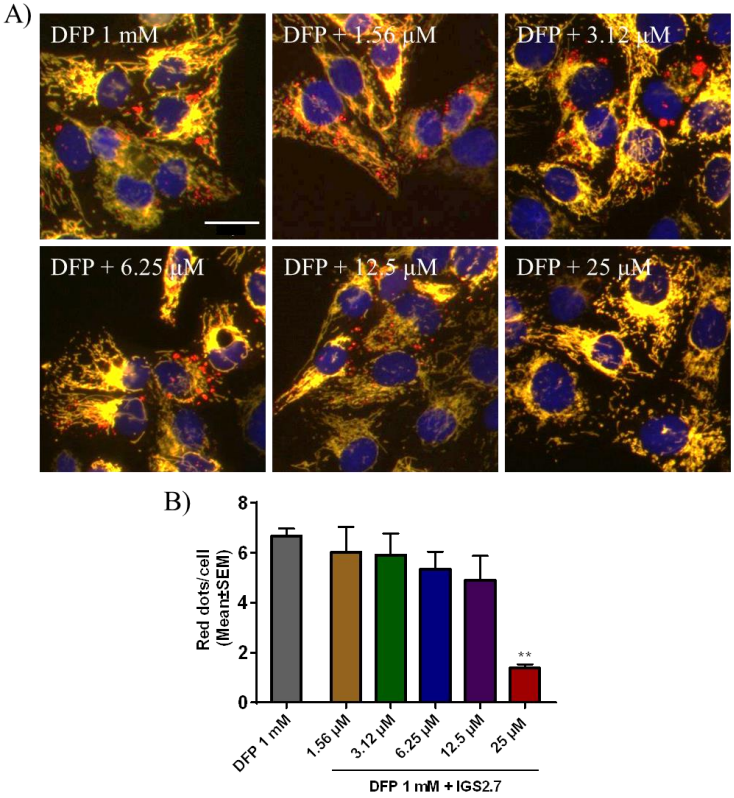

Figure 33. IGS2.7 reduces DFP- induced mitophagy in U2OS-iMLS cells. A) Representation of cells treated with DFP and increasing doses of IGS2.7. B) Quantification of mitophagy flux (red dots only per cell). Data represent mean±SEM of two independent experiments. (Significance was determined by one-way ANOVA followed by Dunnett's multiple comparison test to control, where **p<0.01). Scale bar = 30 µm.

Thus, we confirmed 25 µM as the concentration by which IGS2.7 inhibited DFP-induced mitophagy. But is the compound modulating mitophagy in basal conditions too? Results extracted from the screening (Figure 15) showed no difference in mitophagy when cells were treated alone with the compound compared to control cells (Figure 34). With this, we corroborated that IGS2.7 inhibited DFP-induced mitophagy in U2OS-iMLS but not basal mitophagy.

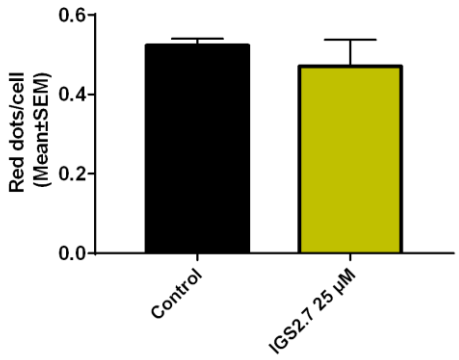

Figure 34. Basal mitophagy modulation by IGS2.7 at 25 µM for 24h. Graph extracted from Figure 15.

4.3.2 IGS2.7 did not modulate basal mitophagy *in vivo*

Next, we examined if the compound could modulate mitophagy in MitoQC mice, which express the reporter MitoQC. IGS2.7 was not able to inhibit the pathway after 8h of administration (Figure 35), probably because mitophagy was not basally enhanced and corroborating the lack of inhibition of basal autophagy found in U2OS-iMLS cells. Animals were also treated for 24h, obtaining similar results (data not shown).

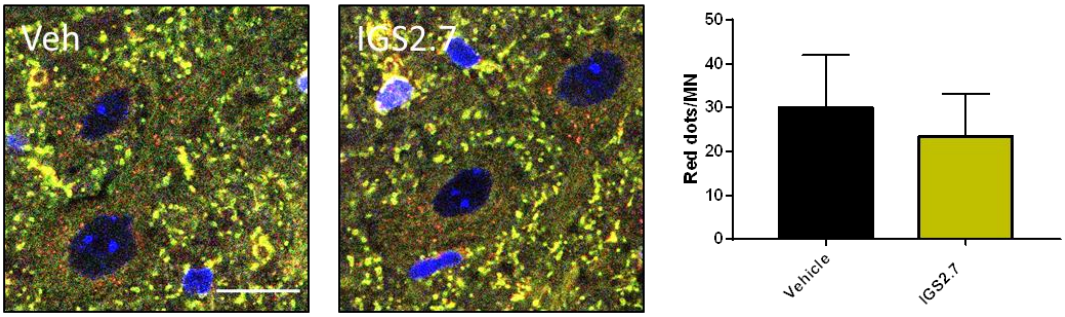

Figure 35. IGS2.7 did not modulate basal mitophagy in MN of MitoQC mice. Histological samples of the anterior horn of the spinal cord of two MitoQC mice treated with IGS2.7 1 mg/Kg for 8h. Mitophagy quantification was done in MN. Data represent mean±SD of one independent experiment. Scale bar = 20 µm.

4.3.3 IGS2.7 as a mitophagy inhibitor in ARPE-19 MitoQC cells

Thus, as IGS2.7 inhibited DFP-induced mitophagy, we proved its mitophagy-inhibitory capacity in ARPE-19 MitoQC cells, which display higher basal mitophagy. Cells were treated with the compound at 25 µM and a decreased of almost 40% of red-only punctae were quantified (Figure 36). This indicates that IGS2.7 is able to inhibit basal mitophagy in ARPE-19 cells.

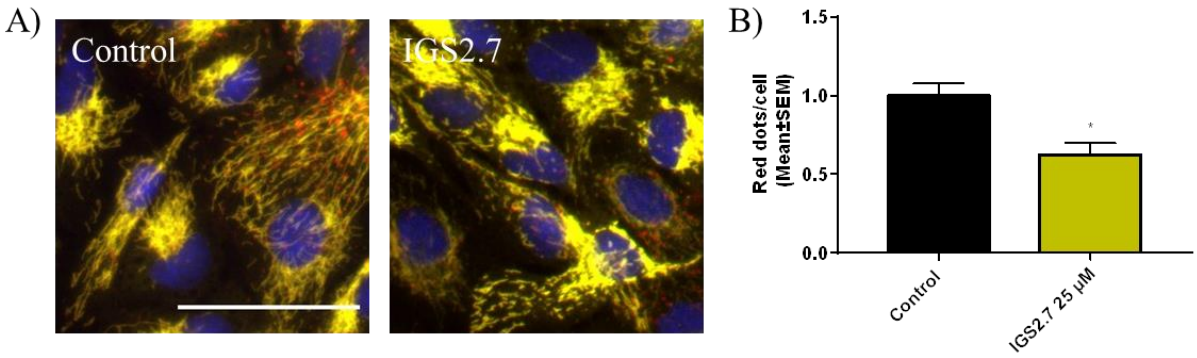

Figure 36. IGS2.7 inhibited basal mitophagy in ARPE-19 MitoQC cells. A) Representation of cells treated with IGS2.7 25 µM for 24h. B) Quantification of mitophagy flux (red dots only per cell). Data represent mean±SEM of three independent experiments. (Significance was determined by unpaired two tailed t-test, where *p<0.05, significantly different from control). Scale bar = 50 µm.

Thus, if we compare mitophagy inhibition by IGS2.7 in the three cell types, we obtained interesting results (Figure 37). As we have already seen, IGS2.7 reduced DFP-induced mitophagy in U2OS-iMLS cells. As this cell line does not express Parkin, CCCP did not induce mitophagy and the co-treatment with IGS2.7 did not change the pathway (Figure 37A). Interestingly, when Parkin is exogenously and endogenously expressed, in U2OS-iMLS-Parkin (Figure 37B) and ARPE-19 MitoQC cells (Figure 37C) respectively, IGS2.7 trended to decrease DFP-induced mitophagy. However, IGS2.7 never blocked CCCP-induced mitophagy.

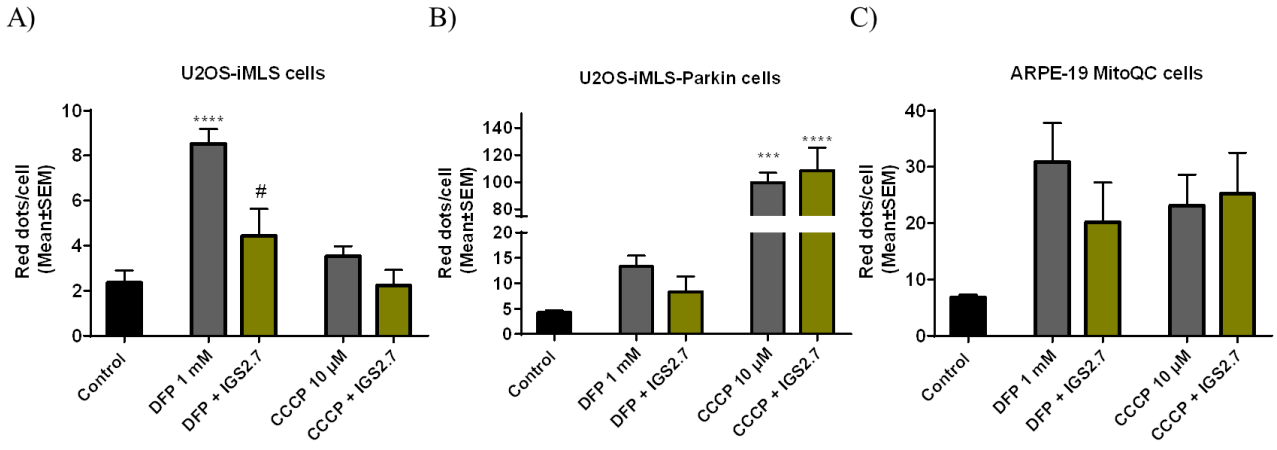

Figure 37. Induced-mitophagy modulation by IGS2.7. U2OS-iMLS, U2OS-iMLS-Parkin cells and ARPE-19 MitoQC cells were treated with the inducers DFP 1 mM and CCCP 10 µM alone and in combination with IGS2.7 25 µM. Data represent mean±SEM of three independent experiments. (Significance was determined by one-way ANOVA followed by Dunnett's multiple comparison test, where ***p<0.001 and ****p<0.0001 different from control and #p < 0.05 different from DFP 1 mM).

With these results, we can conclude that IGS2.7 is capable to block Parkin-independent mitophagy. This effect is confirmed in U2OS-iMLS cells, in which Parkin is not expressed. Besides, similar tendency was observed in the other two cell lines.

4.3.4 Potential mechanism of action of IGS2.7 in mitophagy modulation

The next step was to decipher the mechanism of action by which the compound inhibited mitophagy.

4.3.4.1 IGS2.7 as protein casein kinase 1 (CK1) inhibitor

Our compound IGS2.7 belongs to the MBC library and was synthesized initially in a medicinal chemistry program focused on new casein kinase 1 (CK1) inhibitors.[175] CK1 is one of the kinases involved in the *in vivo* phosphorylation of TDP-43,[176] a hallmark of ALS.[177]

Based on that, CK1 inhibition was firstly considered as a potential mechanism of action by which the hit IGS2.7 reduced mitophagy. However, other CK1 inhibitors, such as IGS3.4 and IGS3.27 (Table 8), from the same chemical family and similar biological potency were included in the initial screening and none of them reduced mitophagy (Figure

17). Thus, we concluded that IGS2.7 modulated mitophagy independently of its activity on CK1.

Table 8. Chemical structures of CK1 inhibitors included in the screening phase, their IC_{50} and the percentage of activity of the kinase ULK1.

Compound	Structure	CK1δ/ε IC_{50} (nM)	ULK1 %Inhibition @10μM
IGS2.7	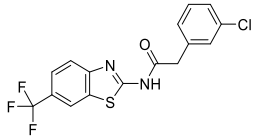	23/840	59
IGS3.27	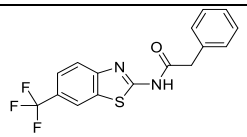	47/750	11.4
IGS3.4	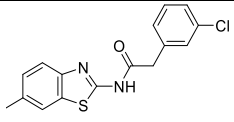	83/880	9

4.3.4.2 IGS2.7 as UNC51 like kinase-1 (ULK1) inhibitor

Benzothiazole IGS2.7 is an ATP-competitive inhibitor when targets CK1. This fact highlights the chance of inhibiting other kinases and lack of kinase selectivity. Previous results from our lab determined the selectivity of IGS2.7 at 10 μM against a panel of 456 protein kinases. As expected, the compound inhibited close to 100% the activity of CK1, its primary target. Besides, IGS2.7 reduced almost 60% the activity of the autophagy-related kinase ULK1.[175] Interestingly, we evaluated the rest of compounds described in Table 8 in a kinase assay against ULK1, and none of them inhibited its kinase activity (Table 8). Thus, ULK1 inhibition appeared as a possible mechanism of action by which IGS2.7 inhibited mitophagy. ULK1 is a serine/threonine-specific protein kinase that plays a central role in starvation-induced autophagy.[178]

To probe this hypothesis, we compared autophagy and mitochondria-related protein profiles in ARPE-19 MitoQC cells treated with MRT68921, an ULK1 inhibitor commonly used to reduce autophagy and IGS2.7 (Figure 38).

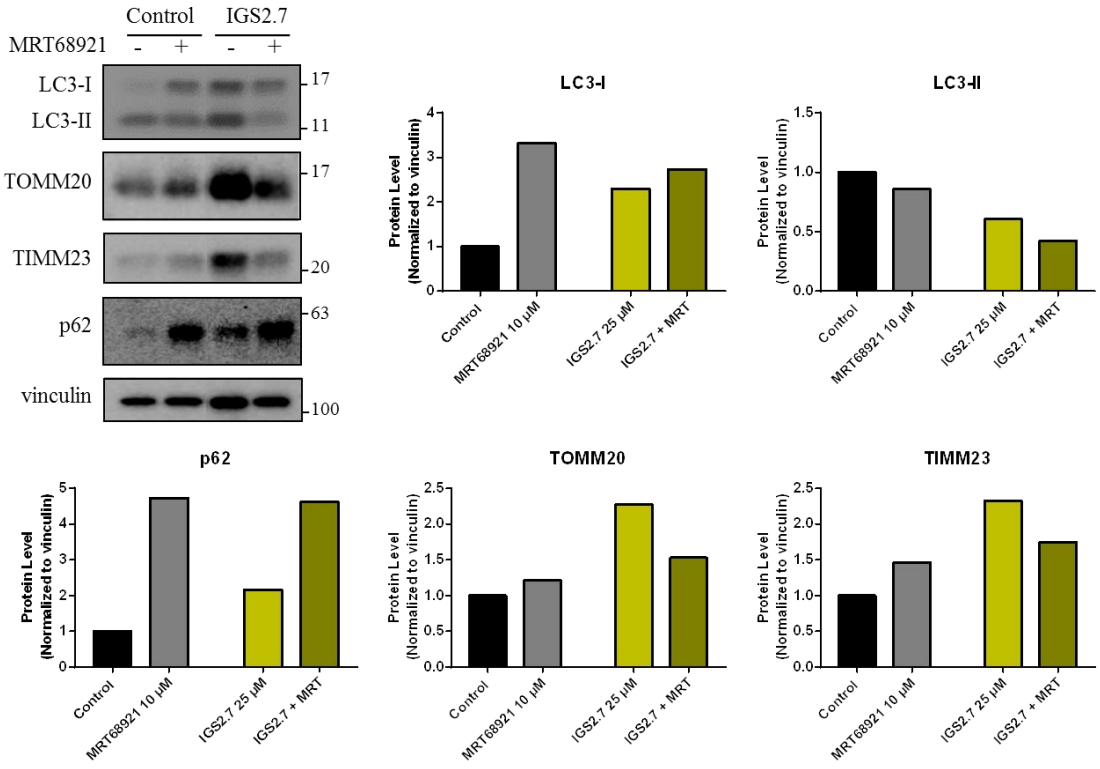

Figure 38. IGS2.7 acted like the ULK1 inhibitor, MRT68921. Western blot and quantification of LC3-I, LC3-II, p62, TOMM20 and TIMM23. ARPE-19 MitoQC cells were treated with MRT68921 10 µM and IGS2.7 25 µM 24h. Data represent results from one experiment and were normalized to control.

The first interesting result obtained was the accumulation LC3-I when cells were treated with MRT68921 and IGS2.7. The co-treatment of both inhibitors also induced an accumulation of LC3-I, although there was not a synergy, which could mean both compounds modulate the same pathway. However, LC3-II was not increased, but a tendency in lower protein accumulation was reporter with the inhibitors. This suggests a blockage in the initial steps of autophagy, when LC3-II lipidation occurs. Interestingly, p62, another autophagy surrogate marker, which is accumulated if autophagy is blocked, was also increased upon treatment with both inhibitors. This showed again how IGS2.7 inhibited the pathway, similar to MRT68921.

Then, to prove whether this blockage on autophagy is related to mitophagy, the mitochondrial mass proteins TOMM20 and TIMM23 were also analyzed. MRT68921 slightly induced accumulation of mitochondrial proteins, while the accumulation of both proteins was relevant upon treatment with IGS2.7.

Thus, with these results we demonstrated that IGS2.7 inhibited autophagy similar to MRT68921, probably by inhibiting ULK1, and promoted mitochondrial mass accumulation. This could be translated in mitophagy inhibition, which corroborates our results from the phenotypic assay.

To further confirm autophagy modulation by IGS2.7, an immunofluorescence of LC3 was studied in U2OS-iMLS cells. LC3 punctae was decreased in U2OS cells treated with IGS2.7 at 25 µM for 24h compared to control (Figure 39). This supports our hypothesis of IGS2.7 acting as an initiation phase inhibitor, which could block the recruitment of LC3, thus acting as an autophagy and a mitophagy inhibitor.

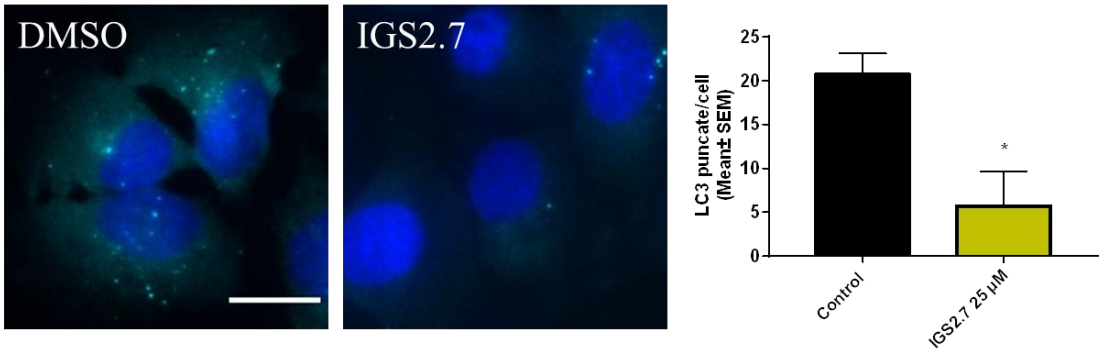

Figure 39. IGS2.7 reduced LC3 punctae in U2OS-iMLS. Cells were treated with IGS2.7 25 µM for 24h and then immunostained for LC3. Data represent the mean±SEM of three independent experiments. (Significance was determined by unpaired two tailed t-test, where *p<0.05, significantly different from control). Scale bar = 20 µm.

4.3.5 Therapeutic potential of IGS2.7 as autophagy/mitophagy inhibitor

Last, we explored the therapeutic potential of IGS2.7 as an autophagy/mitophagy inhibitor. Previous results from our group showed the efficacy of IGS2.7, as a CK1 inhibitor, to restore hallmarks of ALS in two different models of the disease. In lymphoblasts from ALS patients, IGS2.7 restored the pathology of TDP-43 and it also modulated the disease in the TDP-43^{A315T} mice model.[179]

ALS models showed alteration in autophagy and mitophagy pathways.[108] However, some results reported an increase in the processes,[99,103] while others showed a block in autophagy flux.[102] Thus, the upregulation and downregulation of the pathway by molecules have been explored and again, controversial results have been obtained.[104,106] Thus, we

proceeded to study autophagy and mitophagy in our models and the treatment with our inhibitor, IGS2.7, in order to decipher the mechanism of action responsible of the efficacy of this compound.

4.3.5.1 Cellular and animal SOD1 model of ALS

We explored the levels of autophagy in immortalized lymphoblasts from patients with ALS. We distinguish three different groups: control subjects, samples from sporadic ALS patients (sALS) and samples from ALS patients bearing a mutation in superoxide dismutase 1 or SOD1 (SOD1-ALS). The best way to study autophagy is by measuring 'autophagy flux'. As autophagy is a very dynamic process, with this measurement we can compare LC3-II accumulation with and without lysosomal inhibitors. For that, samples were treated for 3h with HCQ. HCQ affects the last phase of autophagy by increasing lysosomal pH and inhibiting the fusion between autophagosomes and lysosomes.[180] Thus, LC3-II accumulation was determined, and the ratio was calculated to measure autophagy flux (Figure 40).

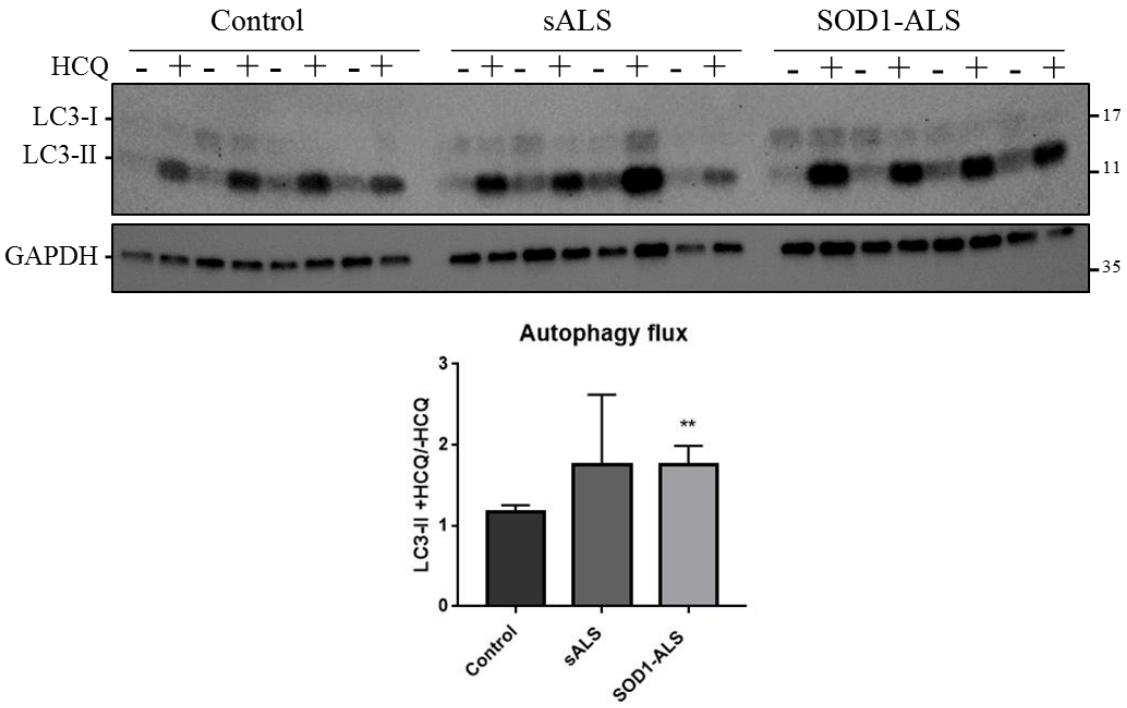

Figure 40. SOD1-ALS samples showed higher autophagy flux. Western blot of lymphoblasts from control, sALS and SOD1-ALS samples treated with 30 µg/mL HCQ for 3h. Data were normalized to control and represent mean±SEM of three independent experiments. (Significance was determined by one-way ANOVA followed by Dunnett's multiple comparison test to control, where **p<0.01).

SOD1-ALS samples showed higher autophagy flux compared to control samples. In contrast, sALS samples showed higher variability, and no differences were found.

Then, as autophagy was only increased in SOD1-ALS samples, we explored the therapeutic ability of the inhibitor IGS2.7 in these samples to restore autophagy flux to normal levels. Importantly, although 25 µM was the concentration of IGS2.7 effective in inhibiting autophagy in previous characterization experiments, here we decreased the dose of IGS2.7 to treat lymphoblasts to 5 µM, as this was the concentration known to decrease TDP-43 phosphorylation in these cells.[179] Similarly, cells were treated with IGS2.7 for 24h. To measure autophagy flux, HCQ was added for the last 3h of incubation (Figure 41). Results revealed a decrease in autophagy flux in SOD1-ALS when the samples were treated with IGS2.7. However, autophagy flux was similar in control samples with and without the inhibitor. Thus, these results confirmed again that IGS2.7 inhibited autophagy or mitophagy only when they are increased and not under basal conditions.

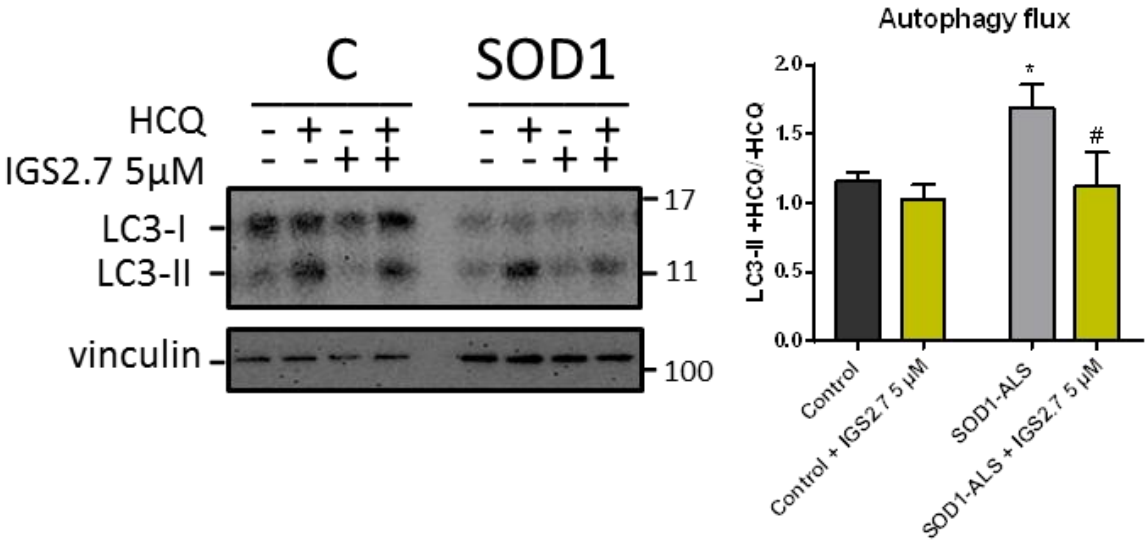

Figure 41. IGS2.7 restored autophagy flux in SOD1-ALS samples. Cells were treated with IGS2.7 5 µM for 24h. 30 µg/mL HCQ 30 µg/mL was added during the last 3h. Data represent mean±SEM of four independent experiments. (Significance was determined by one-way ANOVA followed by Dunnett's multiple comparison test, where *p<0.05 versus control and #p<0.05 versus SOD1-ALS).

Since SOD1 was described as the first gene known to be mutated in ALS, several mice models have been developed. The most used is SOD1^{G93A}, which recapitulates better human pathology.[181]

Here, we studied autophagy levels in this model compared with wild-type animals. Mice were sacrificed at 112-115 days. We performed an immunostaining of autophagy and mitochondrial proteins in the ventral horn, where the MN are localized. As the animals were not treated with an autophagy blocker, autophagy flux could not be measured. However, we used p62 levels as a surrogate marker for autophagy and TOMM20 to measure mitochondrial mass. Figure 42 revealed a decrease in the amount of p62 protein per MN in transgenic mice compared to WT. Thus, an increase in autophagy flux could be considered in these samples, similar to the findings from SOD1 lymphoblasts. Moreover, the amount of mitochondrial mass, measured by TOMM20, was also decreased in the model. This highlights the hypothesis of a possible induction of mitophagy.

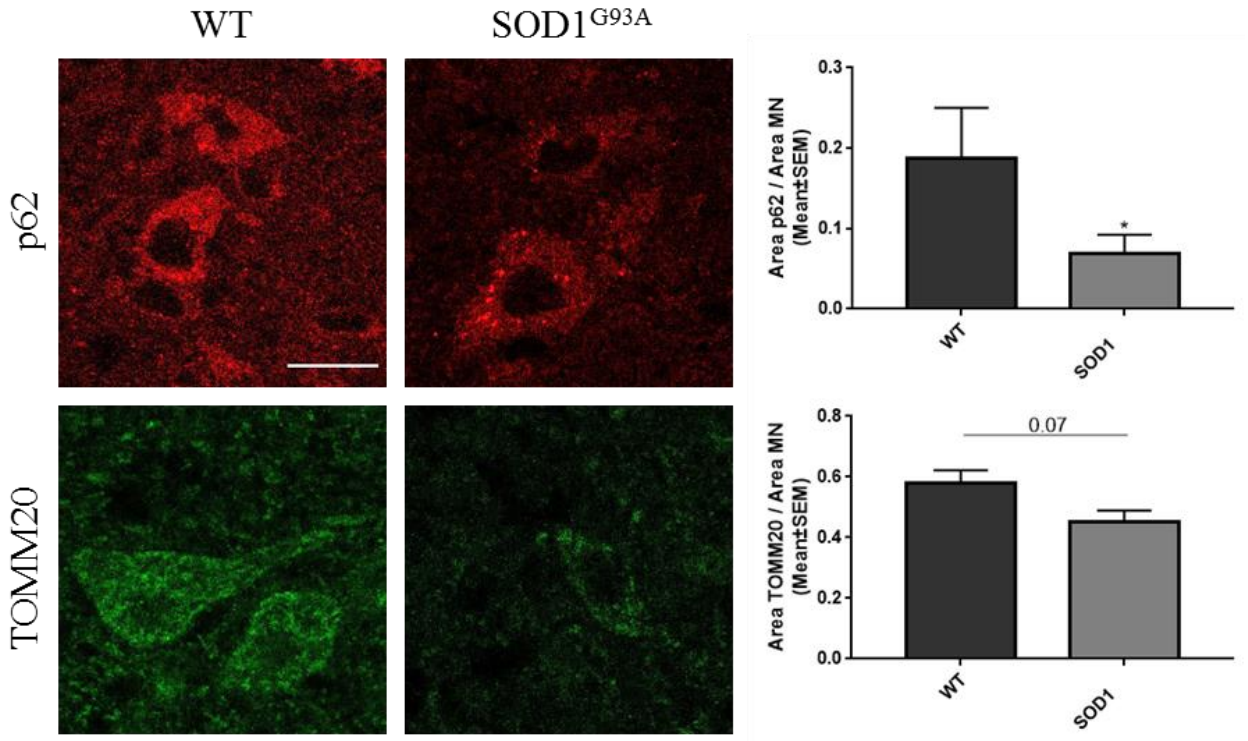

Figure 42. Autophagy was increased in SOD1 mouse model of ALS. Histological samples of the anterior horn of the spinal cord of SOD1^{G93A} and wild-type mice. Tissues were immunostained for p62 and TOMM20 and quantified per MN. Data represents mean±SEM of four different control and nine transgenic mice. (Significance was determined by unpaired two tailed t-test, where *p< 0.05, significantly different from control). Scale bar = 20 µm.

What was interesting was the loss of MN in SOD1^{G93A} animals compared to WT mice. As seen in Figure 43, where a field of view is represented, less number of MN can be quantified. In addition, although there were less p62 level in the remaining MN of SOD1^{G93A} mice, protein accumulation was found in the extracellular matrix, probably being debris from degenerative MN.

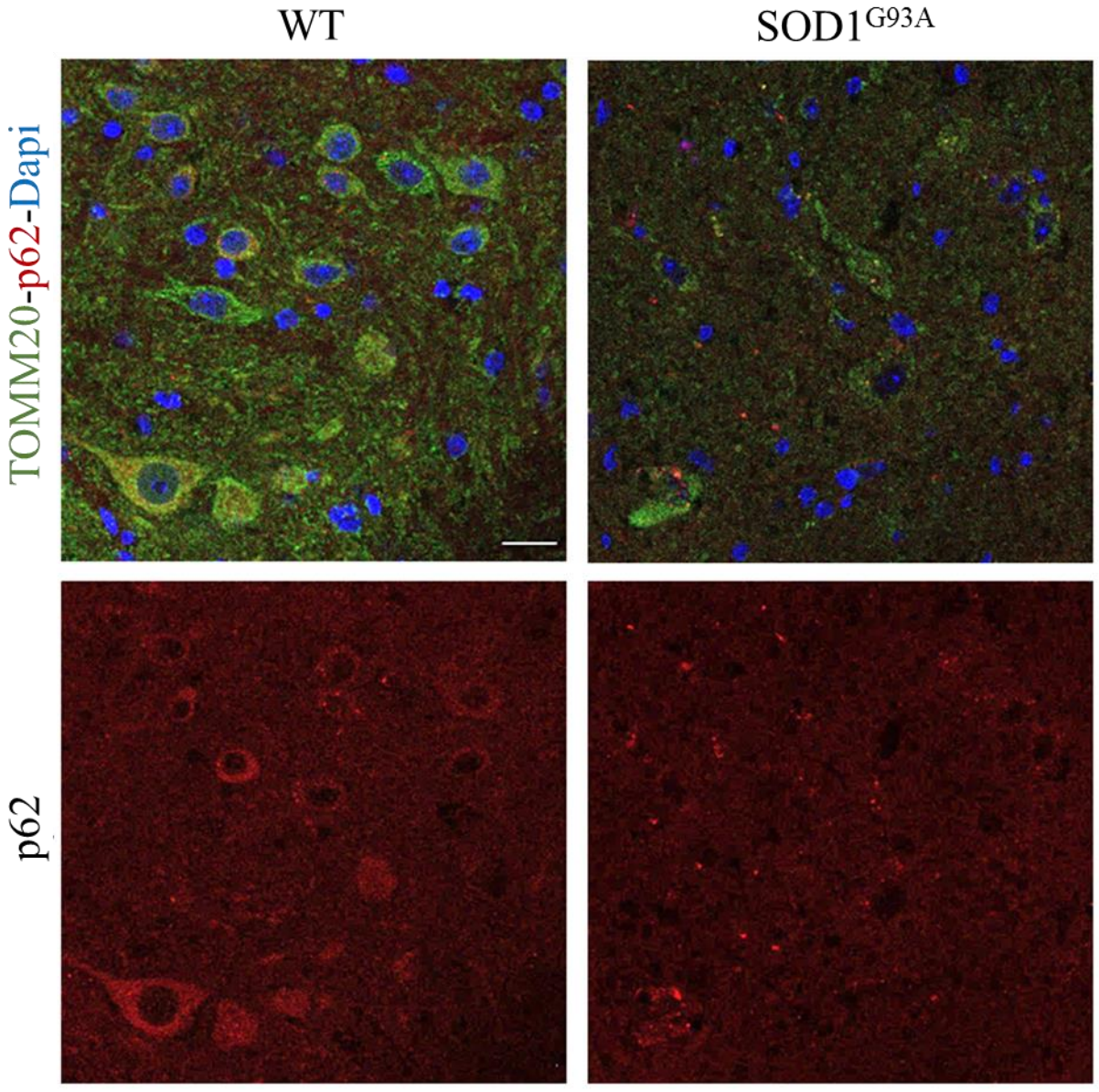

Figure 43. Representation of a field of view of the ventral horn from the spinal cords sections of WT and SOD1^{G93A} mice. Scale bar = 20 µm.

4.3.5.2 Cellular and animal TDP43 model of ALS

In addition, we studied autophagy levels in a new batch of samples from two patients bearing a mutation in TDP-43 (TDP43-ALS). Based on the results obtained from SOD1 lymphoblasts, these new samples were directly treated with the inhibitor IGS2.7 at 5 µM. Results showed an increase in autophagy flux in TDP43-ALS compared to control subjects. The treatment with IGS2.7 restored autophagy levels to control (Figure 44).

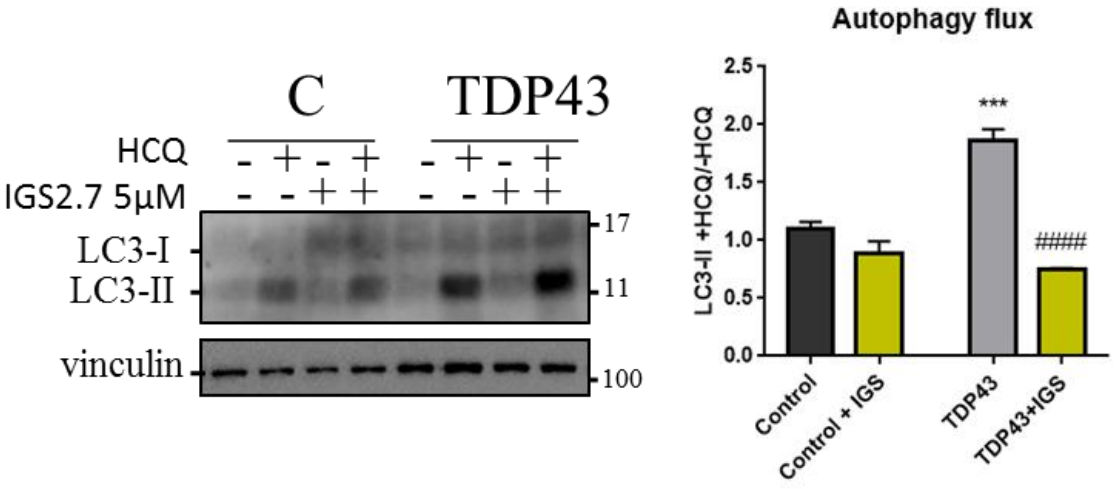

Figure 44. IGS2.7 restored autophagy flux in TDP43-ALS samples. Cells were treated with IGS2.7 5 µM for 24. 30 µg/mL HCQ was added during the last 3h. Data represent mean±SEM of three independent experiments. (Significance was determined by one-way ANOVA followed by Dunnett's multiple comparison test, where ***p<0.005 versus control and ####p<0.001 versus TDP43-ALS).

Finally, we studied the potential of IGS2.7 of modulating autophagy and mitophagy in a transgenic mouse model of ALS with a mutation in TDP-43^{A315T}.[182] Four groups were studied: wild-type animals treated with vehicle (WT), transgenic animals treated with vehicle (TDP-Veh), and transgenic animal treated with two doses of IGS2.7, 0.5 mg/Kg (TDP-0.5) and 1 mg/Kg (TDP-1). Animals were treated from the age of 65 days up to 95 days. Then, we performed an immunostaining of p62 and TOMM20 in the ventral horn (Figure 45).

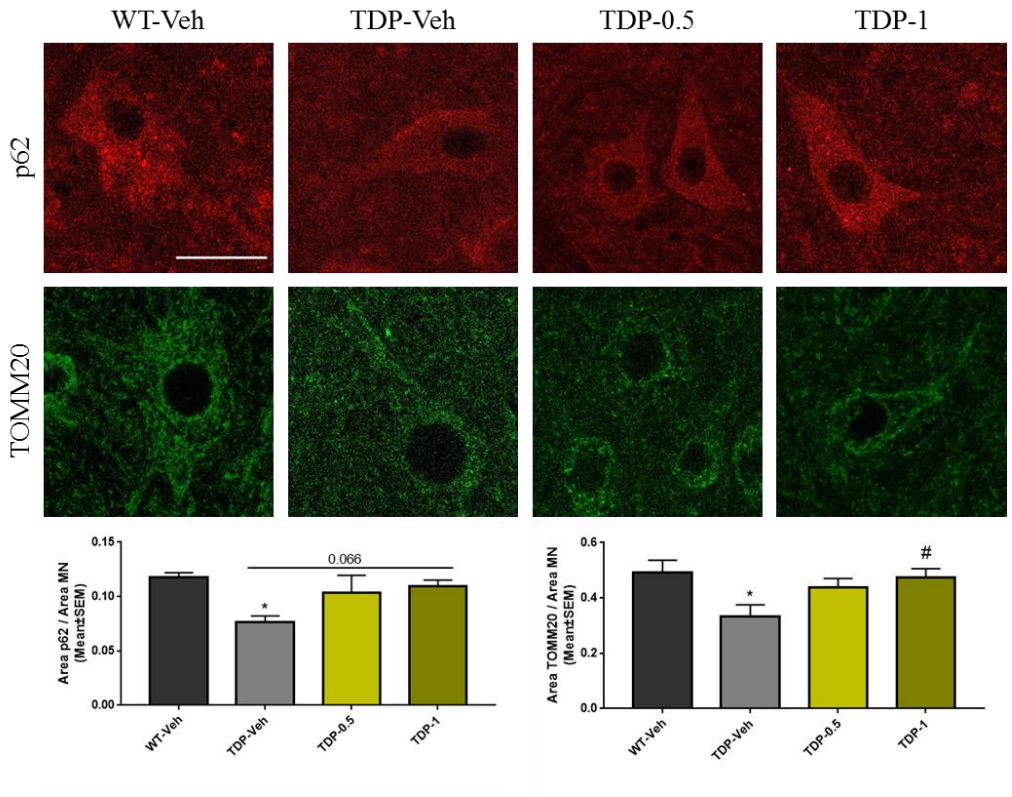

Figure 45. IGS2.7 restored p62 and mitochondrial mass levels to control. Histological samples of the anterior horn of the spinal cord of wild-type and TDP-43 mice treated with 0.5 and 1 mg/Kg for 30 days. Tissues were immunostained for p62 and TOMM20 and quantified per MN. Data represents mean±SEM of four different animals. (Significance was determined by one-way ANOVA followed by Dunnett's multiple comparison test, where *p< 0.05 versus WT and # p<0.05 versus TG-Veh). Scale bar = 20 µm.

We could report a clear decrease in p62 protein level in TDP-Veh compared to WT-Veh. These results suggest an increase in autophagy in TDP-Veh mice, as p62 is degraded by the pathway. Then, the treatment with the inhibitor, IGS2.7, restored p62 protein level almost to WT-Veh, in a dose dependent fashion.

TOMM20 was significantly decreased in TDP-Veh compared to WT-Veh. Similar to $SOD1^{G93A}$, this result together with higher autophagy determined by lower p62 protein level could denote an increase in mitophagy. Interestingly, the treatment with IGS2.7 inhibited the pathway, leading to an increase in mitochondrial mass in TDP-43 mice, similar to WT-Veh.

Previous work from our lab already reported a decrease in the amount of MN and their preservation upon IGS2.7 treatment in this model.[179] However, in this case, we did not see p62 accumulation in the extracellular matrix (data not shown).

4.4 Inhibitors of SGK1 as a promising tool to restore mitochondrial homeostasis in neurodegenerative diseases

4.4.1 Reverse Chemical Genetics

In this last chapter we followed a reverse chemical genetics approach in order to identify a new set of compounds that can modulate mitophagy by regulating a specific target. In that sense, a pool of compounds was screened against the selected target and only those compounds able to modulate this target were further tested in a phenotypic assay to show mitophagy modulation.[126]

4.4.2 Target identification

Target identification is the first step in early drug discovery, and it can be achieved by several methods. In the present case, the target was selected based on recent data reported in the literature. As protein kinases are good druggable targets, we picked out a kinase which has been recently associated with autophagy: serum and glucocorticoid-induced kinase 1 (SGK1).[134] Our main goal is to check if SGK1 inhibitors may be agents that not only modulate autophagy but also the specific mitophagy process.

SGK1 belongs to the AGC kinase family and it has three isoforms, SGK1, SGK2 and SGK3. The sequences of the three isoforms share 80% homology in the catalytic domain, 44–68% in the C-terminal domain, and lower homology in the N-terminal domain. While SGK1 and SGK3 are ubiquitously expressed, SGK2 is expressed only in the liver, kidney, pancreas, and brain.[183]

SGK1 has been the most studied and as its name suggests, it is regulated by serum, and glucocorticoids.[184] Moreover, it can also be modulated by other stimuli, like DNA damage or oxidative stress.[185] Those stimuli are the responsible of the translocation of SGK1 between the cytoplasm and nuclei. It is predominantly located in the surface of the mitochondria by the N—terminal domain, leaving the C-terminus facing the cytoplasm. Thus, SGK1 stays accessible to be activated by cytoplasmic kinases.[186]

Structurally, SGK1 is a 431-amino-acid protein which presents a bilobal kinase fold with an N-terminal β-strand domain (residues 60–179) and a C-terminal α-helical domain (residues 180–431).[187] These two domains are linked by the activation loop (Figure 46).

There are three crystals of SGK1 characterized with different ATP competitive inhibitors (2R5T, 3HDM and 3HDN). In all three crystals, the inhibitors form hydrogen bonds with the main-chain carbonyl and amide groups of residues Asp177 and Ile179.[157] To become active, SGK1 has to be phosphorylated first by the mechanistic target of rapamycin complex 2 (mTORC2) in Ser422, and then by PDK1 in Thr256, in the activation loop of the kinase.

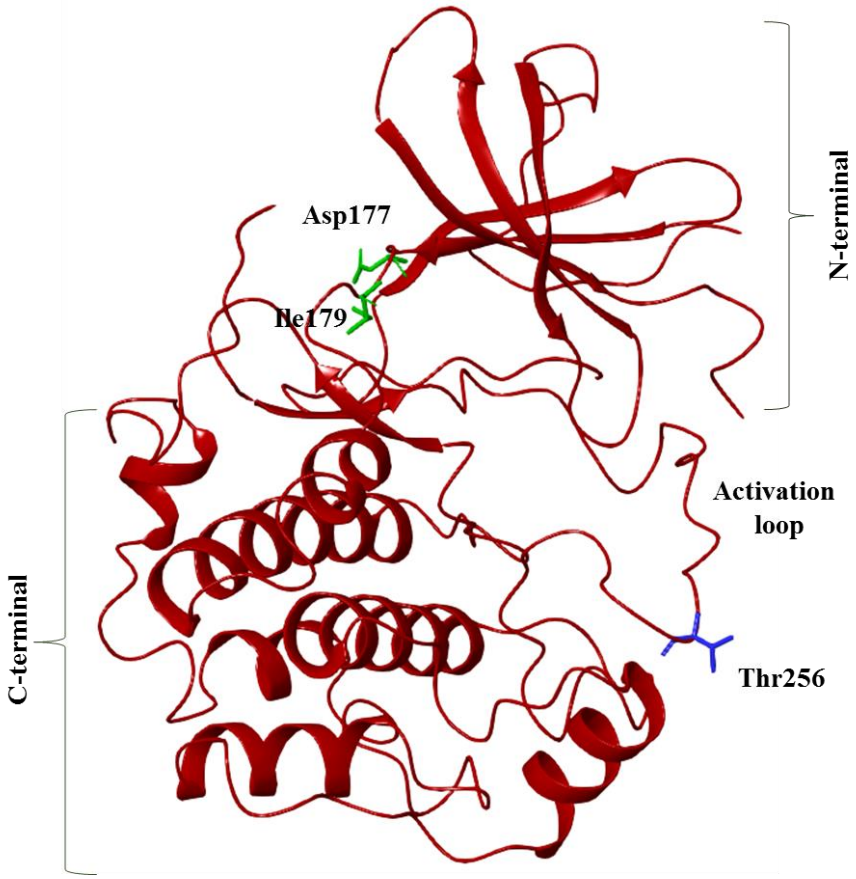

Figure 46. A ribbon diagram of the SGK1 kinase. The N-terminal domain has a β-strand structure while the C-terminal domain has an α-helical secondary structure. The two domains are linked by the activation loop. Residues of the hinge region (Asp177 and Ile179), which form hydrogen bonds with SGK1 inhibitors in the catalytic site, are depicted in green. One of the key amino acid residues (Thr256) phosphorylated by PDK1 during activation of SGK1 is highlighted in blue.

SGK1 is mainly described as an ion channel regulator, as it modulates Na^+, K^+ or Ca^{2+} channels, among others. It is also involved in glucose metabolism by the phosphorylation of the glucose transporters GLUT1 and GLUT4 that increase the plasma membrane abundance of the transporters. It also participates in the regulation of the immune system by favouring a Th17-pro-inflamatory phenotype.[133] Dysregulation of the kinase has been

found predominantly in cancer, but recently it has also been described in other pathological conditions, summarized in Table 9.

Table 9. Diseases in which SGK1 upregulation has been described.

Disease type	Disease
Cancer	Non-small cell lung cancer[188] Gliomas[189] Hepatocellular carcinoma[190] Colorectal cancer[191]
Cardiac	Stroke[192] Ischemia[193] Increased blood pressure and hypertension[194]
Metabolim	Obesity[184] Type 2 Diabetes[195] Diabetic nephropathy[196] Lafora Disease[197]
Immune System	Multiple Sclerosis[198]
Neurological	Alzheimer's disease[199] Parkinson's disease[200] Amyotrophic Lateral Sclerosis[201]
Other	Chron's disease[202] Fibrotic process[203]

These data make SGK1 a suitable pharmacological target for different pathological situations. In fact, there are already some SGK1 inhibitors described in the literature. The most used are GSK650394 (IC_{50}: 62 nM), a pyrrolo-pyridine compound from GlaxoSmithKline,[204] EMD638683 (IC_{50}: 3 µM), a phenylbenzohydrazide developed by Merck,[205] and SI113 (IC_{50}: 600 nM), a pyrazolopyrimidine-based compound[206] (Figure 47). However, they have been mainly applied in cancer research.

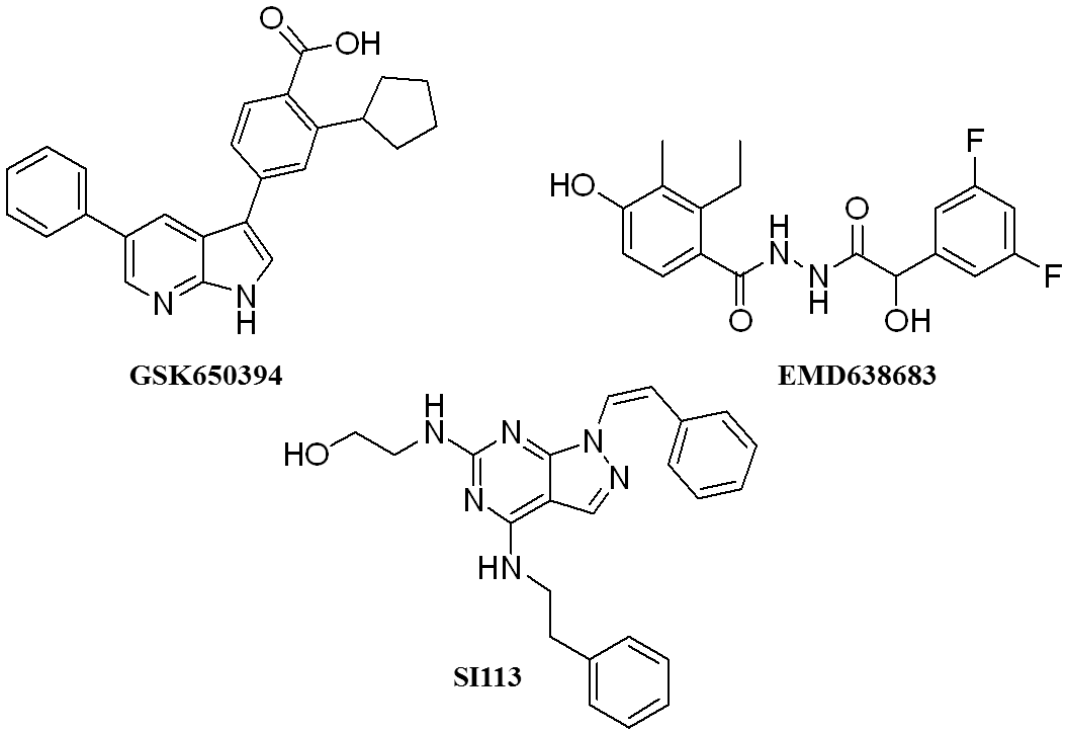

Figure 47. Structure of commercial inhibitors of SGK1.

In addition, its role in autophagy has been recently studied.[207] However, there are some divergences about the modulation of the pathway.[134-135] Thus, in order to explore the role of SGK1 in autophagy and mitophagy, we designed a research program aimed to find new inhibitors to be used as pharmacological tools or drug candidates for the study of neurodegenerative diseases therapy. It is known that the kinase is upregulated in those severe pathologies.

4.4.3 Compound selection

In order to identify new SGK1 inhibitors, a virtual screening on this kinase was done (See Material and Methods). Among the three crystals available in PDB, 2R5T, 3HDM and 3HDN, we selected those with small molecules bound to the catalytic site (Figure 48). Moreover, as the resolution of the crystal was lower in 3HDN (3.10 Å), we decided to use the 3D coordinates corresponding to the crystal structure of SGK1, named 3HDM (2.60 Å), for our virtual screening.

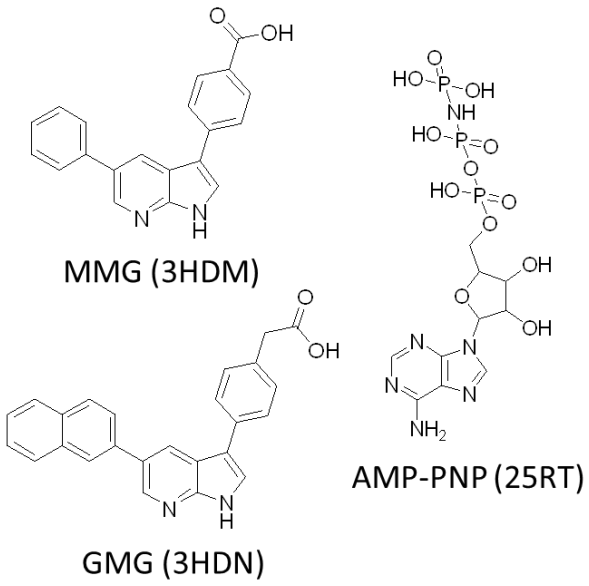

Figure 48. Structure of ligands forming the complex with the crystals.

Docking studies with the MBC chemical library[160] in the ATP binding site or catalytic site were done using the software Glide (Schrodinger). As the 3D SGK1 structure used in the study is a complex with the ligand MMG, this ligand was included in the chemical set used in the screening as internal reference. Furthermore, in the crystal structure 3HDM, the ligand (MMG) interacts with Asp177 and Ile179 (Figure 49). Thus, these two interactions were considered to select only the compounds from the chemical library able to make them.

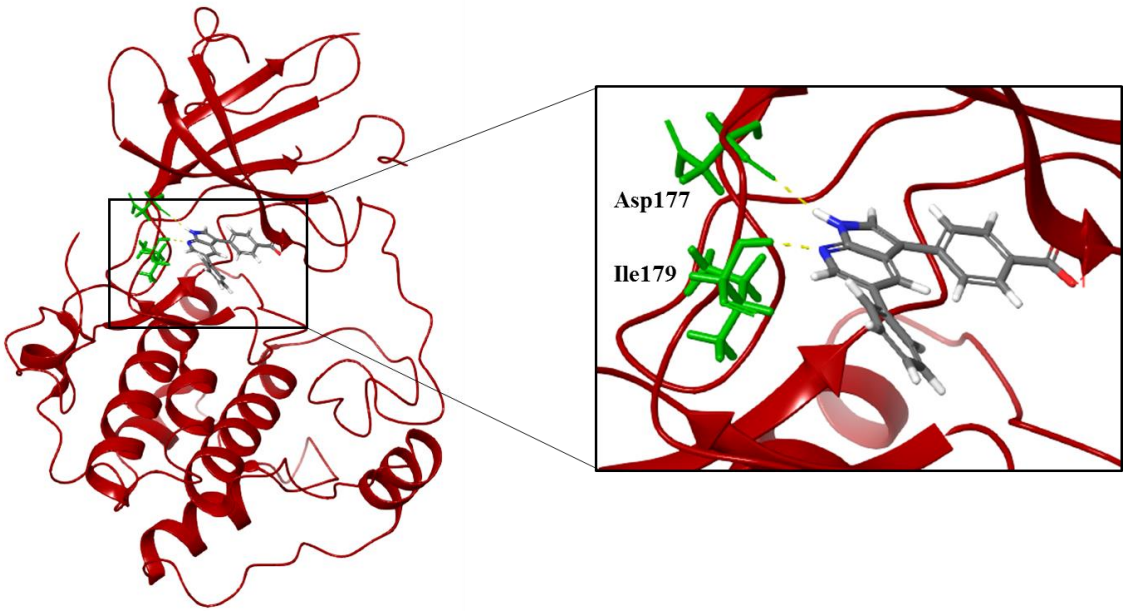

Figure 49. SGK1 crystallized with MMG. The inhibitor (in grey) makes two hydrogen bonds (in yellow) with Asp177 and Ile179 residues (in green).

When the docking was finished, results were ordered by docking score (XP Gscore), selecting the values <-8 Kcal/mol. All the compounds had values of docking score greater than the standard reference (-11.261 Kcal/mol), pointed to less potent compounds. However, as the binding energies are good enough to identify new inhibitors, we selected a set of compounds based on chemical diversity to be experimentally confirmed. Thus, a total of nine compounds, with different chemical scaffolds, were picked for the next step (Table 10).

Table 10. Compounds selected from the structure-based screening based on their docking score (XP Gscore) and structural diversity.

Compound	XP Gscore (Kcal/mol)	Structure	Compound	XP Gscore (Kcal/mol)	Structure
SC695	-8.924	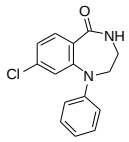	**IGS4.18**	-8.299	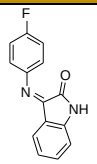
VNG1.6	-8.893	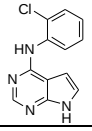	**AC074**	-8.105	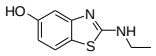
AEL024	-8.507	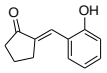	**GMH1.1**	-8.072	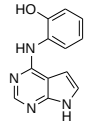
LG1.31	-8.474	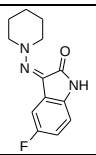	**AM101**	-8.068	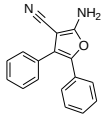
DM1.55	-8.428	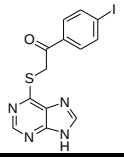			

4.4.4 *In vitro* evaluation of the compounds

A total of nine compounds coming from the target-based screening were evaluated against SGK1. This biological screening was performed in the MRC Unit of Dundee University using a radioactive methodology with ^{32}ATP. In addition, the commercial SGK1 inhibitor, GSK650394 was also included in the study as reference standard. Kinase

inhibition evaluation was performed in two steps. Firstly, all the compounds were assayed at a fixed concentration of 10 µM and only when the kinase inhibition was more than 40% their half maximal inhibitory concentration (IC_{50}) was determined. Results are summarized in Table 11.

Table 11. Inhibitory values of compounds against SGK1

Compound	SGK1 % Inhibition@10 µM	IC_{50} (µM)
GSK650394[a]	92.6	0.1
SC695	3	-
VNG1.6	48	5.2
AEL024	1	-
LG1.31	5	-
DM1.55	7	-
IGS4.18	1	-
AC074	2	-
GMH1.1	28	-
AM101	1	-

[a] IC_{50}: 62 nM[204]

Compound VNG1.6 showed an IC_{50} value of low micromolar (5.2 µM), following by GMH1.1 with a 28% of inhibition at 10 µM. These two compounds shared the heterocyclic scaffold of deazapurine and bound similarly to the catalytic site of SGK1 (Figure 50).

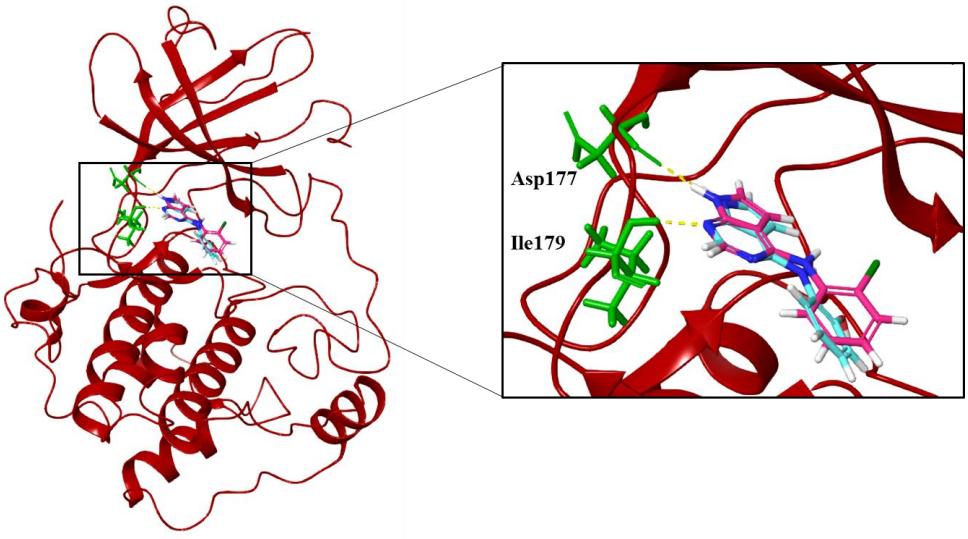

Figure 50. Docking of VNG1.6 (pink) and GMH1.1 (light blue) in the catalytic site of SGK1.

Finally, we proceeded to select a focused subset of compounds from MBC library structurally like VNG1.6. Nine compounds were selected and experimentally evaluated. Data are collected in Table 12. In almost all the cases, we obtained moderate SGK1 inhibitors with IC_{50} values ranged from 3 to 10 µM, confirming that deazapurine moiety is a privileged scaffold for SGK1 inhibition.

Table 12. Inhibitory values of VNG1.6 structural family against SGK1 and their IC_{50}.

Compound	SGK1 % Inh@10 µM	IC_{50} (µM)	Structure	Compound	SGK1 % Inh@10 µM	IC_{50} (µM)	Structure
GSK650394	92.6	0.1	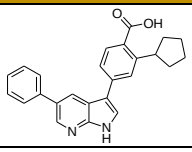	**GMH1.12**	74.3	5.5	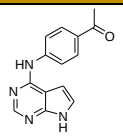
VNG1.7	54.0	9.3	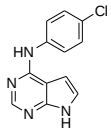	**ERP2.14**	52.6	6.4	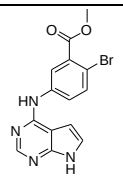
VNG1.52	60.5	2.4	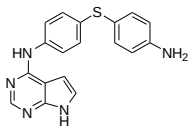	**ERP1.32**	6.6	-	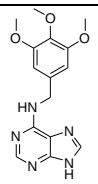
VNG1.65	62.6	3.4	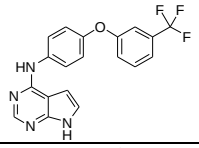	**ERP1.22**	21.9	-	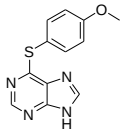
AEV1.40	65.3	6.5	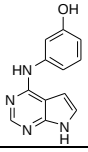	**ERP1.19**	3.9	-	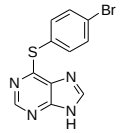

It is worth mentioning the lack of inhibitory kinase activity in purine derivatives. This may be explained by the tautomerism between both nitrogen atoms in the imidazole ring. With the software MarvinSketch (version 18.10.0, ChemAxon Ltd.) we could determine that the most abundant species of ERP1.22 at physiological pH is number 1 (Figure 51). This may decrease the interaction with Asp177 and Ile179, the two key aminoacids within the catalytic site, which translates in the lack of inhibitory potency.

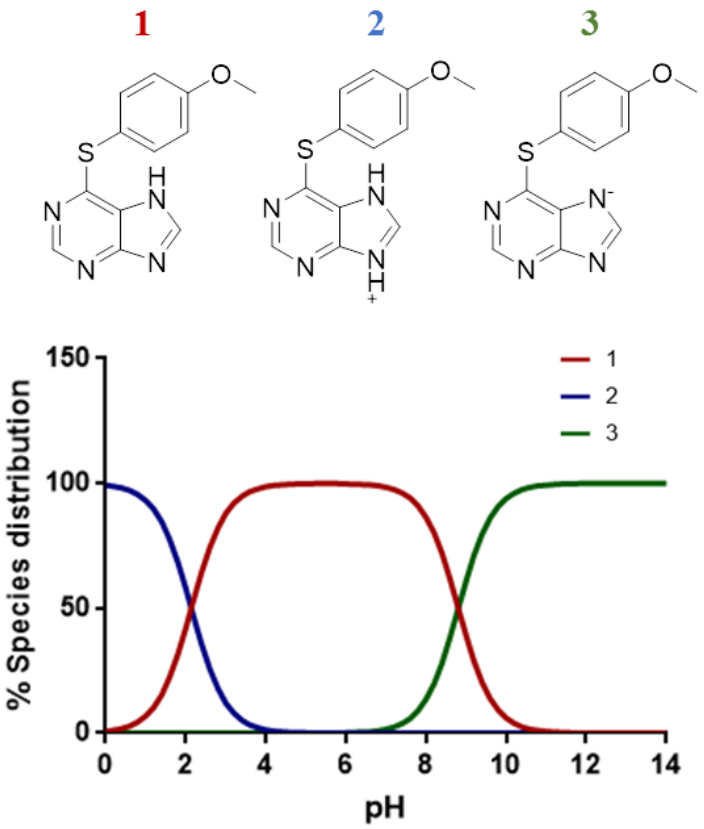

Figure 51. ERP1.22 specie distribution at different pH.

4.4.5 Phenotypic evaluation of new hits in mitophagy assay

Once the new hits were identified and following the scheme of reverse chemical genetics, we determined the role of SGK1 in mitophagy. Thus, the next step was to evaluate the active compounds selected in the *in vitro* step in a phenotypic assay to check the required modulation. Additionally, the commercial inhibitor of SGK1, GSK650394 was also included.

Similar to the screening described in Chapter 1, the ability of SGK1 inhibitors to induce or inhibit mitophagy was studied. Cells were treated with the compounds alone and in combination with mitophagy inducers: FCCP in U2OS-iMLS-Parkin cells (Figure 51) and DFP in U2OS-iMLS cells (Figure 52). In those assays, compounds which produced a 2-fold increase in mitophagy (horizontal red line) were considered inducers and compounds reducing mitophagy more than 50% were considered inhibitors (horizontal yellow line).

As seen on the left part of Figure 52, neither GSK650394 nor our compounds induced mitophagy. Similar, none of the treatment reduced FCCP-induced mitophagy. The mitophagy reduction produced by BafA1 (a control reference) treatment, showed that the assay conditions were adequate. So, SGK1 inhibitors did not modulate Parkin-dependent mitophagy

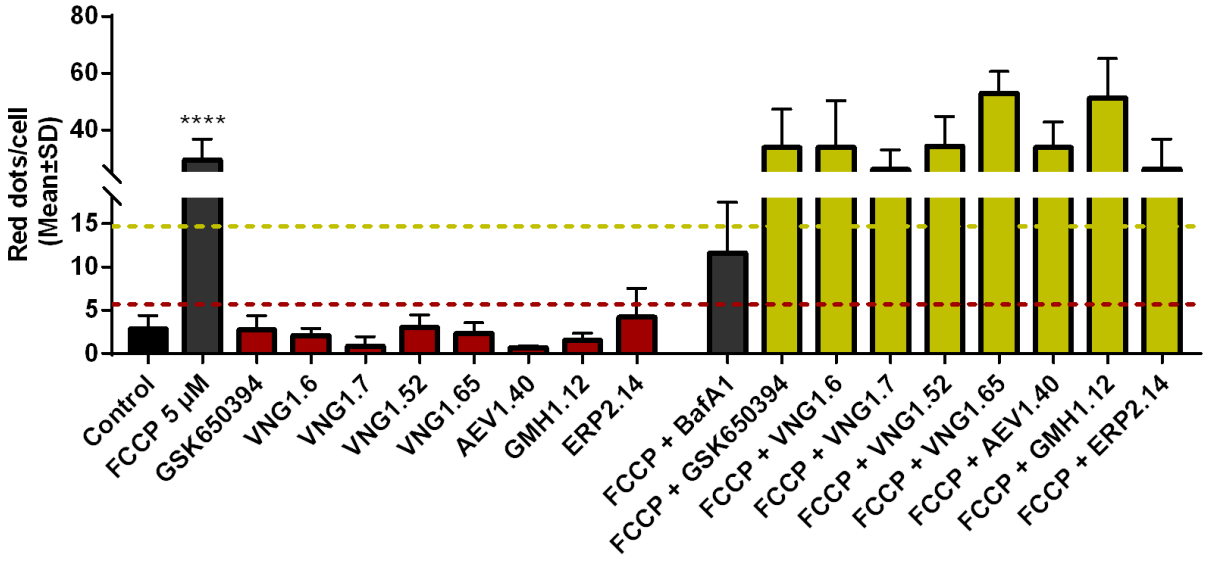

Figure 52. **Parkin-mediated mitophagy modulation by SGK1 inhibitors.** U2OS-iMLS-Parkin cells were treated with the compounds at 10 µM for 24h alone (in red) and in combination with FCCP 5 µM (in yellow). Data represents mean±SD of replicates from one experiment. (Significance was determined by one-way ANOVA followed by Dunnett's multiple comparison test to control, where ****p<0.0001).

The same screening was done in U2OS-iMLS cells, which lack Parkin (Figure 53). Again, none of the compounds induced mitophagy. Interestingly, besides the control (BafA1), two compounds reduced mitophagy more than 50%: the commercial inhibitor, GSK650394, whose inhibition was statistically significant, and the compound from the MBC library, AEV1.40, whose p-value was 0.0562. Moreover, compounds GMH1.12 and ERP2.14 also decreased mitophagy more than 40%. Interestingly, these three compounds from our chemical library reduced also basal mitophagy close to half, indicating the trend of these three compounds to inhibit mitophagy.

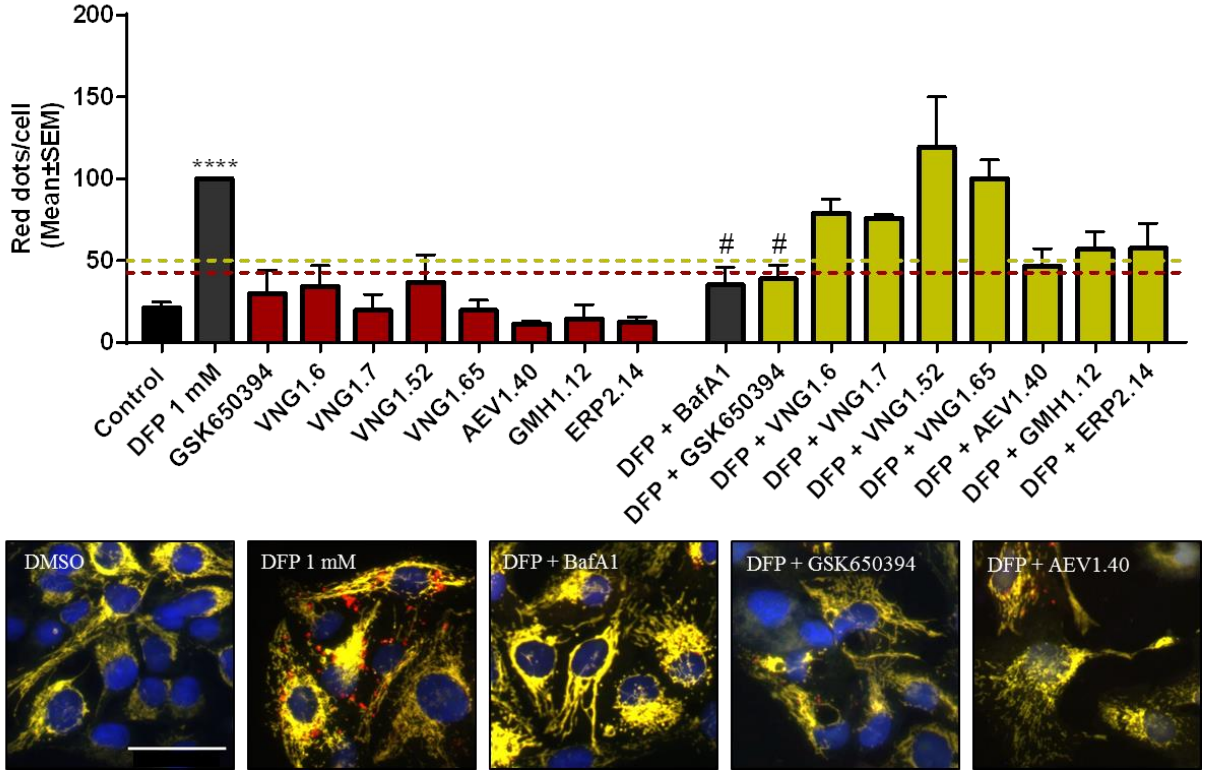

Figure 53. **Receptor-mediated mitophagy modulation by SGK1 inhibitors**. U2OS-iMLS cells were treated with the compounds at 10 µM for 24h alone (in red) and in combination with DFP 1 mM (in yellow). Data were normalized to DFP and represent mean±SEM of three independent experiments. (Significance was determined by one-way ANOVA followed by Dunnett's multiple comparison test, where ****$p<0.0001$ versus control and # $p<0.05$ versus DFP). Scale bar = 50 µm.

4.4.6 Therapeutic applicability of SGK1 inhibitors

Then, we tried to explore the therapeutic applicability of SGK1 inhibition in neurodegeneration. A bibliographic search reported the phosphorylation of tau by SGK1 in Ser214,[208] a residue prone to be hyperphoshorylated and related to Alzheimer's disease (AD).[209] Thus, we proceeded to study the neuroprotection of SGK1 inhibitors against a damage mimicking AD.

With this purpose, the neuroblastoma cell line, SH-SY5Y, was treated with okadaic acid (OA). OA is a toxin that inhibits the serine/threonine phosphatases 1 and 2A, thus inducing the hyperphosphorylation of tau *in vitro* and *in vivo*.[210] This hyperphosphorylation causes cell death. Thus, cells were pre-treated with the compounds at 10 µM for 1h. After

that, OA was added to the culture at a final concentration of 30 nM for 24h. Cell viability was measured by crystal violet.[211]

Results are collected in Figure 54. Cell viability with the different compounds treated at 10 µM for 24h is depicted in Figure 54A. Compound VNG1.52 and VNG1.65 slightly reduced cell viability, thus they were discarded. In Figure 54B is shown how OA reduced cell viability more than 65% and interestingly, the pre-treatment with GSK650394 protected cells from death caused by the toxin. Interestingly, the pre-treatment with AEV1.40, GMH1.12 and ERP2.14, which also tended to inhibit mitophagy, reduced the cell death caused by OA.

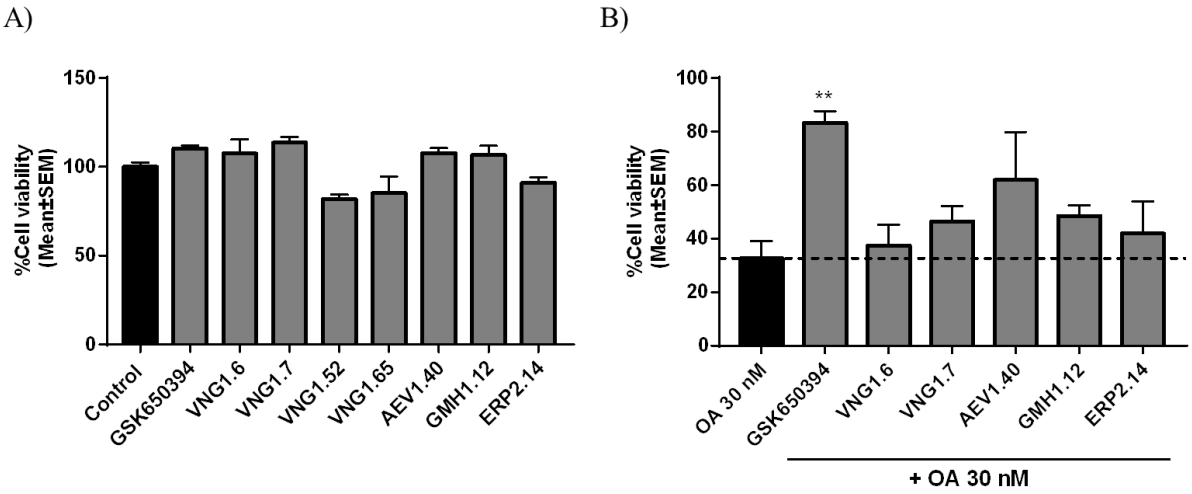

Figure 54. Neuroprotective effect of SGK1 inhibitors in AD cellular model. A) SH-SY5Y cells were treated with the compounds at 10 µM for 24h. B) Cells were pre-treated with the compounds at 10 µM for 1h followed by the treatment with OA 30 nM for 24h. Data were normalized to control and represent mean±SEM of three independent experiments. (Significance was determined by one-way ANOVA followed by Dunnett's multiple comparison test to control, where **p<0.01 versus OA).

Based on these results, we continued characterizing the effect of SGK1 inhibition only with GSK650394, while a medicinal chemistry program is being designed to optimize our hits based on deazapurine scaffold.

Using the SH-SY5Y cells expressing the reporter MitoQC, we here treated with OA and GSK650394 to evaluate the influence of OA on mitophagy. The concentration of the toxin was reduced from 30 nM to 10 nM due to the high cell death produced by the highest concentration.

SH-SY5Y MitoQC cells did not show any mitophagy modulation when they were treated with OA (Figure 55A). Thus, we could confirm that: i) OA induced cell death in SH-SY5Y cells independently of mitophagy and ii) the mechanism by which GSK650394 rescued from OA-induced cell death must differ from its ability to reduced mitophagy. However, in this assay, it was detected that cells lost a great part of mitochondrial mass (yellow network) upon OA treatment (Figure 55). In the other hand, mitochondrial mass was somehow maintained with the pre-treatment with GSK650394. Quantification of the mitochondrial mass (Figure 55B) showed clearly a reduction with OA treatment and an increase when cells were incubated with the SGK1 inhibitor, GSK650394. Furthermore, mitochondrial biogenesis is also observed by the treatment with GSK650394 in control cells.

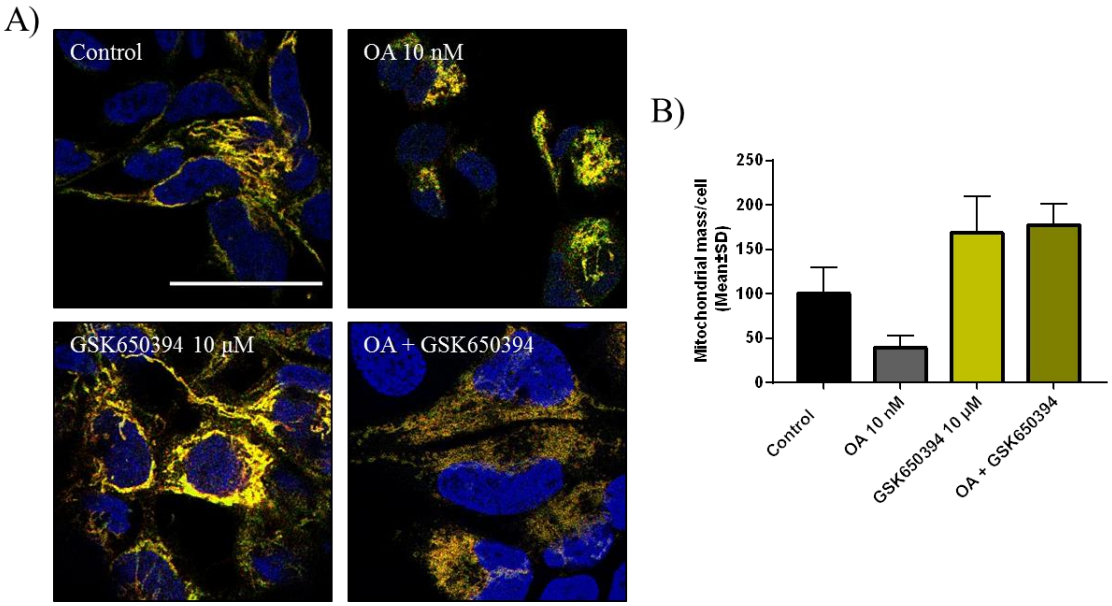

Figure 55. Mitophagy modulation of SGK1 inhibition in AD cellular model. A) Representation of SH-SY5Y MitoQC cells treated with OA 10 nM and GSK650394 10 µM. B) Quantification of the mitochondrial mass upon treatment. Data represents mean±SD of replicates from one experiment. Scale bar = 30 µm.

To check the ability of GSK650394 to increase the mitochondrial mass we used U2OS-iMLS cells showing in Figure 56A, a significant increase in mitochondrial network. Moreover, we measured the mRNA level of the main regulator of mitochondrial biogenesis, *PPARGC1A* (Figure 56B). A 5-fold increase in the gene expression was reported after the treatment with GSK650394 compared to control cells.

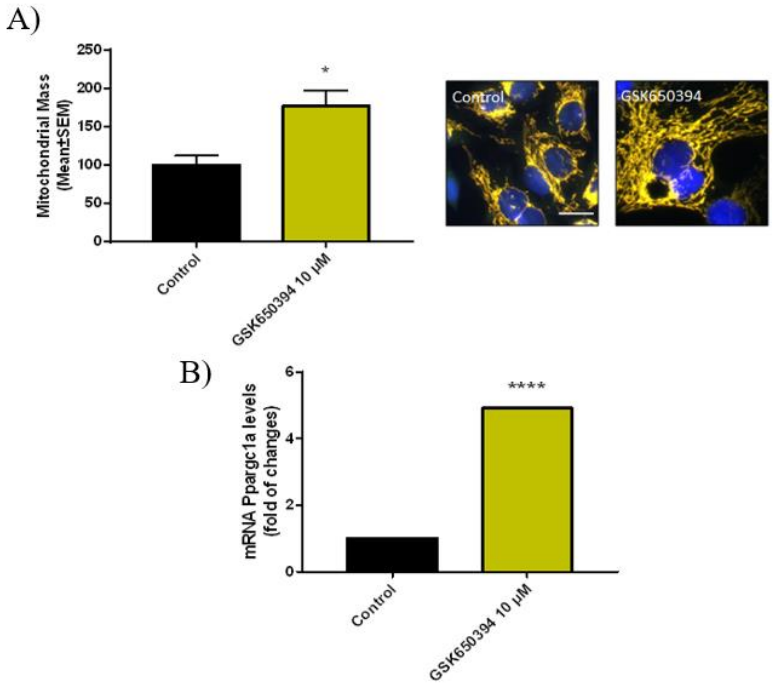

Figure 56. SGK1 inhibition induced mitochondrial biogenesis. A) Quantification of mitochondrial mass and B) *PPARGC1A* expression levels of U2OS-iMLS cells treated with GSK650394 10 µM for 24h. Data represent the mean±SEM of A) four and B) two independent experiments. (Significance was determined by unpaired two tailed t-test, where *p<0.05 and ****p<0.0001, significantly different from control).

All together, these results show that SGK1 inhibitors decreased mitophagy in cells without Parkin. Furthermore, in OA model of AD, these compounds trend to rescue from the neuronal death. We have confirmed that the SGK1 inhibitor, GSK650394, induced mitochondrial biogenesis, regulating the expression of *PPARGC1A*, and increasing in mitochondrial mass in cell cultures. If that relevant biological action is due to SGK1 inhibition or to the specific physicochemical properties of GSK650394, remains to be deciphered. Further studies are ongoing in order to identify the mechanism of action by which SGK1 inhibitors rescued from OA cell death, being the decrease of tau phosphorylation and mitochondrial biogenesis our two-working hypothesis.

5. DISCUSSION

5.1 Discovery of mitophagy modulators

The main objective of this PhD project was to discover mitophagy modulators that could represent new therapies for neurodegeneration. So, with the idea of reaching the patients in the future, compound selection was a crucial step. To cut time and costs, drug repurposing is widely used in the field. That is why the first approach of the project was to filtered libraries of compounds already approved or at least in phase II clinical trials. Pharmakon drug collection, from MicroSource Discovery Systems, Inc, is a perfect source of compounds to start a drug discovery programme based on drug repurposing. They can be easily obtained from the company, but a deeply study of the list should be done in order to remove uninteresting compounds from being included in the screening.

Thus, only drugs allowed for human treatment should be considered for the study, to avoid unexpected events at the end of the process. Therefore, we could reduce time and costs. For that, a bibliographic search was essential to eliminate those compounds that are not safe for human use, like pesticides or those for veterinary use. Moreover, drugs with known side effects can also be discarded to avoid undesirable events. The second filter was to remove the compounds unable to cross the human BBB. Again, a bibliographic search was used to find data related to BBB penetration.

Importantly, during the process of drug discovery and development, a big amount of many drugs fails due to poor ADME and toxicity properties. That is why there are several assays developed to study drug-like properties as early as possible to increase the chances of getting to the market. Those include turbidimetry to measure solubility, LC-MS and HPLC to study integrity and lipophilicity or PAMPA (parallel artificial membrane permeability assay) for BBB penetration.[212]

However, recent advances in cheminformatics allow scientists to predict drug-like properties, physicochemical properties and biological activity of compounds based on their chemical structures.[213] Although those properties depend on the way of administration, the well-known Lipinski's rule of five (MW < 500 Da, Log P < 5, H-bond acceptors < 10 and H-bond donors < 5) refers to oral absorption compounds and represents around 90% of orally active drugs that have reached phase II in clinical trials.[214]

So, although we have already reduced greatly the number of compounds from the Pharmakon drug collection, we added additional filters to fit more those drug-like properties. Filters were applied by computational tools. In this step, our in-house chemical library (MBC) was added to the already filtered list from the Pharmakon drug collection.

Finally, by all these filters, 71 compounds in addition to 19 extra compounds more from the MBC library, chosen due to known biological activity, were selected to be tested in the phenotypic screening assay.

Several years ago, drug discovery process was basically target-based. However, recently, phenotypic-based drug discovery, which is independent on a specific target, is increasing in interest.[215] Phenotypic assays mimics more the physiological environment in which a drug will be involved compared to isolated target. This is quite useful not only in identifying new drugs, but also in identifying tool compounds as chemical probes to study a biological system or repurposing. However, this approach also presents limitations. It is very important to understand the biological endpoint, and to select the best cell type for each assay. Moreover, target deconvolution, which is essential to determine the final mechanism of action, is also a challenge.[216]

Another important issue in phenotypic-based drug discovery is the source of the compounds to be screened. Ideally, chemical libraries should contain high chemical diversity and chemical tractability, like synthesis feasibility, up-scaling or cost.[217]

As autophagy and mitophagy are appearing as potential targets for several diseases, phenotypic assays are needed in order to find compounds that modulate them. The main tools used to study mitophagy and autophagy are described in section 1.4. Of them, the most common ones are fluorescent-based assays, in which a protein involved in autophagy is linked to a fluorescent protein, like GFP-LC3. However, as autophagy is a very dynamic process, autophagy flux has to be measured with the addition of a lysosomal inhibitor. To avoid this step, other fluorescent assays have been developed to study autophagy flux. They use two fluorophores, like GFP and mCherry, and they take advantage of GFP quenching and the stability of the red fluorophore in acidic compartments (lysosomes)[218] to compare between autophagosomes (in yellow, when both fluorophores fluoresce) and autolysosomes

(in red).[121] To monitor mitophagy flux, the reporter is linked to a mitochondrial protein, like or NIPSNAP1[142] or FIS1.[143]

In this project we have used the cell line U2OS. This is an osteosarcoma cell line, which grows fast and presents good cytoplasm for microscopy. As our phenotypic assay is fluorescent based, this fact is very important in the selection of an appropriate cell line. More interestingly, U2OS cell line expresses low levels of Parkin,[164] which are not sufficient to induce Parkin-mediated mitophagy. Thus, Parkin-independent and receptor-mediated mitophagy can be studied. However, as we did not want to lose the chance of exploring Parkin-mediated mitophagy, U2OS cells transduced with Parkin were also used. As there are processes that depend more on one pathway than the other, it would be interested to find drugs able to modulate mitophagy via different signalling pathways. That is why four conditions were studied in the phenotypic assay.

Regarding to mitophagy inducers, none of the compounds enhanced mitophagy when cells did not express Parkin, while two compounds (JAR1.39 and VP07) induced mitophagy in cells expressing Parkin. On the other hand, only one compound (IGS2.7) was able to reduce DFP-induced mitophagy in U2OS-iMLS, but none in U2OS-iMLS-Parkin cells, in which mitophagy was induced with FCCP. Probably, mitophagy enhancement with FCCP was excessive as the mitochondrial network is almost completely lost. Although this detrimental mitophagy induction could be blocked by BafA1, none of the compounds were potent enough to stop the process.

5.2 Characterization and therapeutic potential of mitophagy enhancers

With the aim to verify the mitophagy induction found in U2OS-iMLS-Parkin cells by the two candidates named JAR1.39 and VP07, different approaches were followed. The first one was to study dose-response studies. Compounds were stocked in DMSO at 25 mM, and to avoid toxic effects caused by DMSO, the highest tested concentration was 25 µM. At this concentration, mitophagy was known to be induced, but the aim of the assay was to find an effective lower dose. However, although JAR1.39 showed certain effect at the second highest concentration (12.5 µM), the difference with the control was not

significant and we maintain 25 µM at the best concentration to use each of these two compounds in cellular assays.

In this assay we could also observe mitochondrial morphology and thus assess mitochondrial fragmentation. Fission of mitochondria is part of mitochondrial quality control, and it gives rise to smaller mitochondrial fragments that can be engulfed by autophagosomes. Thus, we decide to measure the area of mitochondrial fragments to determine if fission provokes the mitochondria degradation.[219] For that, a pipeline in CellProfiler[146] was developed, first to identify mitochondria network and then to measure their area. If mitochondria were fissed, the program identified smaller fragments than in untreated cells. In fact, at 25 µM compounds induced mitophagy and a decrease in the mitochondrial area was observed. Thus, we confirmed that the compounds induced fission to obtain smaller fragments of mitochondria to be degraded by mitophagy.

However, this fission effect was also observed in U2OS-iMLS cells upon treatment with the JAR1.39 and VP07, although mitophagy was not induced, due to the low protein level of Parkin expression in this cell type (Figure 21). As Parkin-mediated mitophagy needs former mitochondrial fission,[166] we can conclude that JAR1.39 and VP07 induced mitochondrial fragmentation in both cell lines, but they only modified mitophagy when Parkin is expressed, confirming their Parkin-mediated role in mitophagy.

Additional assays, based on indirect measurement were also used for mitophagy determination. As mitochondria are degraded by mitophagy, we could measure the quantity of remaining mitochondria. Thus, the level of two mitochondrial proteins, TOMM20 and TIMM23, were used to determine mitochondrial mass upon treatment. TOMM20 is part of the complex responsible of the translocation of cytosolic proteins into the mitochondria, and it is placed in the mitochondrial surface.[220] As outer mitochondrial proteins can be degraded by the proteasome,[221] to ensure mitochondrial degradation by mitophagy, the inner mitochondrial protein, TIMM23 was also studied. Similarly, it also allows the transport of proteins through the inner mitochondrial membrane.[220] As expected, both compounds reduced the protein level of both markers. (Figure 22), confirming the mitophagy enhancement by the two drugs treatment.

The second indirect assay used was to measure the activity of a mitochondrial enzyme. In this case, citrate synthase activity was determined. Citrate synthase is an enzyme placed in the mitochondrial matrix with a role in Kreb's cycle. It catalyzes the first reaction of the cycle generating citrate from oxaloacetate and acetyl-CoA.[222] Its activity could be a sign of the amount of mitochondria in a sample. In fact, studies demonstrated the correlation between mitochondrial content and citrate assay activity.[223] The more mitochondrial mass, the more enzymatic activity. In this case, the treatment with JAR1.39 and VP07 reduced mitochondrial content and citrate synthase activity (Figure 23), showing again the mitophagy enhancement.

Last, as it is described, mitophagy induction can be measured by the recruitment of the autophagy machinery to mitochondria. When mitophagy is started, mitochondria are targeted and engulfed by LC3-positive autophagosomes. It is already demonstrated that LC3 was accumulated in mitochondria when MEFs overexpressing Parkin were treated with CCCP.[224] Similarly, we also observed an increase in LC3 punctae and its accumulation in mitochondria when U2OS-iMLS-Parkin cells were treated with the hits (Figure 24).

Overall, all these results confirm the increased of Parkin-mediated mitophagy in U2OS-iMLS-Parkin cells after the treatment with the hits, JAR1.39 and VP07.

Next, we verified mitophagy induction by the compounds in another cell type. Thus, ARPE-19, a human retinal pigment epithelial cell line was used. Interestingly, as ARPE-19 cell line constitutively expresses Parkin,[167] we could measure Parkin-mediated mitophagy in a more physiological way. The induction of mitophagy in this cell line, as seen in Figure 25, confirmed again that Parkin is required for the compounds to induce mitophagy in ARPE-19, in U2OS and in probable any cell type.

Further, both cell lines differ in the mitophagy reporter they harbor. While iMLS reporter is constituted by the tandem fluorophore EGFP-mCherry bound to a matrix protein, NIPSNAP1,[142] MitoQC reporter is based on fusion of mCherry-GFP to the OMM protein FIS1.[143] As stated above, proteins in the OMM are degraded by the proteasome.[221] However, we obtained similar results with both reporters. So, we also validated the use of these two reporters for the proper study of mitophagy.

Mechanism of action characterization is an important milestone in drug discovery process. We tried to decipher which mechanism of action was behind the mitophagy increase produced by JAR1.39 and VP07. As these two compounds belonged to our in-house chemical library, MBC library,[160] their primary target is already known. The compounds were synthesized in medicinal chemistry program to target the kinase GSK3.[168] GSK3 is a serine/threonine kinase involved in glycogen metabolism and in other cellular processes, such as cell cycle, proliferation, differentiation, or inflammation.[225] Moreover, it is overexpressed in pathological conditions like cancer, diabetes, or neurodegeneration.[226] Thus, GSK3 inhibitors are important tools for the treatment of chronic diseases.[227]

Based in the previous background, initially, GSK3 inhibition was assumed as the potential mechanism of action to modulate mitophagy. Indeed, there are works showing the effect of GSK3 modulation in autophagy, although the results are controversial (Figure 57). GSK3 was shown to maintain active mTOR,[228] or to repress AMPK,[229] thus inhibiting autophagy. However, other works showed the overexpression of GSK3 decreased the phosphorylation of a substrate of mTOR, S6K, via TSC2, an mTOR repressor. On the contrary, the treatment with GSK3 inhibitors, increased S6K phosphorylation,[230] thus proving the negative effect of GSK3 on mTOR pathway. In addition, a recent work showed a positive relationship between GSK3 and autophagy. GSK3 phosphorylated and activated ULK1, thus triggering the recruitment of autophagy machinery.[169]

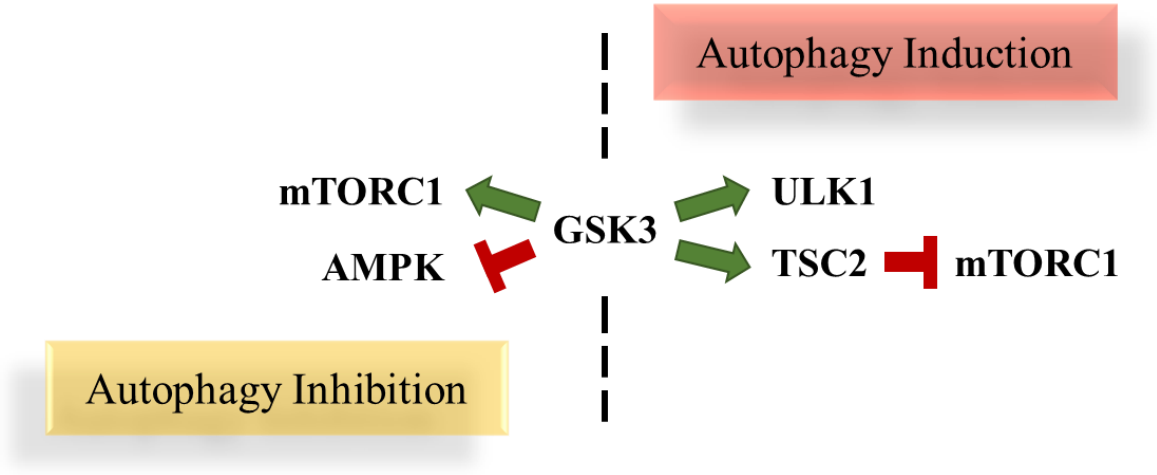

Figure 57. Autophagy modulation by GSK3.

In our case, the hypothesis of GSK3 inhibition as the pathway to induce mitophagy by JAR1.39 and VP07 was rejected, as there were other GSK3 inhibitors chemically diverse included in the mitophagy assay which did not induce mitophagy. Therefore, the ability of our hits to induce mitophagy independently of their GSK3 inhibition was confirmed.

SAR studies were the next approach. As Parkin was overexpressed in U2OS-iMLS-Parkin cells, these analyses were done in ARPE-19 MitoQC cells, which express endogenously Parkin.[167]

Then, the several compounds belonged to the structural family of JAR1.39 and VP07 based on a quinolone scaffold, synthetized against GSK3[168] were evaluated in a mitophagy assay in ARPE-19 MitoQC cells. Results showed the importance of a long aliphatic chain of eleven carbon atoms, the presence of the quinolone scaffold and the hydrophobicity of the substituents in the aromatic nitrogen to induce mitophagy.

These chemical features present in JAR1.39 and VP07 looked similar to other mitophagy regulators, such as cardiolipin (CL) and ceramide, described in the literature (Figure 57).[57] CL is a phospholipid present in the inner mitochondrial membrane. It has a polar head and four flexible acyl chains[231] (Figure 58) that can interact with several mitochondrial complexes. Under several stresses, like harmful agents as rotenone or CCCP, CL externalizes to the outer mitochondrial membrane, and there, it binds to LC3.[57 59] The aliphatic chains of CL remain facing the mitochondrial matrix, while its polar head is exposed to interact with LC3 N-terminus. The LC3 C-terminus binds to the forming autophagosome, thus targeting cargo for mitophagy.[232]

Ceramide is a sphingolipid synthetized by the enzyme CerS1 in the endoplasmic reticulum and it localizes in the plasma membrane or in the mitochondria.[233] In mitochondria it can bind to the LC3 N-terminus, probably in a similar way as CL, thus bridging mitochondria to the autophagosome.[60]

Moreover, metformin, another compound that activates mitophagy by AMPK-ULK1 axis, has been structurally modified.[234] A triphenylphosphonium cationic moiety (TPP+) aliphatic chain was added to the compound, bound by an aliphatic chain with different length. Interestingly, when the alkyl chain was elongated, like in Mito-Met10, with an alkyl

chain of 10 carbons, the compound was more potent activating AMPK,[235] an autophagy initiator.

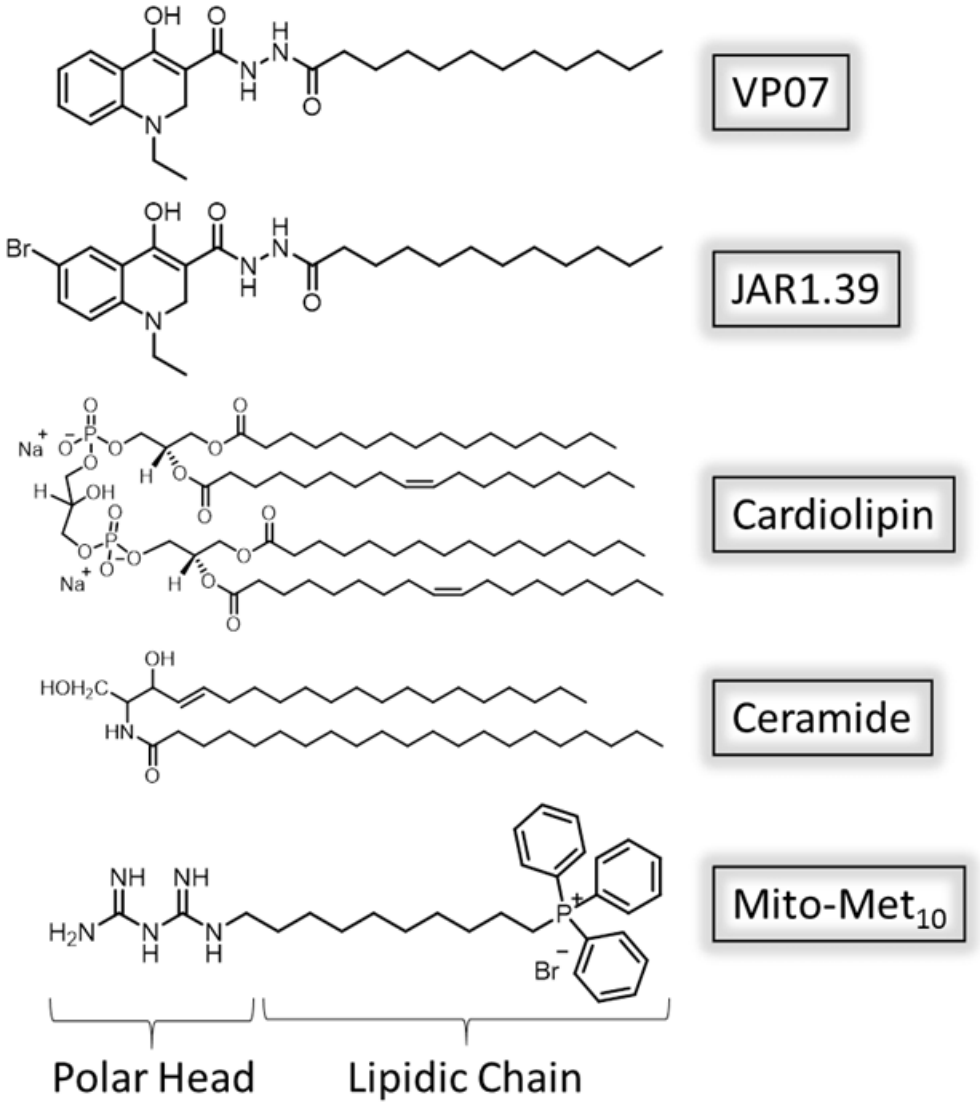

Figure 58. Structural comparison of the hits, JAR1.39 and VP07, with other mitophagy modulators.

Therefore, based on the results obtained from our SAR studies (Section 4.2.3.2) and the chemical similarity of the hits with CL, ceramide or Mito-Met_{10}, our hypothesis is that JAR1.39/VP07 compounds family may associate with the OMM by anchoring the aliphatic chain in it. Thus, the polar head would face the cytoplasm to interact with LC3 N-terminus in a similar way as CL or ceramide. Then, the signal should be boosted by PINK1/Parkin

signalling pathway, as the compound, JAR1.39 and VP07, are Parkin-dependent mitophagy modulators (Figure 59)

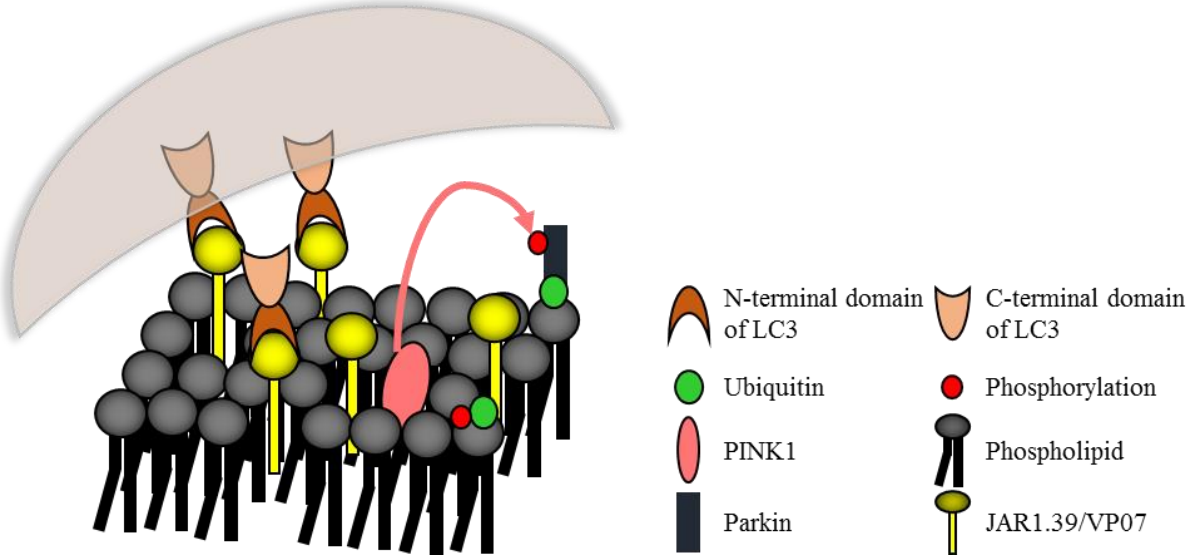

Figure 59. Proposed mechanism of action of hits compounds JAR1.39 and VP07. The illustration shows how the lipidic chain of the compounds may anchor in the mitochondrial membrane, like phospholipids, while the polar head faces to the cytosol. There, it can be directly recognized by the N-terminal domain of LC3 as a mitophagy receptor. Then, the anchoring of the lipidic chain and LC3 recognition favours PINK1 stabilization, amplifying the signal to trigger PINK1/Parkin-mediated mitophagy.

This was supported by the ability of the compounds to induce mitophagy only when Parkin was expressed (Figures 19-21) and by the recruitment of LC3 to mitochondria when U2OS-iMLS-Parkin cells were treated with the hits (Figure 24).

However, another hypothesis could be also considered. Thus, based on the need of an aliphatic chain and the high concentration required, the compounds may disrupt the OMM. This would trigger autophagosome formation to engulf mitochondria without any interaction between the compounds and LC3. So, further studies will be done to decipher the molecular mechanism of action of the compounds to induced Parkin-mediated mitophagy.

Finally, as the main objective of this project is to discover new drugs for neurological disorders, the therapeutic applicability of the hits here found was studied. For that, the human neuronal cell line SH-SY5Y cell line was used. SH-SY5Y is a neuroblastoma cell

line widely used in neuronal studies. They can be differentiated upon several treatments and neurodegeneration and neuroprotection can be evaluated, as well. Specifically, SH-SY5Y cell line is extensively used as PD cellular model, as they have characteristics similar to dopaminergic neurons, the affected cells in PD.[236]

Mitochondrial homeostasis is one of the hallmarks of neurodegeneration. Specifically, defective mitophagy and autophagy have been reported in *in vitro* and *in vivo* models of PD and post-mortem brains of PD patients.[237] In addition, as it is described in the Introduction (Section 1.3.1), there are mitophagy-related genes mutated in PD. So, the need of mitophagy modulators to treat this pathology is manifested.[72, 238]

To mimic PD in cell culture, here we have used two different toxins: PQ and 6-OHDA. On one hand, PQ, which induces oxidative stress and PD-like injuries in mice and rats[5] triggers alpha-synuclein aggregation in mice and neurodegeneration. On the other hand, 6-OHDA, a neurotoxin that induces oxidative stress, as well, and disrupts complexes I and IV of the electron transport chain,[239] decreases PINK1 expression and increases PD-related genes like SNCA (α-synuclein).[240]

Results from our mitophagy assay using SH-SY5Y MitoQC cells showed a reduction in basal mitophagy with both toxins, which mimics somehow this pathomolecular characteristic of PD. Pre-treatment with the hit, VP07, recovered the phenotype, showing its therapeutic potential for PD therapy.

As autophagy and mitophagy enhancers have been showed as a potential therapeutic approach to treat PD, here we have discovered a family of compounds that modulate mitophagy and can prevent the defects in mitophagy pathway, characteristic of the disease

5.3 Characterization and therapeutic potential of a mitophagy inhibitor

The characterization of this new mitophagy inhibitor first of all revealed its ability to modulate only DFP-induced but not basal mitophagy in U2OS-iMLS cells. As these cells present low basal levels of mitophagy, the treatment with the inhibitor did not modulate the pathway. Similar results were obtained in the spinal cords of MitoQC mice. However, the

treatment with IGS2.7 of ARPE-19 MitoQC cells, which have higher basal mitophagy, clearly reduced the formation of mitolysosomes.

This led us to analyse mitophagy in our three cell types in induced conditions. In order to study all the possibilities, we used DFP as receptor-mediated mitophagy enhancer, and CCCP as Parkin-mediated mitophagy inducer. The compound reduced DFP-induced mitophagy in the three cell lines. As expected, CCCP did not induce mitophagy in U2OS-iMLS cells, as they did not express Parkin but, it induced massive mitophagy in the other two cell lines. The co-treatment with IGS2.7 did not block CCCP-induced mitophagy (Figure 37). However, this result did not clarify if IGS2.7 did not work via Parkin, or it was unable to restore the huge amount of mitolysosomes obtained after CCCP treatment. Thus, what we can conclude at this point is the modulation of receptor-mediated mitophagy by IGS2.7.

IGS2.7 was previously synthesized to target CK1. This is a kinase widely studied in ALS, due to its important role in TDP-43 phosphorylation.[176] However, its role in autophagy is still under study. Recently, CK1δ has been reported to be crucial in autophagy with a key role in autophagosome formation. Its deletion triggered p62 accumulation similar to our results with IGS2.7. Moreover, they showed LC3-II accumulation upon CK1δ depletion, claiming a role of the kinase after LC3-II lipidation (Figure 60).[241]

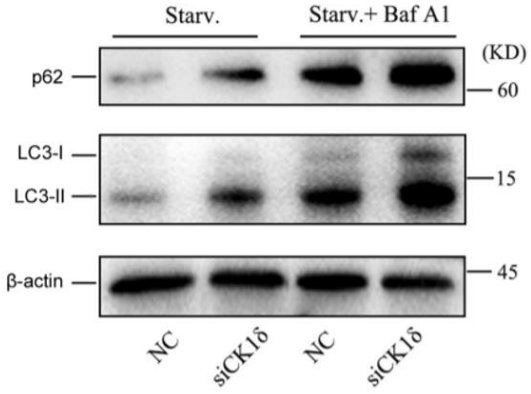

Figure 60. CK1δ deletion impaired autophagy after LC3 lipidation. Immunoblotting of LC3 and p62 in negative control (NC) and CK1δ-depleted HeLa cells. Cells were starved in EBSS for 2.5h with or without bafilomycin A1 (100 nM, 6h). Modified from Ref [241].

However, our results reported LC3-I accumulation and a decrease in LC3-II after the treatment with IGS2.7, which could denote a role of the compound before LC3 lipidation

(Figure 37 and 38). Moreover, other CK1 inhibitors were included in the screening and none of them inhibited mitophagy (Table 8). Thus, its possible role before LC3 lipidation in addition to its exclusiveness in mitophagy modulation among its structural family, suggest a CK1-independent role of IGS2.7 in mitophagy.

Then, another possible mechanism of action was explored. In a previous work from our laboratory, IGS2.7 was screened against a panel of 456 kinases in order to evaluate its selectivity to target CK1. Indeed, the kinase was inhibited almost 100%. Interestingly, the compound showed certain potency to inhibit the autophagy-related kinase, ULK1.[175] ULK1 is a kinase with a key role in the first phases of autophagy, as it triggers the activation of VPS34 complex, which leads to autophagosome formation.[6] The kinase assay was done with a final concentration of IGS2.7 of 10 μM. With that, there was a decrease of almost 60% of ULK1 activity. In this work we are using a higher concentration of the compound, 25 μM. Thus, we considered this concentration increase very important to potentiate more its inhibitory capacity against ULK1.

Moreover, ULK1 inhibition by small molecule ULK1 inhibitor known as MRT68921 lowered LC3 immunofluorescence in MEF cells.[242] This is in coherence with our results in U2OS-iMLS cells, where IGS2.7 reduced LC3 punctae (Figure 38). In addition, there is a clear similarity of protein profiles by western blot between cells treated with MRT68921 and IGS2.7 (Figure 37). Altogether, these results support the idea of IGS2.7 as an initiation phase inhibitor of autophagy and mitophagy, which block LC3 recruitment, via ULK1 inhibition.

Last, we explored the use of the inhibitor as a pharmacological tool in different diseases models. In fact, the therapeutic use of IGS2.7 has been already validated in human cellular models derived from frontotemporal lobar degeneration (FTLD) patients[243] and ALS patients,[179] in which the compound restored TDP-43 hyperphosphorylation. In addition, MN preservation was reported in an ALS mouse model with a mutation in TDP-43 (TDP-43^{A315T}). Thus, although the therapeutic potency of the compound was already manifested, we questioned if the modulation of autophagy and mitophagy could revealed a new mechanism of action responsible of its efficacy.

The study of autophagy and mitophagy in ALS is recently having more attention in order to comprehend better the pathophysiology of this complex disease, not only in MN but in non-cell autonomous mechanisms.[108] However, as we discussed in section 1.3.3 from the Introduction, results are very controversial. Some works reported enhanced autophagy in ALS,[99, 103] while others claimed a clear block of the pathway.[100,102] These opposite results bring together differences in the treatment and outcomes. While autophagy inhibition could be beneficial in some models,[106] its enhancement ameliorated the disease in others.[244]

Results from our cellular ALS models reported an increase in autophagy in those patients with SOD1 and TDP-43 mutation, and the treatment with our inhibitor reduced those levels to control samples. Thus, we agree with those results showed detrimental autophagy enhancement in the pathology and the therapeutic applicability of an autophagy inhibitor, only for familiar patients with these specific mutations.

Moreover, we could confirm those results in two ALS animal models. SOD1^{G93A} mouse is the most studied. It presents a gain of function mutation which triggers the degeneration and loss of MN, with metabolic defects, gliosis and muscle weakness.[245] And the TDP-43^{A315T} mouse model, in which the overexpression of the mutated protein leads to MN degeneration, loss of weight, protein accumulation and gliosis.[182]

Similar results were found in both ALS models: decrease p62 and TOMM20 inside MN. However, while p62 inclusions were found in the extracellular matrix of SOD1^{G93A}, samples from TDP-43^{A315T} model did not. Results from SOD1 are in line with previous data that reported p62 aggregated structures among MN and non-MN cells, but a decrease in its expression inside MN.[246] We hypothesized that these aggregates came from dead MN, which were more apparent in that model. Animals from both models were sacrificed with a difference of around ten days, which could be enough to see differences in MN degeneration and extracellular release of their content.

Moreover, it is important to be aware of the regulation of p62. It is known to be degraded by autophagy. Thus, when p62 is accumulated, a blockage in autophagy flux is considered. However, its regulation is quite complex, other parameters as mRNA levels of p26 or LC3-II turnover could be useful to support the results.[247] In this case, the results

from lymphoblasts, and the decrease in TOMM20, support the outcome: autophagy induction in both ALS animal models. This also agrees with other works which showed enhanced glycolysis and lactate production in ALS.[248] Moreover, a glycolytic shift has been proved to be promoted by enhanced mitophagy in different situations.[63, 249] Thus, the treatment of the models with an inhibitor is logical.

In addition, Parkin protein levels are not detected in spinal cords (Figure 61). This indicates that the possible increase in mitophagy in spinal cords of ALS animal models is Parkin-independent. Then, the treatment with IGS2.7, which inhibited mitophagy independently of Parkin is very appropriate.

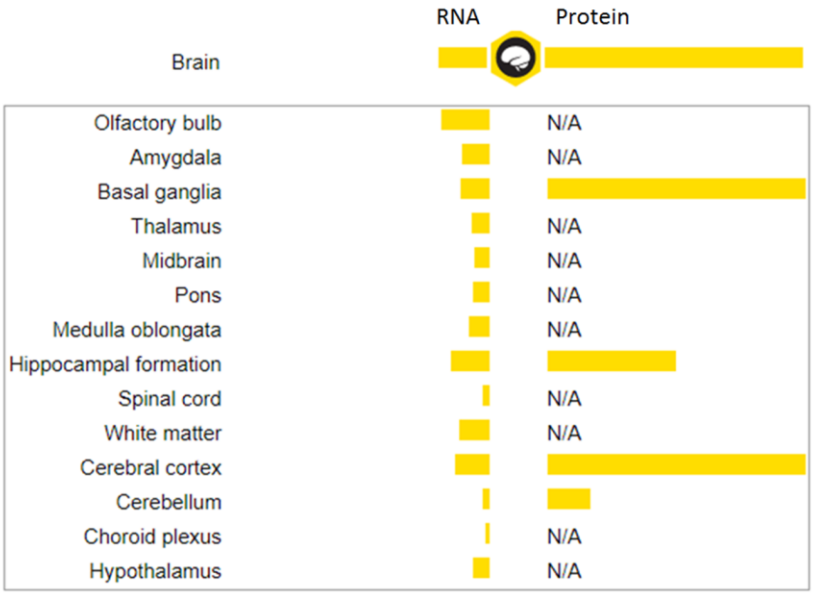

Figure 61. Parkin RNA and protein levels in the brain. Data obtained from ProteinAtlas.[250]

Although we did not know the effect of IGS2.7 on autophagy in SOD1^{G93A} mice model, the hit restored autophagic high levels to control in both lymphoblast ALS groups and in TDP-43^{A315T} mice.

With these new results, we accentuated the relevant value of IGS2.7 as potential therapy for ALS, which restored TDP-43 pathology, MN preservation and now also autophagy defects in SOD1 and TDP-43 patients. Thus, IGS2.7 may be a broad-spectrum ALS therapeutic agent restoring pathological features of genetic patients.

5.4 Inhibitors of SGK1 as a promising tool to restore mitochondrial homeostasis in neurodegenerative diseases

Finally, we took advantages of computational tools to find new mitophagy modulators. First, we identified the target. SGK1 has been recently related to autophagy and it is upregulated in several pathological conditions. Moreover, there are already some inhibitors that modulate the kinase, which makes this protein druggable and suitable for drug discovery programs.[133] However, those inhibitors have been mainly tested in cancer related models.

With the aim of find new inhibitors to target the kinase, we followed SBDD approach. With that, we could discard compounds with low affinity or weak interactions with the kinase. Therefore, we reduced the number of compounds from more than 2000 from the MBC library to nine. With that, we could also decrease costs and time in the experimental validation.

VNG1.6 was the only drug from the initial set of compounds that modulated the kinase, followed by GMH1.1. As both compounds share a deazapurine heterocyclic scaffold, a focused subset of compounds with this scaffold was tested against the kinase. After the analysis of the inhibitory results and the chemical structure of these compounds, only the pyrrolo-pyrimidine compounds inhibited the kinase (See compounds VNG1.6, VNG1.7, VNG1.52, VNG1.65, AEV1.40, GMH1.12 and ERP2.14, Table 12). Interestingly, the commercial inhibitor GSK650394, which is a pyrrolo-pyridine, reduced completely the activity of the kinase (Table 11).

Surprisingly, the purines were inactive in the kinase assay, probably due to the tautomerism found in those compounds. As at pH 7.2 the donor nitrogens in those compounds lack the hydrogen, they cannot make the hydrogen bond with Asp177. Thus, losing their capacity to interact with and inhibit SGK1.

The connection between SGK1 and autophagy/mitophagy has been recently explored. As mTORC2 participates in SGK1 activation and inhibits autophagy,[251] SGK1 could be considered as a negative regulator of the pathway.[252] In fact, autophagy was upregulated in SGK1-deficient mice.[134] Thus, the inhibition of the kinase by the compound GSK650394 induced autophagy.[253-254] However, a recent work done in HEI-OC1, a mouse auditory cell

line, showed an upregulation of SGK1 and autophagy when cells were treated with caffeine, This event was inhibited when cells were co-treated with the inhibitor GSK650394.[135] So, again, there are controversial results around the role of this kinase in autophagy, which we wanted to explore with our mitophagy assay. Interestingly, SGK1 inhibition by GSK650394, AEV1.40, GMH1.12 and ERP2.14 reduced DFP-induced mitophagy in U2OS-iMLS cells (Figure 52).

SGK1 is upregulated in several neurodegenerative diseases, like ALS,[201] or PD.[200, 255] Interestingly, SGK1 overexpression in mouse hippocampus triggered neurodegeneration, a decline in cognitive function and an increase in phospho-tau in Ser214,[256] which is found in AD.[208-209] Moreover, the treatment with EMD638683, a SGK1 inhibitor, reduced tau phosphorylation. Thus, we decided to search the therapeutic applicability of SGK1 inhibition in a cellular AD model.

The treatment of the neuroblastoma cell line SH-SY5Y with OA has been reported as a cellular model to study AD. OA is a toxin that inhibits the activity of serine/threonine phosphatases 1 and 2A, which leads to an increase in phospho-tau.[210] The toxicity caused by the toxin was avoided after the pre-treatment with GSK650394. Moreover, AEV1.40, GMH1.12 and ERP2.14 also tended to increase cell viability. However, we have checked that this neuroprotection was not mitophagy-mediated, as OA did not modulate the pathway. Thus, the compounds must protect from the damage caused by OA by other mechanisms of action. Interestingly, OA clearly reduced the amount of mitochondrial network, which was recovered with the pre-treatment of GSK650394. Therefore, the induction of mitochondrial biogenesis produced by GSK650394 treatment raised as a plausible route to explain the neuroprotected effect observed. Although these data do not allow us to decipher if mitochondrial biogenesis is produced by SGK1 inhibition or by the specific physico-chemical properties of GSK650394, a recent paper showed an increase in mitochondrial biogenesis in glial cells by SGK1 inhibition (Figure 62),[255] which is in agreement with our results and point to a mitochondrial biogenesis modulation by SGK1 inhibitors.

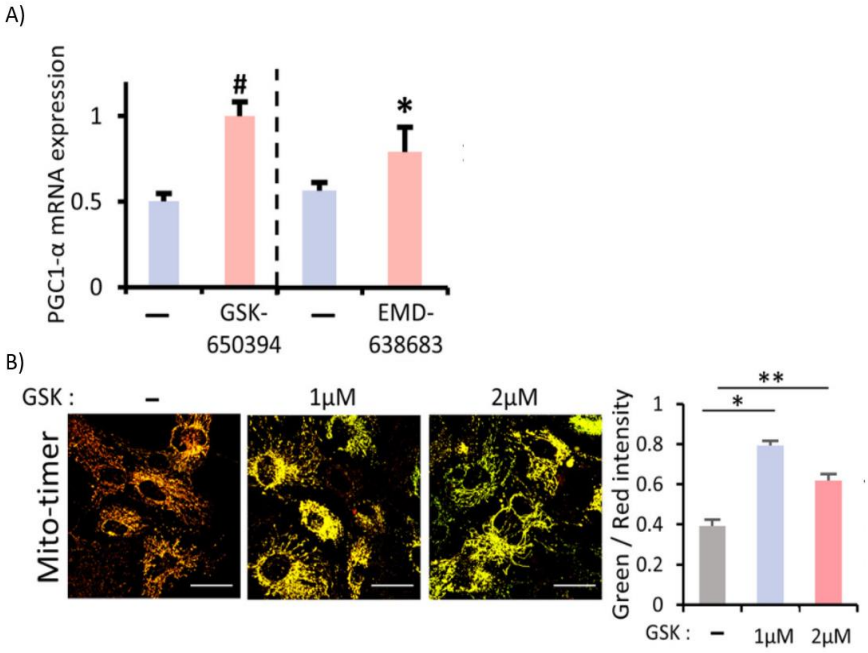

Figure 62. SGK1 induces mitochondrial biogenesis in glial cells. A) PGC1α upregulation in glia treated with SGK1 inhibitors. B) Mito-Timer assay (Green fluorescence indicates newly synthesized mitochondria, and red fluorescence indicates old or damaged mitochondria). Modified from Ref[255].

In fact, there are new approaches to treat neurodegenerative diseases based on the enhancement of mitochondrial biogenesis. PGC1α overexpression improved mitochondrial dysfunction in AD mouse models. In addition, compounds like thiazolidinediones, resveratrol or melatonin induced mitochondrial biogenesis and decreased neuronal degeneration.[257] Our preliminary data may suggest a new strategy to treat neurodegenerative conditions based on the mitochondrial biogenesis increase by the inhibition of the kinase SGK1.

However, OA is known to increase the phosphorylation of tau. Then, a new hypothesis emerges. If SGK1 phosphorylates tau, its inhibition could also contribute to decrease that pathological hallmark of AD. This would place SGK1 as an excellent target for AD, which not only rescued cell death by mitochondrial biogenesis, but also by regulating the homeostasis of tau. Thus, further studies are ongoing to confirm this idea.

6. CONCLUSIONS

6.1 Starting from a collection of more than 3700 compounds and after performing several filters like bibliographic search, computational tools and selection of compounds based on chemical diversity, we had a list of 90 putative compounds to test in our phenotypic assay. Although a decrease in the number of drugs reduces the possibility of finding hits, we were able to identify two mitophagy inducers and one inhibitor, from the MBC library, which were further characterized in the following sections.

6.2 The inducers, JAR1.39 and VP07, were characterized as Parkin-mediated mitophagy modulators. Although they were designed as GSK3 inhibitors, they modulated mitophagy independently of this activity. SAR studies revealed that quinolones with an aliphatic chain of eleven carbon atoms, and hydrophobic substituents in the aromatic nitrogen were more prone to induce mitophagy.

6.3 A potential mechanism of action was hypothesized based on the similarity of the compounds with other mitophagy modulators, like CL or ceramide. They may anchor the aliphatic chain in the OMM, facing the polar head to the cytoplasm where it could act to attract LC3 N-terminus. The mitophagy signal may be amplified by PINK1/Parkin-signalling to produce mitochondrial degradation.

6.4 The therapeutic applicability of the compounds was studied in a SH-SY5Y MitoQC cells treated with PQ or 6-OHDA, two PD cellular models. Both models showed decreased basal mitophagy, which was recovered with the pre-treatment with VP07. Thus, confirming the potency of the hit to be used as a chemical tool for pathologies with defective mitophagy.

6.5 The compound IGS2.7 was characterized as a receptor-mediated mitophagy inhibitor, blocking DFP-induced mitophagy and basal mitophagy in a cell type-dependent manner.

6.6 IGS2.7 modulated autophagy and mitophagy independently of their potency to inhibit CK1, its main target. Results from kinase assays and the similarity with MRT68921, suggested ULK1 inhibition as the mechanism of action by which the compound inhibit the pathway.

6.7 Lymphoblasts from familiar ALS patients bearing a mutation in SOD1 and TDP-43 and transgenic mice with a mutation in the same genes showed enhanced autophagy. The treatment of both models with IGS2.7 restored autophagy to control level.

6.8 SGK1 was selected a promising target to modulate mitophagy. With computational tools, a virtual screening with compounds from the MBC library was performed against the kinase. The compound VNG1.6 obtained from the screening showed inhibitory ability in an in *vitro kinase* assay. Thus, a batch of new compounds with a similar heterocyclic scaffold was evaluated. Only the pyrrolo-pyrimidine compounds inhibited the kinase.

6.9 The pyrrolo-pyrimidine compounds and the commercial inhibitor GSK650394 were evaluated in our phenotypic assay. Three compounds from the MBC library (AEV1.40, GMH1.12 and ERP2.14) and GSK650394 inhibited DFP-induced mitophagy in U2OS-iMLS cells.

6.10 GSK650394 rescued from cell death the cell line SH-SY5Y treated with the toxin OA, which mimics Alzheimer's disease *in vitro*. In addition, AEV1.40, GMH1.12 and ERP2.14 also reduced cell death caused by the toxin.

6.11 SH-SY5Y mitoQC cells did not show mitophagy modulation upon OA treatment. Thus, GSK650394 did not rescue OA-induced cell death via mitophagy inhibition. However, mitochondrial mass was reduced in cells treated with OA. The pre-treatment with GSK650394 maintained the mitochondrial mass, probably by PGC1α regulation, as it increased its transcriptional levels.

7. BIBLIOGRAPHY

1. Levine, B.; Klionsky, D. J., Autophagy wins the 2016 Nobel Prize in Physiology or Medicine: Breakthroughs in baker's yeast fuel advances in biomedical research. *Proc Natl Acad Sci U S A* **2017,** *114* (2), 201-205.
2. Mehrpour, M.; Esclatine, A.; Beau, I.; Codogno, P., Overview of macroautophagy regulation in mammalian cells. *Cell Res* **2010,** *20* (7), 748-62.
3. Maiuri, M. C.; Kroemer, G., Autophagy in stress and disease. *Cell Death Differ* **2015,** *22* (3), 365-6.
4. Sahu, R.; Kaushik, S.; Clement, C. C.; Cannizzo, E. S.; Scharf, B.; Follenzi, A.; Potolicchio, I.; Nieves, E.; Cuervo, A. M.; Santambrogio, L., Microautophagy of cytosolic proteins by late endosomes. *Dev Cell* **2011,** *20* (1), 131-9.
5. Cuervo, A. M.; Wong, E., Chaperone-mediated autophagy: roles in disease and aging. *Cell Res* **2014,** *24* (1), 92-104.
6. Zachari, M.; Ganley, I. G., The mammalian ULK1 complex and autophagy initiation. *Essays Biochem* **2017,** *61* (6), 585-596.
7. Hurley, J. H.; Young, L. N., Mechanisms of Autophagy Initiation. *Annu Rev Biochem* **2017,** *86*, 225-244.
8. Abounit, K.; Scarabelli, T. M.; McCauley, R. B., Autophagy in mammalian cells. *World J Biol Chem* **2012,** *3* (1), 1-6.
9. Nishimura, T.; Tooze, S. A., Emerging roles of ATG proteins and membrane lipids in autophagosome formation. *Cell Discov* **2020,** *6* (1), 32.
10. Takahashi, Y.; He, H.; Tang, Z.; Hattori, T.; Liu, Y.; Young, M. M.; Serfass, J. M.; Chen, L.; Gebru, M.; Chen, C.; Wills, C. A.; Atkinson, J. M.; Chen, H.; Abraham, T.; Wang, H. G., An autophagy assay reveals the ESCRT-III component CHMP2A as a regulator of phagophore closure. *Nat Commun* **2018,** *9* (1), 2855.
11. Kauffman, K. J.; Yu, S.; Jin, J.; Mugo, B.; Nguyen, N.; O'Brien, A.; Nag, S.; Lystad, A. H.; Melia, T. J., Delipidation of mammalian Atg8-family proteins by each of the four ATG4 proteases. *Autophagy* **2018,** *14* (6), 992-1010.
12. Lorincz, P.; Juhasz, G., Autophagosome-Lysosome Fusion. *J Mol Biol* **2020,** *432* (8), 2462-2482.
13. Yim, W. W.; Mizushima, N., Lysosome biology in autophagy. *Cell Discov* **2020,** *6*, 6.
14. Feng, Y.; Yao, Z.; Klionsky, D. J., How to control self-digestion: transcriptional, post-transcriptional, and post-translational regulation of autophagy. *Trends Cell Biol* **2015,** *25* (6), 354-63.
15. Kim, J.; Kundu, M.; Viollet, B.; Guan, K. L., AMPK and mTOR regulate autophagy through direct phosphorylation of Ulk1. *Nat Cell Biol* **2011,** *13* (2), 132-41.
16. Settembre, C.; Di Malta, C.; Polito, V. A.; Garcia Arencibia, M.; Vetrini, F.; Erdin, S.; Erdin, S. U.; Huynh, T.; Medina, D.; Colella, P.; Sardiello, M.; Rubinsztein, D. C.; Ballabio, A., TFEB links autophagy to lysosomal biogenesis. *Science* **2011,** *332* (6036), 1429-33.
17. Zhang, W.; Li, X.; Wang, S.; Chen, Y.; Liu, H., Regulation of TFEB activity and its potential as a therapeutic target against kidney diseases. *Cell Death Discov* **2020,** *6*, 32.
18. Mizushima, N.; Levine, B., Autophagy in mammalian development and differentiation. *Nat Cell Biol* **2010,** *12* (9), 823-30.
19. Yin, Z.; Pascual, C.; Klionsky, D. J., Autophagy: machinery and regulation. *Microb Cell* **2016,** *3* (12), 588-596.

20. Hansen, M.; Rubinsztein, D. C.; Walker, D. W., Autophagy as a promoter of longevity: insights from model organisms. *Nat Rev Mol Cell Biol* **2018,** *19* (9), 579-593.
21. Cuervo, A. M.; Bergamini, E.; Brunk, U. T.; Droge, W.; Ffrench, M.; Terman, A., Autophagy and aging: the importance of maintaining "clean" cells. *Autophagy* **2005,** *1* (3), 131-40.
22. Saha, S.; Panigrahi, D. P.; Patil, S.; Bhutia, S. K., Autophagy in health and disease: A comprehensive review. *Biomed Pharmacother* **2018,** *104*, 485-495.
23. Yun, C. W.; Lee, S. H., The Roles of Autophagy in Cancer. *Int J Mol Sci* **2018,** *19* (11).
24. Zhu, J.; Cai, Y.; Xu, K.; Ren, X.; Sun, J.; Lu, S.; Chen, J.; Xu, P., Beclin1 overexpression suppresses tumor cell proliferation and survival via an autophagydependent pathway in human synovial sarcoma cells. *Oncol Rep* **2018,** *40* (4), 1927-1936.
25. Dikic, I.; Elazar, Z., Mechanism and medical implications of mammalian autophagy. *Nat Rev Mol Cell Biol* **2018,** *19* (6), 349-364.
26. Schiattarella, G. G.; Hill, J. A., Therapeutic targeting of autophagy in cardiovascular disease. *J Mol Cell Cardiol* **2016,** *95*, 86-93.
27. Gomes, L. C.; Dikic, I., Autophagy in antimicrobial immunity. *Mol Cell* **2014,** *54* (2), 224-33.
28. Paludan, C.; Schmid, D.; Landthaler, M.; Vockerodt, M.; Kube, D.; Tuschl, T.; Munz, C., Endogenous MHC class II processing of a viral nuclear antigen after autophagy. *Science* **2005,** *307* (5709), 593-6.
29. Loi, M.; Muller, A.; Steinbach, K.; Niven, J.; Barreira da Silva, R.; Paul, P.; Ligeon, L. A.; Caruso, A.; Albrecht, R. A.; Becker, A. C.; Annaheim, N.; Nowag, H.; Dengjel, J.; Garcia-Sastre, A.; Merkler, D.; Munz, C.; Gannage, M., Macroautophagy Proteins Control MHC Class I Levels on Dendritic Cells and Shape Anti-viral CD8(+) T Cell Responses. *Cell Rep* **2016,** *15* (5), 1076-1087.
30. Wei, J.; Long, L.; Yang, K.; Guy, C.; Shrestha, S.; Chen, Z.; Wu, C.; Vogel, P.; Neale, G.; Green, D. R.; Chi, H., Autophagy enforces functional integrity of regulatory T cells by coupling environmental cues and metabolic homeostasis. *Nat Immunol* **2016,** *17* (3), 277-85.
31. Deretic, V., Autophagy in inflammation, infection, and immunometabolism. *Immunity* **2021,** *54* (3), 437-453.
32. Henderson, P.; Stevens, C., The role of autophagy in Crohn's disease. *Cells* **2012,** *1* (3), 492-519.
33. Henckaerts, L.; Cleynen, I.; Brinar, M.; John, J. M.; Van Steen, K.; Rutgeerts, P.; Vermeire, S., Genetic variation in the autophagy gene ULK1 and risk of Crohn's disease. *Inflamm Bowel Dis* **2011,** *17* (6), 1392-7.
34. Lieberman, A. P.; Puertollano, R.; Raben, N.; Slaugenhaupt, S.; Walkley, S. U.; Ballabio, A., Autophagy in lysosomal storage disorders. *Autophagy* **2012,** *8* (5), 719-30.
35. Sandri, M.; Coletto, L.; Grumati, P.; Bonaldo, P., Misregulation of autophagy and protein degradation systems in myopathies and muscular dystrophies. *J Cell Sci* **2013,** *126* (Pt 23), 5325-33.
36. Kim, J.; Cheon, H.; Jeong, Y. T.; Quan, W.; Kim, K. H.; Cho, J. M.; Lim, Y. M.; Oh, S. H.; Jin, S. M.; Kim, J. H.; Lee, M. K.; Kim, S.; Komatsu, M.; Kang, S. W.; Lee, M. S., Amyloidogenic peptide oligomer accumulation in autophagy-deficient beta cells induces diabetes. *J Clin Invest* **2014,** *124* (8), 3311-24.

37. Towers, C. G.; Thorburn, A., Therapeutic Targeting of Autophagy. *EBioMedicine* **2016,** *14*, 15-23.
38. Kocak, M.; Ezazi Erdi, S.; Jorba, G.; Maestro, I.; Farres, J.; Kirkin, V.; Martinez, A.; Pless, O., Targeting autophagy in disease: established and new strategies. *Autophagy* **2021**, 1-23.
39. Zaffagnini, G.; Martens, S., Mechanisms of Selective Autophagy. *J Mol Biol* **2016,** *428* (9 Pt A), 1714-24.
40. Birgisdottir, A. B.; Lamark, T.; Johansen, T., The LIR motif - crucial for selective autophagy. *J Cell Sci* **2013,** *126* (Pt 15), 3237-47.
41. Gatica, D.; Lahiri, V.; Klionsky, D. J., Cargo recognition and degradation by selective autophagy. *Nat Cell Biol* **2018,** *20* (3), 233-242.
42. Nthiga, T. M.; Kumar Shrestha, B.; Lamark, T.; Johansen, T., The soluble reticulophagy receptor CALCOCO1 is also a Golgiphagy receptor. *Autophagy* **2021,** *17* (8), 2051-2052.
43. Herst, P. M.; Rowe, M. R.; Carson, G. M.; Berridge, M. V., Functional Mitochondria in Health and Disease. *Front Endocrinol (Lausanne)* **2017,** *8*, 296.
44. van der Bliek, A. M.; Sedensky, M. M.; Morgan, P. G., Cell Biology of the Mitochondrion. *Genetics* **2017,** *207* (3), 843-871.
45. Osellame, L. D.; Blacker, T. S.; Duchen, M. R., Cellular and molecular mechanisms of mitochondrial function. *Best Pract Res Clin Endocrinol Metab* **2012,** *26* (6), 711-23.
46. Brand, M. D.; Orr, A. L.; Perevoshchikova, I. V.; Quinlan, C. L., The role of mitochondrial function and cellular bioenergetics in ageing and disease. *Br J Dermatol* **2013,** *169 Suppl 2*, 1-8.
47. Chen, H.; Chan, D. C., Mitochondrial dynamics--fusion, fission, movement, and mitophagy--in neurodegenerative diseases. *Hum Mol Genet* **2009,** *18* (R2), R169-76.
48. Liu, Y. J.; McIntyre, R. L.; Janssens, G. E.; Houtkooper, R. H., Mitochondrial fission and fusion: A dynamic role in aging and potential target for age-related disease. *Mech Ageing Dev* **2020,** *186*, 111212.
49. Gureev, A. P.; Shaforostova, E. A.; Popov, V. N., Regulation of Mitochondrial Biogenesis as a Way for Active Longevity: Interaction Between the Nrf2 and PGC-1alpha Signaling Pathways. *Front Genet* **2019,** *10*, 435.
50. Popov, L. D., Mitochondrial biogenesis: An update. *J Cell Mol Med* **2020,** *24* (9), 4892-4899.
51. Ge, P.; Dawson, V. L.; Dawson, T. M., PINK1 and Parkin mitochondrial quality control: a source of regional vulnerability in Parkinson's disease. *Mol Neurodegener* **2020,** *15* (1), 20.
52. Shiba-Fukushima, K.; Imai, Y.; Yoshida, S.; Ishihama, Y.; Kanao, T.; Sato, S.; Hattori, N., PINK1-mediated phosphorylation of the Parkin ubiquitin-like domain primes mitochondrial translocation of Parkin and regulates mitophagy. *Sci Rep* **2012,** *2*, 1002.
53. Yamano, K.; Matsuda, N.; Tanaka, K., The ubiquitin signal and autophagy: an orchestrated dance leading to mitochondrial degradation. *EMBO Rep* **2016,** *17* (3), 300-16.
54. Lamark, T.; Johansen, T., Mechanisms of Selective Autophagy. *Annu Rev Cell Dev Biol* **2021,** *37*, 143-169.
55. Onishi, M.; Yamano, K.; Sato, M.; Matsuda, N.; Okamoto, K., Molecular mechanisms and physiological functions of mitophagy. *EMBO J* **2021,** *40* (3), e104705.
56. Killackey, S. A.; Philpott, D. J.; Girardin, S. E., Mitophagy pathways in health and disease. *J Cell Biol* **2020,** *219* (11).

57. Teresak, P.; Lapao, A.; Subic, N.; Boya, P.; Elazar, Z.; Simonsen, A., Regulation of PRKN-independent mitophagy. *Autophagy* **2021**, 1-16.
58. Dudek, J., Role of Cardiolipin in Mitochondrial Signaling Pathways. *Front Cell Dev Biol* **2017,** *5*, 90.
59. Chu, C. T.; Ji, J.; Dagda, R. K.; Jiang, J. F.; Tyurina, Y. Y.; Kapralov, A. A.; Tyurin, V. A.; Yanamala, N.; Shrivastava, I. H.; Mohammadyani, D.; al., e., Cardiolipin externalization to the outer mitochondrial membrane acts as an elimination signal for mitophagy in neuronal cells. *Nat Cell Biol* **2013,** *15* (10), 1197-1205.
60. Dany, M.; Ogretmen, B., Ceramide induced mitophagy and tumor suppression. *Biochim Biophys Acta* **2015,** *1853* (10 Pt B), 2834-45.
61. Rojansky, R.; Cha, M. Y.; Chan, D. C., Elimination of paternal mitochondria in mouse embryos occurs through autophagic degradation dependent on PARKIN and MUL1. *Elife* **2016,** *5*.
62. Um, J. H.; Yun, J., Emerging role of mitophagy in human diseases and physiology. *BMB Rep* **2017,** *50* (6), 299-307.
63. Esteban-Martinez, L.; Sierra-Filardi, E.; McGreal, R. S.; Salazar-Roa, M.; Marino, G.; Seco, E.; Durand, S.; Enot, D.; Grana, O.; Malumbres, M.; Cvekl, A.; Cuervo, A. M.; Kroemer, G.; Boya, P., Programmed mitophagy is essential for the glycolytic switch during cell differentiation. *EMBO J* **2017,** *36* (12), 1688-1706.
64. Doblado, L.; Lueck, C.; Rey, C.; Samhan-Arias, A. K.; Prieto, I.; Stacchiotti, A.; Monsalve, M., Mitophagy in Human Diseases. *Int J Mol Sci* **2021,** *22* (8).
65. Gan, L.; Cookson, M. R.; Petrucelli, L.; La Spada, A. R., Converging pathways in neurodegeneration, from genetics to mechanisms. *Nat Neurosci* **2018,** *21* (10), 1300-1309.
66. Kim, M.; Ho, A.; Lee, J. H., Autophagy and Human Neurodegenerative Diseases-A Fly's Perspective. *Int J Mol Sci* **2017,** *18* (7).
67. Komatsu, M.; Waguri, S.; Chiba, T.; Murata, S.; Iwata, J.; Tanida, I.; Ueno, T.; Koike, M.; Uchiyama, Y.; Kominami, E.; Tanaka, K., Loss of autophagy in the central nervous system causes neurodegeneration in mice. *Nature* **2006,** *441* (7095), 880-4.
68. Hara, T.; Nakamura, K.; Matsui, M.; Yamamoto, A.; Nakahara, Y.; Suzuki-Migishima, R.; Yokoyama, M.; Mishima, K.; Saito, I.; Okano, H.; al., e., Suppression of basal autophagy in neural cells causes neurodegenerative disease in mice. *Nature* **2006,** *441* (7095), 885-9.
69. Menzies, F. M.; Fleming, A.; Caricasole, A.; Bento, C. F.; Andrews, S. P.; Ashkenazi, A.; Fullgrabe, J.; Jackson, A.; Jimenez Sanchez, M.; Karabiyik, C.; al., e., Autophagy and Neurodegeneration: Pathogenic Mechanisms and Therapeutic Opportunities. *Neuron* **2017,** *93* (5), 1015-1034.
70. Lee , T. K., Yankee, E.L., A review on Parkinson's disease treatment. In *Neuroimmunology and Neuroinflammation*, 2021; Vol. 8, pp 222-44.
71. Stoker, T. B.; Barker, R. A., Recent developments in the treatment of Parkinson's Disease. *F1000Res* **2020,** *9*.
72. Liu, J.; Liu, W.; Li, R.; Yang, H., Mitophagy in Parkinson's Disease: From Pathogenesis to Treatment. *Cells* **2019,** *8* (7).
73. Hou, X.; Watzlawik, J. O.; Fiesel, F. C.; Springer, W., Autophagy in Parkinson's Disease. *J Mol Biol* **2020,** *432* (8), 2651-2672.
74. Dehay, B.; Bove, J.; Rodriguez-Muela, N.; Perier, C.; Recasens, A.; Boya, P.; Vila, M., Pathogenic lysosomal depletion in Parkinson's disease. *J Neurosci* **2010,** *30* (37), 12535-44.

75. Park, H.; Kang, J. H.; Lee, S., Autophagy in Neurodegenerative Diseases: A Hunter for Aggregates. *Int J Mol Sci* **2020,** *21* (9).
76. Singh, F.; Prescott, A. R.; Rosewell, P.; Ball, G.; Reith, A. D.; Ganley, I. G., Pharmacological rescue of impaired mitophagy in Parkinson's disease-related LRRK2 G2019S knock-in mice. *Elife* **2021,** *10*.
77. Yakhine-Diop, S. M. S.; Rodriguez-Arribas, M.; Canales-Cortes, S.; Martinez-Chacon, G.; Uribe-Carretero, E.; Blanco-Benitez, M.; Duque-Gonzalez, G.; Paredes-Barquero, M.; Alegre-Cortes, E.; Climent, V.; al., e., The parkinsonian LRRK2 R1441G mutation shows macroautophagy-mitophagy dysregulation concomitant with endoplasmic reticulum stress. *Cell Biol Toxicol* **2021**.
78. Poewe, W.; Antonini, A.; Zijlmans, J. C.; Burkhard, P. R.; Vingerhoets, F., Levodopa in the treatment of Parkinson's disease: an old drug still going strong. *Clin Interv Aging* **2010,** *5*, 229-38.
79. Feyder, M.; Plewnia, C.; Lieberman, O. J.; Spigolon, G.; Piccin, A.; Urbina, L.; Dehay, B.; Li, Q.; Nilsson, P.; Altun, M.; al., e., Involvement of Autophagy in Levodopa-Induced Dyskinesia. *Mov Disord* **2021,** *36* (5), 1137-1146.
80. Liu, J.; Li, L., Targeting Autophagy for the Treatment of Alzheimer's Disease: Challenges and Opportunities. *Front Mol Neurosci* **2019,** *12*, 203.
81. Funderburk, S. F.; Marcellino, B. K.; Yue, Z., Cell "self-eating" (autophagy) mechanism in Alzheimer's disease. *Mt Sinai J Med* **2010,** *77* (1), 59-68.
82. Li, H., Wei, Y., Wang, Z. and Wang, Q Application of APP/PS1 Transgenic Mouse Model for Alzheimer Disease. *J Alzheimer's and Parkinsonism* **2015,** *5* (201).
83. Xiao, Q.; Yan, P.; Ma, X.; Liu, H.; Perez, R.; Zhu, A.; Gonzales, E.; Tripoli, D. L.; Czerniewski, L.; Ballabio, A.; al., e., Neuronal-Targeted TFEB Accelerates Lysosomal Degradation of APP, Reducing Abeta Generation and Amyloid Plaque Pathogenesis. *J Neurosci* **2015,** *35* (35), 12137-51.
84. Long, Z.; Chen, J.; Zhao, Y.; Zhou, W.; Yao, Q.; Wang, Y.; He, G., Dynamic changes of autophagic flux induced by Abeta in the brain of postmortem Alzheimer's disease patients, animal models and cell models. *Aging (Albany NY)* **2020,** *12* (11), 10912-10930.
85. Rocchi, A.; Yamamoto, S.; Ting, T.; Fan, Y.; Sadleir, K.; Wang, Y.; Zhang, W.; Huang, S.; Levine, B.; Vassar, R.; al., e., A Becn1 mutation mediates hyperactive autophagic sequestration of amyloid oligomers and improved cognition in Alzheimer's disease. *PLoS Genet* **2017,** *13* (8), e1006962.
86. Manczak, M.; Calkins, M. J.; Reddy, P. H., Impaired mitochondrial dynamics and abnormal interaction of amyloid beta with mitochondrial protein Drp1 in neurons from patients with Alzheimer's disease: implications for neuronal damage. *Hum Mol Genet* **2011,** *20* (13), 2495-509.
87. Manczak, M.; Kandimalla, R.; Yin, X.; Reddy, P. H., Hippocampal mutant APP and amyloid beta-induced cognitive decline, dendritic spine loss, defective autophagy, mitophagy and mitochondrial abnormalities in a mouse model of Alzheimer's disease. *Hum Mol Genet* **2018,** *27* (8), 1332-1342.
88. Yiannopoulou, K. G.; Papageorgiou, S. G., Current and Future Treatments in Alzheimer Disease: An Update. *J Cent Nerv Syst Dis* **2020,** *12*, 1179573520907397.
89. Lin, M. W.; Chen, Y. H.; Yang, H. B.; Lin, C. C.; Hung, S. Y., Galantamine Inhibits Abeta1-42-Induced Neurotoxicity by Enhancing alpha7nAChR Expression as a

Cargo Carrier for LC3 Binding and Abeta1-42 Engulfment During Autophagic Degradation. *Neurotherapeutics* **2020,** *17* (2), 676-689.
90. Song, G.; Li, Y.; Lin, L.; Cao, Y., Anti-autophagic and anti-apoptotic effects of memantine in a SH-SY5Y cell model of Alzheimer's disease via mammalian target of rapamycin-dependent and -independent pathways. *Mol Med Rep* **2015,** *12* (5), 7615-22.
91. Hirano, K.; Fujimaki, M.; Sasazawa, Y.; Yamaguchi, A.; Ishikawa, K. I.; Miyamoto, K.; Souma, S.; Furuya, N.; Imamichi, Y.; Yamada, D.; Saya, H.; Akamatsu, W.; Saiki, S.; Hattori, N., Neuroprotective effects of memantine via enhancement of autophagy. *Biochem Biophys Res Commun* **2019,** *518* (1), 161-170.
92. Evans, C. S.; Holzbaur, E. L. F., Autophagy and mitophagy in ALS. *Neurobiol Dis* **2019,** *122*, 35-40.
93. Hasegawa, M.; Arai, T.; Nonaka, T.; Kametani, F.; Yoshida, M.; Hashizume, Y.; Beach, T. G.; Buratti, E.; Baralle, F.; Morita, M.; al., e., Phosphorylated TDP-43 in frontotemporal lobar degeneration and amyotrophic lateral sclerosis. *Ann Neurol* **2008,** *64* (1), 60-70.
94. Blokhuis, A. M.; Groen, E. J.; Koppers, M.; van den Berg, L. H.; Pasterkamp, R. J., Protein aggregation in amyotrophic lateral sclerosis. *Acta Neuropathol* **2013,** *125* (6), 777-94.
95. Sun, R.; He, X.; Jiang, X.; Tao, H., The new role of riluzole in the treatment of pancreatic cancer through the apoptosis and autophagy pathways. *J Cell Biochem* **2019**.
96. Cruz, M. P., Edaravone (Radicava): A Novel Neuroprotective Agent for the Treatment of Amyotrophic Lateral Sclerosis. *P T* **2018,** *43* (1), 25-28.
97. Yin, J.; Zhou, Z.; Chen, J.; Wang, Q.; Tang, P.; Ding, Q.; Yin, G.; Gu, J.; Fan, J., Edaravone inhibits autophagy after neuronal oxygen-glucose deprivation/recovery injury. *Int J Neurosci* **2019,** *129* (5), 501-510.
98. Liu, N.; Shang, J.; Tian, F.; Nishi, H.; Abe, K., In vivo optical imaging for evaluating the efficacy of edaravone after transient cerebral ischemia in mice. *Brain Res* **2011,** *1397*, 66-75.
99. Nguyen, D. K. H.; Thombre, R.; Wang, J., Autophagy as a common pathway in amyotrophic lateral sclerosis. *Neurosci Lett* **2019,** *697*, 34-48.
100. Giovedi, S.; Ravanelli, M. M.; Parisi, B.; Bettegazzi, B.; Guarnieri, F. C., Dysfunctional Autophagy and Endolysosomal System in Neurodegenerative Diseases: Relevance and Therapeutic Options. *Front Cell Neurosci* **2020,** *14*, 602116.
101. Bilsland, L. G.; Sahai, E.; Kelly, G.; Golding, M.; Greensmith, L.; Schiavo, G., Deficits in axonal transport precede ALS symptoms in vivo. *Proc Natl Acad Sci U S A* **2010,** *107* (47), 20523-8.
102. Xie, Y.; Zhou, B.; Lin, M. Y.; Wang, S.; Foust, K. D.; Sheng, Z. H., Endolysosomal Deficits Augment Mitochondria Pathology in Spinal Motor Neurons of Asymptomatic fALS Mice. *Neuron* **2015,** *87* (2), 355-70.
103. Palomo, G. M.; Granatiero, V.; Kawamata, H.; Konrad, C.; Kim, M.; Arreguin, A. J.; Zhao, D.; Milner, T. A.; Manfredi, G., Parkin is a disease modifier in the mutant SOD1 mouse model of ALS. *EMBO Mol Med* **2018,** *10* (10).
104. Li, Y.; Guo, Y.; Wang, X.; Yu, X.; Duan, W.; Hong, K.; Wang, J.; Han, H.; Li, C., Trehalose decreases mutant SOD1 expression and alleviates motor deficiency in early but not end-stage amyotrophic lateral sclerosis in a SOD1-G93A mouse model. *Neuroscience* **2015,** *298*, 12-25.

105. Casterton, R. L.; Hunt, R. J.; Fanto, M., Pathomechanism Heterogeneity in the Amyotrophic Lateral Sclerosis and Frontotemporal Dementia Disease Spectrum: Providing Focus Through the Lens of Autophagy. *J Mol Biol* **2020,** *432* (8), 2692-2713.
106. Zhou, Q. M.; Zhang, J. J.; Li, S.; Chen, S.; Le, W. D., n-butylidenephthalide treatment prolongs life span and attenuates motor neuron loss in SOD1(G93A) mouse model of amyotrophic lateral sclerosis. *CNS Neurosci Ther* **2017,** *23* (5), 375-385.
107. Xia, Q.; Wang, H.; Hao, Z.; Fu, C.; Hu, Q.; Gao, F.; Ren, H.; Chen, D.; Han, J.; Ying, Z.; al., e., TDP-43 loss of function increases TFEB activity and blocks autophagosome-lysosome fusion. *EMBO J* **2016,** *35* (2), 121-42.
108. Madruga, E.; Maestro, I.; Martinez, A., Mitophagy Modulation, a New Player in the Race against ALS. *Int J Mol Sci* **2021,** *22* (2).
109. Rubinsztein, D. C.; Marino, G.; Kroemer, G., Autophagy and aging. *Cell* **2011,** *146* (5), 682-95.
110. Xu, T. T.; Li, H.; Dai, Z.; Lau, G. K.; Li, B. Y.; Zhu, W. L.; Liu, X. Q.; Liu, H. F.; Cai, W. W.; Huang, S. Q.; Wang, Q.; Zhang, S. J., Spermidine and spermine delay brain aging by inducing autophagy in SAMP8 mice. *Aging (Albany NY)* **2020,** *12* (7), 6401-6414.
111. Kanamori, H.; Naruse, G.; Yoshida, A.; Minatoguchi, S.; Watanabe, T.; Kawaguchi, T.; Yamada, Y.; Mikami, A.; Kawasaki, M.; Takemura, G.; al., e., Metformin Enhances Autophagy and Provides Cardioprotection in delta-Sarcoglycan Deficiency-Induced Dilated Cardiomyopathy. *Circ Heart Fail* **2019,** *12* (4), e005418.
112. Martin-Montalvo, A.; Mercken, E. M.; Mitchell, S. J.; Palacios, H. H.; Mote, P. L.; Scheibye-Knudsen, M.; Gomes, A. P.; Ward, T. M.; Minor, R. K.; Blouin, M. J.; al., e., Metformin improves healthspan and lifespan in mice. *Nat Commun* **2013,** *4*, 2192.
113. Kodali, M.; Attaluri, S.; Madhu, L. N.; Shuai, B.; Upadhya, R.; Gonzalez, J. J.; Rao, X.; Shetty, A. K., Metformin treatment in late middle age improves cognitive function with alleviation of microglial activation and enhancement of autophagy in the hippocampus. *Aging Cell* **2021,** *20* (2), e13277.
114. Brattas, P. L.; Hersbach, B. A.; Madsen, S.; Petri, R.; Jakobsson, J.; Pircs, K., Impact of differential and time-dependent autophagy activation on therapeutic efficacy in a model of Huntington disease. *Autophagy* **2021,** *17* (6), 1316-1329.
115. Rose, C.; Menzies, F. M.; Renna, M.; Acevedo-Arozena, A.; Corrochano, S.; Sadiq, O.; Brown, S. D.; Rubinsztein, D. C., Rilmenidine attenuates toxicity of polyglutamine expansions in a mouse model of Huntington's disease. *Hum Mol Genet* **2010,** *19* (11), 2144-53.
116. David, M. A.; Tayebi, M., Detection of protein aggregates in brain and cerebrospinal fluid derived from multiple sclerosis patients. *Front Neurol* **2014,** *5*, 251.
117. Dasgupta, A.; Zheng, J.; Perrone-Bizzozero, N. I.; Bizzozero, O. A., Increased carbonylation, protein aggregation and apoptosis in the spinal cord of mice with experimental autoimmune encephalomyelitis. *ASN Neuro* **2013,** *5* (1), e00111.
118. Feng, X.; Hou, H.; Zou, Y.; Guo, L., Defective autophagy is associated with neuronal injury in a mouse model of multiple sclerosis. *Bosn J Basic Med Sci* **2017,** *17* (2), 95-103.
119. Tsukada, M.; Ohsumi, Y., Isolation and characterization of autophagy-defective mutants of Saccharomyces cerevisiae. *FEBS Lett* **1993,** *333* (1-2), 169-74.
120. https://pubmed.ncbi.nlm.nih.gov/ (Consulted 03.01.2022).
121. Klionsky, D. J.; Abdel-Aziz, A. K.; Abdelfatah, S.; Abdellatif, M.; Abdoli, A.; Abel, S.; Abeliovich, H.; Abildgaard, M. H.; Abudu, Y. P.; Acevedo-Arozena, A.; al., e.,

Guidelines for the use and interpretation of assays for monitoring autophagy (4th edition)(1). *Autophagy* **2021,** *17* (1), 1-382.
122. Kola, I.; Landis, J., Can the pharmaceutical industry reduce attrition rates? *Nat Rev Drug Discov* **2004,** *3* (8), 711-5.
123. DiMasi, J. A.; Grabowski, H. G.; Hansen, R. W., Innovation in the pharmaceutical industry: New estimates of R&D costs. *J Health Econ* **2016,** *47*, 20-33.
124. Hughes, J. P.; Rees, S.; Kalindjian, S. B.; Philpott, K. L., Principles of early drug discovery. *Br J Pharmacol* **2011,** *162* (6), 1239-49.
125. Cohen, P., Protein kinases--the major drug targets of the twenty-first century? *Nat Rev Drug Discov* **2002,** *1* (4), 309-15.
126. Bunnage, M. E., *New Frontiers in Chemical Biology: Enabling Drug Discovery* RSC Books 2011.
127. Zanders, E. D.; Bailey, D. S.; Dean, P. M., Probes for chemical genomics by design. *Drug Discov Today* **2002,** *7* (13), 711-8.
128. Kiriiri, G. K., Njogu, P.M., Mwangi, A.N., Exploring different approaches to improve the success of drug discovery and development projects: a review. *Future Journal of Pharmaceutical Sciences* **2020,** *6* (27).
129. https://www.fda.gov/patients/learn-about-drug-and-device-approvals/drug-development-process (Consulted 08.01.2022).
130. Cheng, H. C.; Qi, R. Z.; Paudel, H.; Zhu, H. J., Regulation and function of protein kinases and phosphatases. *Enzyme Res* **2011,** *2011*, 794089.
131. Zhang, J.; Yang, P. L.; Gray, N. S., Targeting cancer with small molecule kinase inhibitors. *Nat Rev Cancer* **2009,** *9* (1), 28-39.
132. Roskoski, R., Jr., Properties of FDA-approved small molecule protein kinase inhibitors: A 2022 update. *Pharmacol Res* **2022,** *175*, 106037.
133. Maestro, I.; Boya, P.; Martinez, A., Serum- and glucocorticoid-induced kinase 1, a new therapeutic target for autophagy modulation in chronic diseases. *Expert Opin Ther Targets* **2020,** *24* (3), 231-243.
134. Zuleger, T.; Heinzelbecker, J.; Takacs, Z.; Hunter, C.; Voelkl, J.; Lang, F.; Proikas-Cezanne, T., SGK1 Inhibits Autophagy in Murine Muscle Tissue. *Oxid Med Cell Longev* **2018,** *2018*, 4043726.
135. Tang, X.; Sun, Y.; Xu, C.; Guo, X.; Sun, J.; Pan, C.; Sun, J., Caffeine Induces Autophagy and Apoptosis in Auditory Hair Cells via the SGK1/HIF-1alpha Pathway. *Front Cell Dev Biol* **2021,** *9*, 751012.
136. Dib, M., Issues for clinical drug development in neurodegenerative diseases. *Drugs* **2005,** *65* (17), 2463-79.
137. Aldewachi, H.; Al-Zidan, R. N.; Conner, M. T.; Salman, M. M., High-Throughput Screening Platforms in the Discovery of Novel Drugs for Neurodegenerative Diseases. *Bioengineering (Basel)* **2021,** *8* (2).
138. Nozal, V.; Garcia-Rubia, A.; Cuevas, E. P.; Perez, C.; Tosat-Bitrian, C.; Bartolome, F.; Carro, E.; Ramirez, D.; Palomo, V.; Martinez, A., From Kinase Inhibitors to Multitarget Ligands as Powerful Drug Leads for Alzheimer's Disease using Protein-Templated Synthesis. *Angew Chem Int Ed Engl* **2021,** *60* (35), 19344-19354.
139. Sliwoski, G.; Kothiwale, S.; Meiler, J.; Lowe, E. W., Jr., Computational methods in drug discovery. *Pharmacol Rev* **2014,** *66* (1), 334-95.

140. Berman, H. M.; Westbrook, J.; Feng, Z.; Gilliland, G.; Bhat, T. N.; Weissig, H.; Shindyalov, I. N.; Bourne, P. E., The Protein Data Bank. *Nucleic Acids Res* **2000,** *28* (1), 235-42.
141. Kontoyianni, M., Docking and Virtual Screening in Drug Discovery. *Methods Mol Biol* **2017,** *1647*, 255-266.
142. Princely Abudu, Y.; Pankiv, S.; Mathai, B. J.; Hakon Lystad, A.; Bindesboll, C.; Brenne, H. B.; Yoke Wui Ng, M.; Thiede, B.; Yamamoto, A.; Mutugi Nthiga, T.; Lamark, T.; Esguerra, C. V.; Johansen, T.; Simonsen, A., NIPSNAP1 and NIPSNAP2 Act as "Eat Me" Signals for Mitophagy. *Dev Cell* **2019,** *49* (4), 509-525 e12.
143. Allen, G. F.; Toth, R.; James, J.; Ganley, I. G., Loss of iron triggers PINK1/Parkin-independent mitophagy. *EMBO Rep* **2013,** *14* (12), 1127-35.
144. Agosta, F.; Al-Chalabi, A.; Filippi, M.; Hardiman, O.; Kaji, R.; Meininger, V.; Nakano, I.; Shaw, P.; Shefner, J.; van den Berg, L. H.; Ludolph, A.; ALS/MND, W. F. N. R. G. o., The El Escorial criteria: strengths and weaknesses. *Amyotroph Lateral Scler Frontotemporal Degener* **2015,** *16* (1-2), 1-7.
145. Koistinen, P., Human peripheral blood and bone marrow cell separation using density gradient centrifugation on Lymphoprep and Percoll in haematological diseases. *Scand J Clin Lab Invest* **1987,** *47* (7), 709-14.
146. Carpenter, A. E.; Jones, T. R.; Lamprecht, M. R.; Clarke, C.; Kang, I. H.; Friman, O.; Guertin, D. A.; Chang, J. H.; Lindquist, R. A.; Moffat, J.; al., e., CellProfiler: image analysis software for identifying and quantifying cell phenotypes. *Genome Biol* **2006,** *7* (10), R100.
147. McWilliams, T. G.; Prescott, A. R.; Allen, G. F.; Tamjar, J.; Munson, M. J.; Thomson, C.; Muqit, M. M.; Ganley, I. G., mito-QC illuminates mitophagy and mitochondrial architecture in vivo. *J Cell Biol* **2016,** *214* (3), 333-45.
148. Maestro, Schrödinger, LLC, New York, NY, 2021.
149. LigPrep, Schrödinger, LLC, New York, NY, 2021.
150. QikProp, S., Schrödinger Release 2015-4; LLC, New York, NY, 2015.
151. Benet, L. Z.; Hosey, C. M.; Ursu, O.; Oprea, T. I., BDDCS, the Rule of 5 and drugability. *Adv Drug Deliv Rev* **2016,** *101*, 89-98.
152. Bhal, K., LogP—Making Sense of the Value. Advanced Chemistry Development, Inc. Toronto, ON, Canada.
153. Kelder, J.; Grootenhuis, P. D.; Bayada, D. M.; Delbressine, L. P.; Ploemen, J. P., Polar molecular surface as a dominating determinant for oral absorption and brain penetration of drugs. *Pharm Res* **1999,** *16* (10), 1514-9.
154. Canvas Version 2.5.015,Canvas, Schrödinger, LLC, New York, NY, 2015.
155. Rogers, D.; Brown, R. D.; Hahn, M., Using extended-connectivity fingerprints with Laplacian-modified Bayesian analysis in high-throughput screening follow-up. *J Biomol Screen* **2005,** *10* (7), 682-6.
156. Duan, J.; Dixon, S. L.; Lowrie, J. F.; Sherman, W., Analysis and comparison of 2D fingerprints: insights into database screening performance using eight fingerprint methods. *J Mol Graph Model* **2010,** *29* (2), 157-70.
157. Hammond, M.; Washburn, D. G.; Hoang, H. T.; Manns, S.; Frazee, J. S.; Nakamura, H.; Patterson, J. R.; Trizna, W.; Wu, C.; Azzarano, L. M.; al., e., Design and synthesis of orally bioavailable serum and glucocorticoid-regulated kinase 1 (SGK1) inhibitors. *Bioorg Med Chem Lett* **2009,** *19* (15), 4441-5.

158. Protein Preparation Wizard; Epik, Schrödinger, LLC, New York, NY, 2021; Impact, Schrödinger, LLC, New York, NY; Prime, Schrödinger, LLC, New York, NY, 2021.
159. Glide, S., LLC, New York, NY, 2017. Glide, Schrödinger, 2017.
160. Sebastian-Perez, V.; Roca, C.; Awale, M.; Reymond, J. L.; Martinez, A.; Gil, C.; Campillo, N. E., Medicinal and Biological Chemistry (MBC) Library: An Efficient Source of New Hits. *J Chem Inf Model* **2017,** *57* (9), 2143-2151.
161. Gil, C.; Martinez, A., Is drug repurposing really the future of drug discovery or is new innovation truly the way forward? *Expert Opin Drug Discov* **2021,** *16* (8), 829-831.
162. Pushpakom, S.; Iorio, F.; Eyers, P. A.; Escott, K. J.; Hopper, S.; Wells, A.; Doig, A.; Guilliams, T.; Latimer, J.; McNamee, C.; al., e., Drug repurposing: progress, challenges and recommendations. *Nat Rev Drug Discov* **2019,** *18* (1), 41-58.
163. Narendra, D.; Tanaka, A.; Suen, D. F.; Youle, R. J., Parkin is recruited selectively to impaired mitochondria and promotes their autophagy. *J Cell Biol* **2008,** *183* (5), 795-803.
164. Tang, M. Y.; Vranas, M.; Krahn, A. I.; Pundlik, S.; Trempe, J. F.; Fon, E. A., Structure-guided mutagenesis reveals a hierarchical mechanism of Parkin activation. *Nat Commun* **2017,** *8*, 14697.
165. Yoshimori, T.; Yamamoto, A.; Moriyama, Y.; Futai, M.; Tashiro, Y., Bafilomycin A1, a specific inhibitor of vacuolar-type H(+)-ATPase, inhibits acidification and protein degradation in lysosomes of cultured cells. *J Biol Chem* **1991,** *266* (26), 17707-12.
166. Tanaka, A.; Cleland, M. M.; Xu, S.; Narendra, D. P.; Suen, D. F.; Karbowski, M.; Youle, R. J., Proteasome and p97 mediate mitophagy and degradation of mitofusins induced by Parkin. *J Cell Biol* **2010,** *191* (7), 1367-80.
167. Huang, C.; Lu, H.; Xu, J.; Yu, H.; Wang, X.; Zhang, X., Protective roles of autophagy in retinal pigment epithelium under high glucose condition via regulating PINK1/Parkin pathway and BNIP3L. *Biol Res* **2018,** *51* (1), 22.
168. Palomo, V.; Perez, D. I.; Roca, C.; Anderson, C.; Rodriguez-Muela, N.; Perez, C.; Morales-Garcia, J. A.; Reyes, J. A.; Campillo, N. E.; Perez-Castillo, A. M.; al., e., Subtly Modulating Glycogen Synthase Kinase 3 beta: Allosteric Inhibitor Development and Their Potential for the Treatment of Chronic Diseases. *J Med Chem* **2017,** *60* (12), 4983-5001.
169. Ryu, H. Y.; Kim, L. E.; Jeong, H.; Yeo, B. K.; Lee, J. W.; Nam, H.; Ha, S.; An, H. K.; Park, H.; Jung, S.; al., e., GSK3B induces autophagy by phosphorylating ULK1. *Exp Mol Med* **2021,** *53* (3), 369-383.
170. Rippin, I.; Eldar-Finkelman, H., Mechanisms and Therapeutic Implications of GSK-3 in Treating Neurodegeneration. *Cells* **2021,** *10* (2).
171. Palomo, V.; Perez, D. I.; Perez, C.; Morales-Garcia, J. A.; Soteras, I.; Alonso-Gil, S.; Encinas, A.; Castro, A.; Campillo, N. E.; Perez-Castillo, A.; al., e., 5-imino-1,2,4-thiadiazoles: first small molecules as substrate competitive inhibitors of glycogen synthase kinase 3. *J Med Chem* **2012,** *55* (4), 1645-61.
172. Martinez, A.; Alonso, M.; Castro, A.; Perez, C.; Moreno, F. J., First non-ATP competitive glycogen synthase kinase 3 beta (GSK-3beta) inhibitors: thiadiazolidinones (TDZD) as potential drugs for the treatment of Alzheimer's disease. *J Med Chem* **2002,** *45* (6), 1292-9.
173. Yakhine-Diop, S. M. S.; Niso-Santano, M.; Rodriguez-Arribas, M.; Gomez-Sanchez, R.; Martinez-Chacon, G.; Uribe-Carretero, E.; Navarro-Garcia, J. A.; Ruiz-Hurtado, G.; Aiastui, A.; Cooper, J. M.; al., e., Impaired Mitophagy and Protein

Acetylation Levels in Fibroblasts from Parkinson's Disease Patients. *Mol Neurobiol* **2019,** *56* (4), 2466-2481.
174. Maestro, I.; de la Ballina, L. R.; Simonsen, A.; Boya, P.; Martinez, A., Phenotypic Assay Leads to Discovery of Mitophagy Inducers with Therapeutic Potential for Parkinson's Disease. *ACS Chem Neurosci* **2021,** *12* (24), 4512-4523.
175. Salado, I. G.; Redondo, M.; Bello, M. L.; Perez, C.; Liachko, N. F.; Kraemer, B. C.; Miguel, L.; Lecourtois, M.; Gil, C.; Martinez, A.; Perez, D. I., Protein kinase CK-1 inhibitors as new potential drugs for amyotrophic lateral sclerosis. *J Med Chem* **2014,** *57* (6), 2755-72.
176. Palomo, V.; Nozal, V.; Rojas-Prats, E.; Gil, C.; Martinez, A., Protein kinase inhibitors for amyotrophic lateral sclerosis therapy. *Br J Pharmacol* **2021,** *178* (6), 1316-1335.
177. Palomo, V.; Tosat-Bitrian, C.; Nozal, V.; Nagaraj, S.; Martin-Requero, A.; Martinez, A., TDP-43: A Key Therapeutic Target beyond Amyotrophic Lateral Sclerosis. *ACS Chem Neurosci* **2019,** *10* (3), 1183-1196.
178. Wong, P. M.; Puente, C.; Ganley, I. G.; Jiang, X., The ULK1 complex: sensing nutrient signals for autophagy activation. *Autophagy* **2013,** *9* (2), 124-37.
179. Martinez-Gonzalez, L.; Rodriguez-Cueto, C.; Cabezudo, D.; Bartolome, F.; Andres-Benito, P.; Ferrer, I.; Gil, C.; Martin-Requero, A.; Fernandez-Ruiz, J.; Martinez, A.; de Lago, E., Motor neuron preservation and decrease of in vivo TDP-43 phosphorylation by protein CK-1delta kinase inhibitor treatment. *Sci Rep* **2020,** *10* (1), 4449.
180. Mauthe, M.; Orhon, I.; Rocchi, C.; Zhou, X.; Luhr, M.; Hijlkema, K. J.; Coppes, R. P.; Engedal, N.; Mari, M.; Reggiori, F., Chloroquine inhibits autophagic flux by decreasing autophagosome-lysosome fusion. *Autophagy* **2018,** *14* (8), 1435-1455.
181. Gurney, M. E.; Pu, H.; Chiu, A. Y.; Dal Canto, M. C.; Polchow, C. Y.; Alexander, D. D.; Caliendo, J.; Hentati, A.; Kwon, Y. W.; Deng, H. X.; et al., Motor neuron degeneration in mice that express a human Cu,Zn superoxide dismutase mutation. *Science* **1994,** *264* (5166), 1772-5.
182. Wegorzewska, I.; Bell, S.; Cairns, N. J.; Miller, T. M.; Baloh, R. H., TDP-43 mutant transgenic mice develop features of ALS and frontotemporal lobar degeneration. *Proc Natl Acad Sci U S A* **2009,** *106* (44), 18809-14.
183. Basnet, R.; Gong, G. Q.; Li, C.; Wang, M. W., Serum and glucocorticoid inducible protein kinases (SGKs): a potential target for cancer intervention. *Acta Pharm Sin B* **2018,** *8* (5), 767-771.
184. Lang, F.; Artunc, F.; Vallon, V., The physiological impact of the serum and glucocorticoid-inducible kinase SGK1. *Curr Opin Nephrol Hypertens* **2009,** *18* (5), 439-48.
185. Lang, F.; Stournaras, C.; Zacharopoulou, N.; Voelkl, J.; Alesutan, I., Serum- and glucocorticoid-inducible kinase 1 and the response to cell stress. *Cell Stress* **2018,** *3* (1), 1-8.
186. Engelsberg, A.; Kobelt, F.; Kuhl, D., The N-terminus of the serum- and glucocorticoid-inducible kinase Sgk1 specifies mitochondrial localization and rapid turnover. *Biochem J* **2006,** *399* (1), 69-76.
187. Zhao, B.; Lehr, R.; Smallwood, A. M.; Ho, T. F.; Maley, K.; Randall, T.; Head, M. S.; Koretke, K. K.; Schnackenberg, C. G., Crystal structure of the kinase domain of serum and glucocorticoid-regulated kinase 1 in complex with AMP PNP. *Protein Sci* **2007,** *16* (12), 2761-9.

188. Abbruzzese, C.; Mattarocci, S.; Pizzuti, L.; Mileo, A. M.; Visca, P.; Antoniani, B.; Alessandrini, G.; Facciolo, F.; Amato, R.; D'Antona, L.; al., e., Determination of SGK1 mRNA in non-small cell lung cancer samples underlines high expression in squamous cell carcinomas. *J Exp Clin Cancer Res* **2012,** *31*, 4.
189. Talarico, C.; Dattilo, V.; D'Antona, L.; Barone, A.; Amodio, N.; Belviso, S.; Musumeci, F.; Abbruzzese, C.; Bianco, C.; Trapasso, F.; al., e., SI113, a SGK1 inhibitor, potentiates the effects of radiotherapy, modulates the response to oxidative stress and induces cytotoxic autophagy in human glioblastoma multiforme cells. *Oncotarget* **2016,** *7* (13), 15868-84.
190. Chung, E. J.; Sung, Y. K.; Farooq, M.; Kim, Y.; Im, S.; Tak, W. Y.; Hwang, Y. J.; Kim, Y. I.; Han, H. S.; Kim, J. C.; al., e., Gene expression profile analysis in human hepatocellular carcinoma by cDNA microarray. *Mol Cells* **2002,** *14* (3), 382-7.
191. Liang, X.; Lan, C.; Jiao, G.; Fu, W.; Long, X.; An, Y.; Wang, K.; Zhou, J.; Chen, T.; Li, Y.; al., e., Therapeutic inhibition of SGK1 suppresses colorectal cancer. *Exp Mol Med* **2017,** *49* (11), e399.
192. Inoue, K.; Leng, T.; Yang, T.; Zeng, Z.; Ueki, T.; Xiong, Z. G., Role of serum- and glucocorticoid-inducible kinases in stroke. *J Neurochem* **2016,** *138* (2), 354-61.
193. Nishida, Y.; Nagata, T.; Takahashi, Y.; Sugahara-Kobayashi, M.; Murata, A.; Asai, S., Alteration of serum/glucocorticoid regulated kinase-1 (sgk-1) gene expression in rat hippocampus after transient global ischemia. *Brain Res Mol Brain Res* **2004,** *123* (1-2), 121-5.
194. von Wowern, F.; Berglund, G.; Carlson, J.; Mansson, H.; Hedblad, B.; Melander, O., Genetic variance of SGK-1 is associated with blood pressure, blood pressure change over time and strength of the insulin-diastolic blood pressure relationship. *Kidney Int* **2005,** *68* (5), 2164-72.
195. Schwab, M.; Lupescu, A.; Mota, M.; Mota, E.; Frey, A.; Simon, P.; Mertens, P. R.; Floege, J.; Luft, F.; Asante-Poku, S.; al., e., Association of SGK1 gene polymorphisms with type 2 diabetes. *Cell Physiol Biochem* **2008,** *21* (1-3), 151-60.
196. Zhuang, L.; Jin, G.; Hu, X.; Yang, Q.; Shi, Z., The inhibition of SGK1 suppresses epithelial-mesenchymal transition and promotes renal tubular epithelial cell autophagy in diabetic nephropathy. *Am J Transl Res* **2019,** *11* (8), 4946-4956.
197. Singh, P. K.; Singh, S.; Ganesh, S., Activation of serum/glucocorticoid-induced kinase 1 (SGK1) underlies increased glycogen levels, mTOR activation, and autophagy defects in Lafora disease. *Mol Biol Cell* **2013,** *24* (24), 3776-86.
198. Wu, C.; Chen, Z.; Xiao, S.; Thalhamer, T.; Madi, A.; Han, T.; Kuchroo, V., SGK1 Governs the Reciprocal Development of Th17 and Regulatory T Cells. *Cell Rep* **2018,** *22* (3), 653-665.
199. Sahin, P.; McCaig, C.; Jeevahan, J.; Murray, J. T.; Hainsworth, A. H., The cell survival kinase SGK1 and its targets FOXO3a and NDRG1 in aged human brain. *Neuropathol Appl Neurobiol* **2013,** *39* (6), 623-33.
200. Iwata, S.; Nomoto, M.; Morioka, H.; Miyata, A., Gene expression profiling in the midbrain of striatal 6-hydroxydopamine-injected mice. *Synapse* **2004,** *51* (4), 279-86.
201. Schoenebeck, B.; Bader, V.; Zhu, X. R.; Schmitz, B.; Lubbert, H.; Stichel, C. C., Sgk1, a cell survival response in neurodegenerative diseases. *Mol Cell Neurosci* **2005,** *30* (2), 249-64.

202. Waldegger, S.; Klingel, K.; Barth, P.; Sauter, M.; Rfer, M. L.; Kandolf, R.; Lang, F., h-sgk serine-threonine protein kinase gene as transcriptional target of transforming growth factor beta in human intestine. *Gastroenterology* **1999,** *116* (5), 1081-8.
203. Yang, M.; Zheng, J.; Miao, Y.; Wang, Y.; Cui, W.; Guo, J.; Qiu, S.; Han, Y.; Jia, L.; Li, H.; al., e., Serum-glucocorticoid regulated kinase 1 regulates alternatively activated macrophage polarization contributing to angiotensin II-induced inflammation and cardiac fibrosis. *Arterioscler Thromb Vasc Biol* **2012,** *32* (7), 1675-86.
204. Sherk, A. B.; Frigo, D. E.; Schnackenberg, C. G.; Bray, J. D.; Laping, N. J.; Trizna, W.; Hammond, M.; Patterson, J. R.; Thompson, S. K.; Kazmin, D.; al., e., Development of a small-molecule serum- and glucocorticoid-regulated kinase-1 antagonist and its evaluation as a prostate cancer therapeutic. *Cancer Res* **2008,** *68* (18), 7475-83.
205. Ackermann, T. F.; Boini, K. M.; Beier, N.; Scholz, W.; Fuchss, T.; Lang, F., EMD638683, a novel SGK inhibitor with antihypertensive potency. *Cell Physiol Biochem* **2011,** *28* (1), 137-46.
206. Ortuso, F.; Amato, R.; Artese, A.; D'Antona, L.; Costa, G.; Talarico, C.; Gigliotti, F.; Bianco, C.; Trapasso, F.; Schenone, S.; al., e., In silico identification and biological evaluation of novel selective serum/glucocorticoid-inducible kinase 1 inhibitors based on the pyrazolo-pyrimidine scaffold. *J Chem Inf Model* **2014,** *54* (7), 1828-32.
207. Conza, D.; Mirra, P.; Cali, G.; Tortora, T.; Insabato, L.; Fiory, F.; Schenone, S.; Amato, R.; Beguinot, F.; Perrotti, N.; al., e., The SGK1 inhibitor SI113 induces autophagy, apoptosis, and endoplasmic reticulum stress in endometrial cancer cells. *J Cell Physiol* **2017,** *232* (12), 3735-3743.
208. Virdee, K.; Yoshida, H.; Peak-Chew, S.; Goedert, M., Phosphorylation of human microtubule-associated protein tau by protein kinases of the AGC subfamily. *FEBS Lett* **2007,** *581* (14), 2657-62.
209. Duka, V.; Lee, J. H.; Credle, J.; Wills, J.; Oaks, A.; Smolinsky, C.; Shah, K.; Mash, D. C.; Masliah, E.; Sidhu, A., Identification of the sites of tau hyperphosphorylation and activation of tau kinases in synucleinopathies and Alzheimer's diseases. *PLoS One* **2013,** *8* (9), e75025.
210. Kamat, P. K.; Rai, S.; Nath, C., Okadaic acid induced neurotoxicity: an emerging tool to study Alzheimer's disease pathology. *Neurotoxicology* **2013,** *37*, 163-72.
211. Feoktistova, M.; Geserick, P.; Leverkus, M., Crystal Violet Assay for Determining Viability of Cultured Cells. *Cold Spring Harb Protoc* **2016,** *2016* (4), pdb prot087379.
212. Di, L.; Kerns, E. H., Profiling drug-like properties in discovery research. *Curr Opin Chem Biol* **2003,** *7* (3), 402-8.
213. Xu J, H. A., Chemoinformatics and Drug Discovery. *Molecules* **2002,** *7* (8), 566-600.
214. Lipinski, C. A., Lead- and drug-like compounds: the rule-of-five revolution. *Drug Discov Today Technol* **2004,** *1* (4), 337-41.
215. Isherwood, B. A., A., *Phenotypic Drug Discovery*. RSC Books 2021.
216. Comley, J., Phenotypic Drug Discovery: Striving towards high level biological relevance. *Drug Discovery World* **2015,** (Winter 2015/16).
217. Swinney, D. C.; Lee, J. A., Recent advances in phenotypic drug discovery. *F1000Res* **2020,** *9*.
218. Shinoda, H.; Shannon, M.; Nagai, T., Fluorescent Proteins for Investigating Biological Events in Acidic Environments. *Int J Mol Sci* **2018,** *19* (6).

219. Rees, D. J.; Roberts, L.; Carla Carisi, M.; Morgan, A. H.; Brown, M. R.; Davies, J. S., Automated Quantification of Mitochondrial Fragmentation in an In Vitro Parkinson's Disease Model. *Curr Protoc Neurosci* **2020,** *94* (1), e105.
220. Chacinska, A.; Koehler, C. M.; Milenkovic, D.; Lithgow, T.; Pfanner, N., Importing mitochondrial proteins: machineries and mechanisms. *Cell* **2009,** *138* (4), 628-44.
221. Karbowski, M.; Youle, R. J., Regulating mitochondrial outer membrane proteins by ubiquitination and proteasomal degradation. *Curr Opin Cell Biol* **2011,** *23* (4), 476-82.
222. Williams, N. C.; O'Neill, L. A. J., A Role for the Krebs Cycle Intermediate Citrate in Metabolic Reprogramming in Innate Immunity and Inflammation. *Front Immunol* **2018,** *9*, 141.
223. Larsen, S.; Nielsen, J.; Hansen, C. N.; Nielsen, L. B.; Wibrand, F.; Stride, N.; Schroder, H. D.; Boushel, R.; Helge, J. W.; Dela, F.; al., e., Biomarkers of mitochondrial content in skeletal muscle of healthy young human subjects. *J Physiol* **2012,** *590* (14), 3349-60.
224. Itakura, E.; Kishi-Itakura, C.; Koyama-Honda, I.; Mizushima, N., Structures containing Atg9A and the ULK1 complex independently target depolarized mitochondria at initial stages of Parkin-mediated mitophagy. *J Cell Sci* **2012,** *125* (Pt 6), 1488-99.
225. Phukan, S.; Babu, V. S.; Kannoji, A.; Hariharan, R.; Balaji, V. N., GSK3beta: role in therapeutic landscape and development of modulators. *Br J Pharmacol* **2010,** *160* (1), 1-19.
226. Jope, R. S.; Yuskaitis, C. J.; Beurel, E., Glycogen synthase kinase-3 (GSK3): inflammation, diseases, and therapeutics. *Neurochem Res* **2007,** *32* (4-5), 577-95.
227. Palomo, V.; Martinez, A., Glycogen synthase kinase 3 (GSK-3) inhibitors: a patent update (2014-2015). *Expert Opin Ther Pat* **2017,** *27* (6), 657-666.
228. Azoulay-Alfaguter, I.; Elya, R.; Avrahami, L.; Katz, A.; Eldar-Finkelman, H., Combined regulation of mTORC1 and lysosomal acidification by GSK-3 suppresses autophagy and contributes to cancer cell growth. *Oncogene* **2015,** *34* (35), 4613-23.
229. Suzuki, T.; Bridges, D.; Nakada, D.; Skiniotis, G.; Morrison, S. J.; Lin, J. D.; Saltiel, A. R.; Inoki, K., Inhibition of AMPK catabolic action by GSK3. *Mol Cell* **2013,** *50* (3), 407-19.
230. Inoki, K.; Ouyang, H.; Zhu, T.; Lindvall, C.; Wang, Y.; Zhang, X.; Yang, Q.; Bennett, C.; Harada, Y.; Stankunas, K.; al., e., TSC2 integrates Wnt and energy signals via a coordinated phosphorylation by AMPK and GSK3 to regulate cell growth. *Cell* **2006,** *126* (5), 955-68.
231. Li, X. X.; Tsoi, B.; Li, Y. F.; Kurihara, H.; He, R. R., Cardiolipin and its different properties in mitophagy and apoptosis. *J Histochem Cytochem* **2015,** *63* (5), 301-11.
232. Anton, Z.; Landajuela, A.; Hervas, J. H.; Montes, L. R.; Hernandez-Tiedra, S.; Velasco, G.; Goni, F. M.; Alonso, A., Human Atg8-cardiolipin interactions in mitophagy: Specific properties of LC3B, GABARAPL2 and GABARAP. *Autophagy* **2016,** *12* (12), 2386-2403.
233. Scarlatti, F.; Bauvy, C.; Ventruti, A.; Sala, G.; Cluzeaud, F.; Vandewalle, A.; Ghidoni, R.; Codogno, P., Ceramide-mediated macroautophagy involves inhibition of protein kinase B and up-regulation of beclin 1. *J Biol Chem* **2004,** *279* (18), 18384-91.
234. Bhansali, S.; Bhansali, A.; Dhawan, V., Metformin promotes mitophagy in mononuclear cells: a potential in vitro model for unraveling metformin's mechanism of action. *Ann N Y Acad Sci* **2020,** *1463* (1), 23-36.

235. Cheng, G.; Zielonka, J.; Ouari, O.; Lopez, M.; McAllister, D.; Boyle, K.; Barrios, C. S.; Weber, J. J.; Johnson, B. D.; Hardy, M.; al., e., Mitochondria-Targeted Analogues of Metformin Exhibit Enhanced Antiproliferative and Radiosensitizing Effects in Pancreatic Cancer Cells. *Cancer Res* **2016,** *76* (13), 3904-15.
236. Xie, H. R.; Hu, L. S.; Li, G. Y., SH-SY5Y human neuroblastoma cell line: in vitro cell model of dopaminergic neurons in Parkinson's disease. *Chin Med J (Engl)* **2010,** *123* (8), 1086-92.
237. Moors, T. E.; Hoozemans, J. J.; Ingrassia, A.; Beccari, T.; Parnetti, L.; Chartier-Harlin, M. C.; van de Berg, W. D., Therapeutic potential of autophagy-enhancing agents in Parkinson's disease. *Mol Neurodegener* **2017,** *12* (1), 11.
238. Dernie, F., Mitophagy in Parkinson's disease: From pathogenesis to treatment target. *Neurochem Int* **2020,** *138*, 104756.
239. Xicoy, H.; Wieringa, B.; Martens, G. J., The SH-SY5Y cell line in Parkinson's disease research: a systematic review. *Mol Neurodegener* **2017,** *12* (1), 10.
240. Yiğit, E. N. S., E.; Söğüt, M. S.; Çakır, T.; Kurnaz, I. A. , Validation of an In-Vitro Parkinson's Disease Model for the Study of Neuroprotection. *Proceedings* **2018,** *2* (1559).
241. Li, Y.; Chen, X.; Xiong, Q.; Chen, Y.; Zhao, H.; Tahir, M.; Song, J.; Zhou, B.; Wang, J., Casein Kinase 1 Family Member CK1delta/Hrr25 Is Required for Autophagosome Completion. *Front Cell Dev Biol* **2020,** *8*, 460.
242. Petherick, K. J.; Conway, O. J.; Mpamhanga, C.; Osborne, S. A.; Kamal, A.; Saxty, B.; Ganley, I. G., Pharmacological inhibition of ULK1 kinase blocks mammalian target of rapamycin (mTOR)-dependent autophagy. *J Biol Chem* **2015,** *290* (48), 28726.
243. Alquezar, C.; Salado, I. G.; de la Encarnacion, A.; Perez, D. I.; Moreno, F.; Gil, C.; de Munain, A. L.; Martinez, A.; Martin-Requero, A., Targeting TDP-43 phosphorylation by Casein Kinase-1delta inhibitors: a novel strategy for the treatment of frontotemporal dementia. *Mol Neurodegener* **2016,** *11* (1), 36.
244. Wang, I. F.; Guo, B. S.; Liu, Y. C.; Wu, C. C.; Yang, C. H.; Tsai, K. J.; Shen, C. K., Autophagy activators rescue and alleviate pathogenesis of a mouse model with proteinopathies of the TAR DNA-binding protein 43. *Proc Natl Acad Sci U S A* **2012,** *109* (37), 15024-9.
245. Stephenson J, A. S., Modelling amyotrophic lateral sclerosis in mice. *Drug Discov Today Dis Model* **2017,** *25-26*, 35-45.
246. Rogers, R. S.; Tungtur, S.; Tanaka, T.; Nadeau, L. L.; Badawi, Y.; Wang, H.; Ni, H. M.; Ding, W. X.; Nishimune, H., Impaired Mitophagy Plays a Role in Denervation of Neuromuscular Junctions in ALS Mice. *Front Neurosci* **2017,** *11*, 473.
247. Liu, W. J.; Ye, L.; Huang, W. F.; Guo, L. J.; Xu, Z. G.; Wu, H. L.; Yang, C.; Liu, H. F., p62 links the autophagy pathway and the ubiqutin-proteasome system upon ubiquitinated protein degradation. *Cell Mol Biol Lett* **2016,** *21*, 29.
248. Lastres-Becker, I.; Porras, G.; Arribas-Blazquez, M.; Maestro, I.; Borrego-Hernandez, D.; Boya, P.; Cerdan, S.; Garcia-Redondo, A.; Martinez, A.; Martin-Requero, A., Molecular Alterations in Sporadic and SOD1-ALS Immortalized Lymphocytes: Towards a Personalized Therapy. *Int J Mol Sci* **2021,** *22* (6).
249. Domenech, E.; Maestre, C.; Esteban-Martinez, L.; Partida, D.; Pascual, R.; Fernandez-Miranda, G.; Seco, E.; Campos-Olivas, R.; Perez, M.; Megias, D.; al., e., AMPK and PFKFB3 mediate glycolysis and survival in response to mitophagy during mitotic arrest. *Nat Cell Biol* **2015,** *17* (10), 1304-16.

250. https://www.proteinatlas.org/ENSG00000185345-PRKN/tissue (Consulted 04.03.2022).
251. Ballesteros-Alvarez, J.; Andersen, J. K., mTORC2: The other mTOR in autophagy regulation. *Aging Cell* **2021,** *20* (8), e13431.
252. Lu, M.; Wang, J.; Jones, K. T.; Ives, H. E.; Feldman, M. E.; Yao, L. J.; Shokat, K. M.; Ashrafi, K.; Pearce, D., mTOR complex-2 activates ENaC by phosphorylating SGK1. *J Am Soc Nephrol* **2010,** *21* (5), 811-8.
253. Liu, W.; Wang, X.; Liu, Z.; Wang, Y.; Yin, B.; Yu, P.; Duan, X.; Liao, Z.; Chen, Y.; Liu, C.; al., e., SGK1 inhibition induces autophagy-dependent apoptosis via the mTOR-Foxo3a pathway. *Br J Cancer* **2017,** *117* (8), 1139-1153.
254. Liu, W.; Wang, X.; Wang, Y.; Dai, Y.; Xie, Y.; Ping, Y.; Yin, B.; Yu, P.; Liu, Z.; Duan, X.; al., e., SGK1 inhibition-induced autophagy impairs prostate cancer metastasis by reversing EMT. *J Exp Clin Cancer Res* **2018,** *37* (1), 73.
255. Kwon, O. C.; Song, J. J.; Yang, Y.; Kim, S. H.; Kim, J. Y.; Seok, M. J.; Hwang, I.; Yu, J. W.; Karmacharya, J.; Maeng, H. J.; al., e., SGK1 inhibition in glia ameliorates pathologies and symptoms in Parkinson disease animal models. *EMBO Mol Med* **2021,** *13* (4), e13076.
256. Elahi, M.; Motoi, Y.; Shimonaka, S.; Ishida, Y.; Hioki, H.; Takanashi, M.; Ishiguro, K.; Imai, Y.; Hattori, N., High-fat diet-induced activation of SGK1 promotes Alzheimer's disease-associated tau pathology. *Hum Mol Genet* **2021,** *30* (18), 1693-1710.
257. Simmons, E. C.; Scholpa, N. E.; Schnellmann, R. G., Mitochondrial biogenesis as a therapeutic target for traumatic and neurodegenerative CNS diseases. *Exp Neurol* **2020,** *329*, 113309.

8. RESULTS DISSEMINATION

Publications from the PhD thesis:

[1] Maestro, I.; Boya, P.; Martinez, A., Serum- and glucocorticoid-induced kinase 1, a new therapeutic target for autophagy modulation in chronic diseases. *Expert Opin Ther Target*. **2020** *24* (3), 231-243

[2] Madruga, E.; Maestro, I.; Martínez, A., Mitophagy Modulation, a New Player in the Race against ALS. *Int J Mol Sci* **2021** *22* (2), 740.

[3] Lastres-Becker, I.; Porras, G.; Arribas-Blázquez, M.; Maestro, I.; Borrego-Hernández, D.; Boya, P.; Cerdán, S.; García-Redondo, A.; Martínez, A.; Martin-Requero, Á., Molecular Alterations in Sporadic and *SOD1*-ALS Immortalized Lymphocytes: Towards a Personalized Therapy. *Int J Mol Sci* **2021** *22* (6), 3007.

[4] Kocak, M*.; Erdi, SE*.; Jorba, G*.; Maestro, I*.; Farres, J.; Kirkin; V.; Martinez, A.; Pless, O., Targeting autophagy in disease: established and new strategies. *Autophagy* **2021** *9*, 1-3.

[5] Maestro, I.; de la Ballina, L. R.; Simonsen, A.; Boya, P.; Martinez, A., Phenotypic Assay Leads to Discovery of Mitophagy Inducers with Therapeutic Potential for Parkinson's Disease. *ACS Chem Neurosci* **2021** *12* (24), 4512-4523.

Other publications:

[1] Gil, C.; Ginex, T.; Maestro, I.; Nozal, V.; Barrado-Gil, L.; Cuesta-Geijo, M. A.; Urquiza, J.; Ramírez, D.; Alonso, C.; Campillo, N. E.; Martinez, A., COVID-19: Drug Targets and Potential Treatments. *J Med Chem*. **2020** *63* (21), 12359-12386.

[2] Ginex, T.; Garaigorta, U.; Ramírez, D.; Castro, V.; Nozal, V.; Maestro, I.; García-Cárceles, J.; Campillo, N. E.; Martinez, A.; Gastaminza, P.; Gil, C.;, Host-Directed FDA-Approved Drugs with Antiviral Activity against SARS-CoV-2 Identified by Hierarchical In Silico/In Vitro Screening Methods. *Pharmaceuticals* **2021** *14* (4), 332.

[3] Nozal, V.; Rojas-Prats, E.; Maestro, I.; Gil, C.; Perez, D.I.; Martinez, A., Improved Controlled Release and Brain Penetration of the Small Molecule S14 Using PLGA Nanoparticles. *Int J Mol Sci* **2021** *22* (6), 3206

9. ANNEXES

Table S1. Structure of compounds selected for the screening in the phenotypic assay. Compounds in yellow and blue were selected from the Pharmakon drug collection and MBC lirbary, respectively, based on the similarity with known mitophagy modulators DFP and CCCP. Compounds in green were selected from the MBC library based on previous biological activity

Compound ID	Structure	Similarity DFP	Similarity CCCP	Biological Activity
FDA001 Acetaminophen	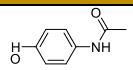	0.854	0.820	analgesic, antipyretic
FDA002 Antipyrine	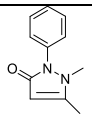	0.875	0.756	analgesic
FDA005 Clozapine	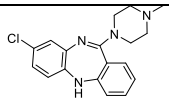	0.633	0.789	antipsychotic
FDA006 Edaravone	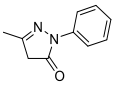	0.852	0.784	antioxidant, lipoxygenase inhibitor
FDA007 Iproniazid phosphate	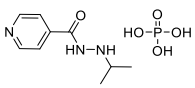	0.785	0.776	monoamine oxidase inhibitor, antidepressant
FDA008 Khellin	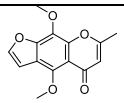	0.790	0.604	vasodilator (coronary), photosensitizer
FDA009 Methimazole		0.884	0.647	antihyperthyroid
FDA010 Phenelzine sulfate	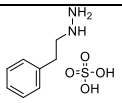	0.741	0.803	antidepressant
FDA011 Phenylbutazone	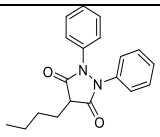	0.786	0.689	antiinflammatory
FDA012 Phenytoin Sodium	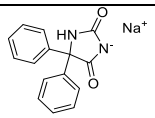	0.762	0.804	anticonvulsant, antieleptic

FDA013 1S,2R-Phenylpropanolamine Hydrochloride	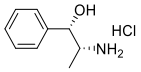	0.819	0.782	vasoconstrictor, decongestant, anorexic
FDA014 Pirfenidone	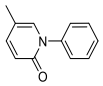	0.868	0.747	antiinflammatory, analgesic, antipyretic
FDA015 Ramifenazone	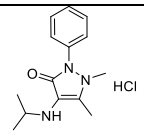	0.851	0.743	analgesic, antipyretic, antiinflammatory
FDA016 Temazepam	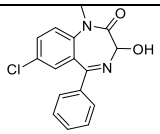	0.729	0.801	sedative, minor tranquilizer
FDA017 Tolazoline Hydrochloride	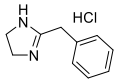	0.726	0.812	adrenergic blocker
FDA018 Tolfenamic acid	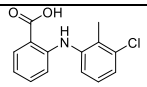	0.776	0.815	antiinflammatory, analgesia
FDA021 Chloropyramine Hydrochloride	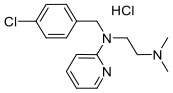	0.688	0.764	antihistamine
FDA022 Clonixin	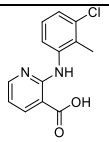	0.760	0.803	antiinflammatory, analgesic
FDA023 Cresopirine	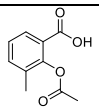	0.809	0.797	antiinflammatory, antpyretic
FDA024 Isaxonine	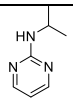	0.793	0.785	nerve growth stimulant

FDA025 Meclofenoxate Hydrochloride	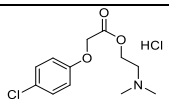	0.766	0.793	nootropic
FDA026 Mephenytoin	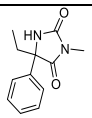	0.766	0.815	anticonvulsant
FDA027 Papaverine Hydrochloride	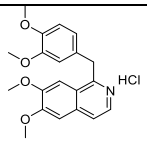	0.645	0.656	muscle relaxant (smooth), cerebral vasodilator
FDA028 Phenacetin	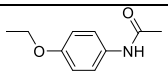	0.782	0.794	analgesic, antipyretic
FDA029 Ractopamine Hydrochloride	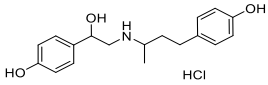	0.738	0.645	beta-adrenergic agonist, growth stimulant
FDA030 Zolmitriptan	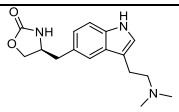	0.673	0.677	antimigraine, 5HT[1B/1D] agonist
FDA033 Diclofenac Sodium	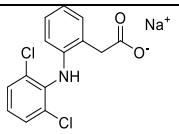	0.710	0.811	antiinflammatory
FDA037 Metoclopramide Hydrochloride	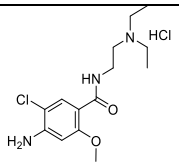	0.711	0.753	antiemetic
AC010a	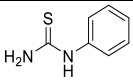	0.749	0.858	
AC047	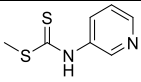	0.756	0.831	
AC053	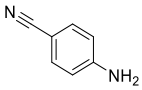	0.765	0.836	
AEL015	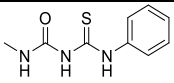	0.773	0.820	

AGF2.38	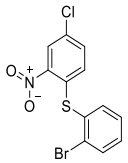	0.707	0.809	
AGF3.40	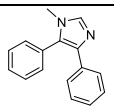	0.815	0.736	
AL029	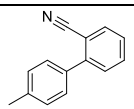	0.782	0.812	
AM008	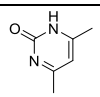	0.874	0.749	
AM034	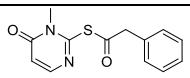	0.817	0.720	
ERP-1.28A	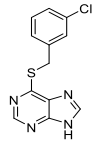	0.631	0.825	
IGS3.4	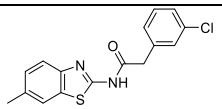	0.706	0.813	
IGS2.6a,b	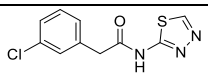	0.710	0.862	
IGS-4.70	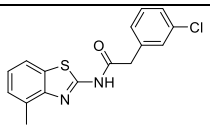	0.713	0.819	
JAR1.42	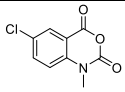	0.836	0.775	
JCB1.19	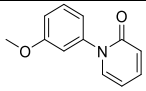	0.847	0.770	
JCB1.4	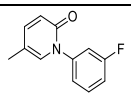	0.851	0.777	
JHD1.18	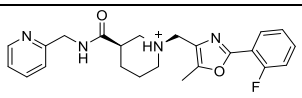	0.639	0.644	
LG1.32	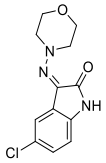	0.680	0.813	

SC116	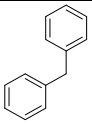	0.769	0.858	
SC162	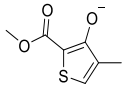	0.829	0.737	
SC290	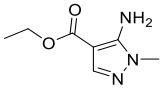	0.831	0.719	
SC296	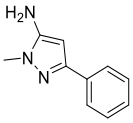	0.821	0.787	
SC298		0.867	0.776	
SC310	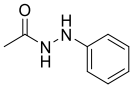	0.810	0.848	
SC448	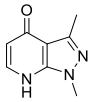	0.874	0.657	
SC450	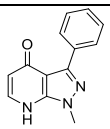	0.831	0.706	
SC456	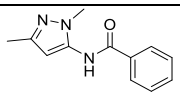	0.819	0.790	
SC695	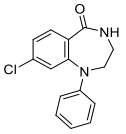	0.980	0.813	
VP0.10	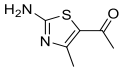	0.819	0.702	
VP2.49	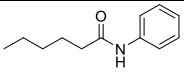	0.761	0.811	
WP020a/b	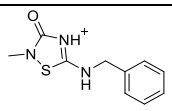	0.834	0.750	
WP031a/b	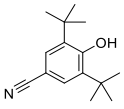	0.829	0.815	

WP042b	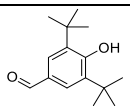	0.848	0.737	
AGF2.20	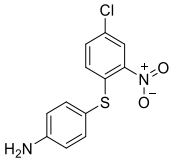	-	-	PDE7A: 0.37 µM PDE7B: 3µM
AZ2	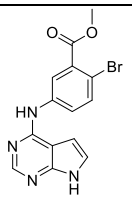	-	-	TTBK1: 2.6 µM TTBK2: 3.2 µM
DM1.55	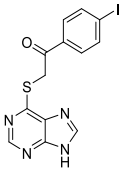	-	-	CDC7: 0.380 µM
ERP1.14	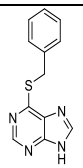	-	-	CDC7: 0.12 µM
ERP2.37	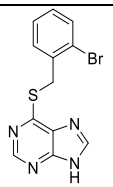	-	-	CDC7: 0.26 µM
IGS2.7	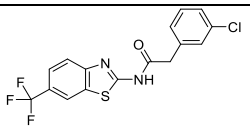	-	-	CK1d: 0.023 µM CK1E: 0.84 µM GSK3 :9.75 µM
IGS3.27	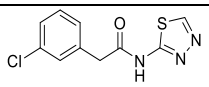	-	-	CK1d: 0.047 µM CK1E: 0.76 µM
JAR1.39	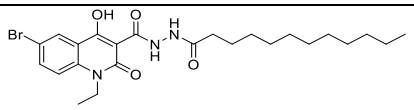	-	-	GSK3: 2.01 µM
MR3.18	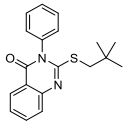	-	-	PDE7A: 0.1 µM PDE7B: 2.51 µM PDE10A: 17 µM
S14	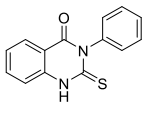	-	-	PDE7A: 4.68 µM PDE7B: 8.8 µM PDE10A: 167 µM

TC3.6	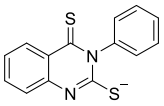	-	-	PDE7A: 0.55 µM
VNG1.6	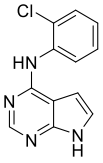	-	-	TTBK1: 21.8 µM
VP07	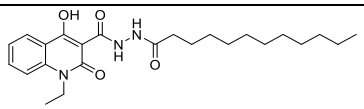	-	-	GSK3: 2.8 µM
VP1.14	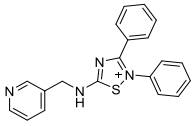	-	-	PDE7A :0.38 µM PDE10A: 3.17 µM GSK3: 1.28 µM
Cdc7VP1.15	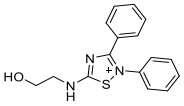	-	-	PDE7A: 1.11 µM PDE10A: 41% @ 10 µM GSK3: 1.95 µM
VP3.15	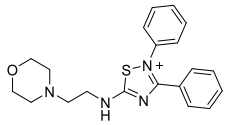	-	-	PDE7A: 1.59 µM PDE10A: 15.4 @ 10 µM GSK3: 0.88 µM
VP4.55	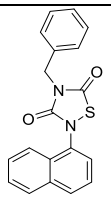	-	-	GSK3: 0.32 µM